

**Aus der Medizinischen Klinik und Poliklinik IV der Ludwig-Maximilians-
Universität München**

Direktor: Prof. Dr. med. Martin Reincke

Role of Murine Double Minute (MDM)-2 in Kidney Injury and Repair

Dissertation

zum Erwerb des Doktorgrades der Humanbiologie

an der Medizinischen Fakultät der

Ludwig-Maximilians-Universität München

vorgelegt von

Shrikant Ramesh Mulay

aus Akole, India

2013

**Mit Genehmigung der Medizinischen Fakultät
der Ludwig-Maximilians-Universität München**

Berichterstatter : Prof. Dr. med. Hans-Joachim Anders

Mitberichterstatter : Prof. Dr. Thomas Knösel

Mitberichterstatter : Prof. Dr. Reinhard Lorenz

Mitberichterstatter : Priv. Doz. Dr. Lutz T. Weber

Mitberichterstatter : Prof. Dr. Peter Nelson

Dekan : Prof. Dr. med. Dr. h.c. M. Reiser, FACR, FRCR

Tag der mündlichen Prüfung : 29.05.2013

Dedicated to MY MOTHER

“What she has is equivalent to a PhD in mothering and my eternal respect”

“No man is poor who has a Godly mother.”

— Sir Abraham Lincoln

TABLE OF CONTENTS

Zusammenfassung	iv
Summary	vi
1. Introduction	1
1.1 Acute Kidney Injury	1
1.1.1 Pathophysiology of renal ischemia/reperfusion injury (IRI)	1
1.2 Chronic Kidney Disease	7
1.2.1 Focal Segmental Glomerulosclerosis	9
1.2.2 Pathogenesis of FSGS	9
1.2.3 Mechanisms of Podocyte death	12
1.2.4 Inflammation in FSGS	13
1.2.5 Adriamycin nephropathy: a model of FSGS	15
1.3. Murine Double Minute (MDM)-2	17
1.3.1 The classical p53-dependent role of MDM2 on cell cycle control	19
1.3.2 p53-independent roles of MDM2 in carcinogenesis	20
1.3.3 Inhibitors of p53-MDM2 interactions	20
1.3.4 Toxicity of MDM2 inhibitors to normal tissue	21
1.4. Role of proliferation in kidney injury and repair	21
1.4.1 Role of proliferation in AKI	21
1.4.2 Role of proliferation in CKD	23
2. Hypotheses	25
3. Material and Methods	26
3.1 Instruments and Chemicals	26
3.2 Experimental procedures	31
3.3 Blood and urine sample collection	34
3.4 Urinary albumin to creatinine ratio	35
3.5 Cytokines Elisa	36
3.6 Immunostaining and Confocal imaging	37

3.7 Periodic acid Schiff staining	38
3.8 Histopathological evaluations	38
3.9 RNA analysis	40
3.10 Protein isolation and western blotting	44
3.11 Magnetic cell sorting technique for isolation of renal cells	44
3.12 Electrophoretic mobility shift assay	45
3.13 <i>In-vitro</i> methods	45
3.14 Statistical analysis	47
4. Results	48
4.1 Part I MDM2 inhibition in ischemia reperfusion induced acute kidney injury	48
4.1.1 MDM2 expression in the healthy and postischemic kidney	48
4.1.2 MDM2 blockade prevents early postischemic AKI	48
4.1.3 MDM2 promotes postischemic renal inflammation in a p53-independent manner	53
4.1.4 MDM2 is required for NF- κ B target gene transcription	58
4.1.5 MDM2 drives tubular regeneration	61
4.2 Part II MDM2 inhibition in adriamycin induced focal segmental glomerulosclerosis	62
4.2.1 MDM2 is expressed in glomerular epithelial cells in healthy & AN kidney	62
4.2.2 MDM2 blockade prevents glomerular pathology and renal dysfunction	65
4.2.3 MDM2 blockade prevents glomerular inflammation and podocyte loss	66
4.2.4 Nutlin-3a prevents adriamycin-induced podocyte death by mitotic catastrophe	68
4.2.5 Effect of MDM2 blockade on p21 expression and podocyte mitosis in AN	68
4.2.6 Delayed MDM2 blockade prevents the progression of AN	70
4.2.7 Delayed MDM2 blockade prevents AN-related tubulointerstitial inflammation	70
4.2.8 Delayed MDM2 blockade prevents AN-related interstitial fibrosis	72
5. Discussion	76
6. References	83
7. Abbreviations	98
8. Appendix	99
9. Acknowledgement	104

Declaration

I hereby declare that all of the present work embodied in this thesis was carried out by me from 01/2010 until 09/2012 under the supervision of Prof. Dr. Hans Joachim Anders, Nephrologisches Zentrum, Medizinische Klinik und Poliklinik IV, Innenstadt Klinikum der Universität München. This work has not been submitted in part or full to any other university or institute for any degree or diploma.

Part of the work was done by others, as mentioned below:

1. Dr. Dana Thomasova, post-doctoral fellow, University of Munich, Germany.

She has performed the *in-vitro* studies to find out the mechanism of pro-inflammatory action of MDM2. The data is presented in the results part I, section 4.1.4 of this thesis.

2. Prof. Paola Romagnani, University of Florence, Italy.

She has performed the *in-vitro* studies to find out the mechanism by which nutlin-3a has protected podocytes from death. The data is presented in the results part II, section 4.2.4 of this thesis.

Part of the work has been published in *Kidney International* (2012 Jun; 81(12):1199-21).

Part of the work has been accepted for publication in *Journal of Pathology* (2013)

Date:

Signature:

Place: Munich, Germany

(Shrikant Ramesh Mulay)

Zusammenfassung

Murine double minute (MDM)-2 fördert als E3 Ubiquitin Ligase das Überleben von Tumorzellen, indem es den Zellzyklus-Regulator p53 degradiert. Die Hemmung von MDM2 durch sogenannte cis-imidazol-Nutline wird zurzeit in klinischen Studien zur Tumorthherapie untersucht. Wir konnten beobachten, dass MDM2 auch in renalen Epithelzellen stark exprimiert wird, beispielsweise in den Tubuluszellen sowie den Podozyten. Um herauszufinden, ob MDM2 regeneratives Zellwachstum fördert, untersuchten wir die Wirkung eines MDM2-Inhibitors, Nutlin-3a, während der tubulären Heilung nach postischämischen akuten Nierenversagen, sowie in den Podozyten nach Adriamycin-induziertem chronischen Nierenversagen.

In Übereinstimmung mit unserer Hypothese konnten wir beobachten, dass der Einsatz von Nutlin-3a nach postischämischen akuten Nierenversagen in C57BL6 Wildtyp-Mäusen die tubuläre epitheliale Heilung verschlechtert. Dieser Effekt war p53-abhängig. Allerdings konnten wir einen zweiten Effekt beobachten, nämlich dass die MDM2-Blockade ebenfalls eine Verringerung der Tubulusnekrose unmittelbar nach Schädigung bewirkte, indem die sterile inflammatorische Reaktion gehemmt wurde. Diesen zweiten Effekt konnten wir ebenfalls in p53-defizienten Mäusen beobachten, was uns schließen lässt, dass es einen zweiten, p53-unabhängigen proinflammatorischen Signalweg von MDM2 gibt. *In vitro*-Experimente bestätigten, dass MDM2 zur mRNA-Expression und Sekretion NF- κ B-abhängiger Zytokine nach Toll-like-Rezeptor-Stimulation benötigt wird, indem die Bindung von NF- κ B an Promoter-Bindestellen verstärkt wird. Folglich verknüpft MDM2 sowohl die Entzündungsreaktion als auch die epitheliale Heilung nach akutem Nierenversagen. Es verstärkt die Entzündungsreaktion unmittelbar nach der Schädigung, fördert dann aber in einer zweiten Phase die Regeneration beschädigter Tubuli. Diesen zusätzlichen biologischen Funktionen muss Beachtung geschenkt werden, wenn eine MDM2-Inhibitionstherapie für die Behandlung des akuten Nierenversagens in Betracht gezogen wird.

Da MDM2 auch in Podozyten stark exprimiert wird vermuteten wir, dass eine MDM2-Blockade während der glomerulären Schädigung die Zahl apoptotischer Podozyten verstärken würde und sich Proteinurie und Glomerulosklerose manifestieren. Die MDM2-Blockade in der frühen Phase der Adriamycin-induzierten Nephropathie in Balb/c-Mäusen hatte jedoch in unerwarteter Weise einen gegenteiligen Effekt und führte zu einer Verringerung der intrarenalen Zytokin- und Chemokinexpression, der Anzahl glomerulären Makrophagen und

T-Zellen, sowie der Kreatinin- und Harnstoff-Plasmaspiegel. Auch in Zellkultur kultivierte Podozyten reagierten nicht mit verstärkter Apoptose, nachdem sie Adriamycin ausgesetzt waren. Vielmehr bewirkte Adriamycin eine Verringerung sowohl abberante Zellkernteilungen als auch des Zelltods aneuploider Podozyten, hier bezeichnet als mitotische Katastrophe (mitotic catastrophe). In Übereinstimmung hierzu bewirkte die MDM2-Blockade einen Anstieg von p21 und verhinderte die Ausbildung von Mitosen *in vivo*, wohingegen TUNEL+ apoptotische Podozyten nicht erkennbar waren. Folglich stellt die mitotische Katastrophe einen bislang unbeachteten Mechanismus für den Verlust von Podozyten dar, in welchem MDM2 die Podozyten zur vollständigen Mitose bewegt. In Abwesenheit der Zytokinese führt dies jedoch zu Aneuploidie und zum Zelltod. Überdies bewirkte die verspätete MDM2-Blockade ebenfalls eine Verringerung der Kreatinin- und Harnstoff-Plasmaspiegel, der Tubulusatrophie, der Leukozyten-Anzahl im Interstitium, der Zytokin-Expression sowie der interstitiellen Fibrose. In Zusammenschau der Erkenntnisse könnte die MDM2-Blockade mit Nutlin-3a einen neuen Therapie-Ansatz für die Prävention von renaler Entzündung, Podozytenverlust, Glomerulosklerose, Proteinurie und fortschreitender Nierenerkrankung darstellen.

Trotz alledem beinhaltet die therapeutische MDM2-Blockade das Risiko einer unvollständigen tubulären Heilung nach akutem Nierenversagen. Auf der anderen Seite könnte es die progressive Zerstörung der Glomeruli stark verlangsamen oder sogar aufhalten und so das chronische Nierenversagen verhindern, indem es die Podozyten direkt vor einem Zelltod durch mitotischen Katastrophe schützt.

Summary

Murine double minute (MDM)-2, an E3 ubiquitin ligase, promotes cancer cell survival and growth, by degrading the cell cycle regulator p53. Antagonism of MDM2 by the small-molecule cis-imidazoline nutlin analogs is currently under study for cancer therapy. We observed that MDM2 is strongly expressed by the epithelial cells in the kidney for example, tubular epithelial cells and podocytes. To test whether MDM2 promotes regenerative cell growth, we studied the effects of MDM2 antagonist, nutlin-3a on tubule cell healing during postischemic acute kidney injury and on podocytes during adriamycin induced chronic renal failure.

Consistent with the hypothesis, we observed that treatment with nutlin-3a impaired tubular cell regeneration during postischemic AKI in C57Bl6 wild-type mice in a p53-dependent manner. However, MDM2 blockade also prevented tubular necrosis by suppressing sterile inflammation during the early postischemic phase. This effect also occurred in *p53*-deficient mice, indicating a second, pro-inflammatory, p53-independent role for MDM2 in AKI. *In vitro* experiments confirmed that MDM2 is required to induce mRNA expression and secretion of NF- κ B-dependent cytokines upon Toll-like receptor stimulation by enhanced binding of NF- κ B to cytokine promoter-binding sites. Thus, MDM2 links inflammation and epithelial healing during AKI. It promotes the inflammatory response after the injury at the same time it drives the regeneration of injured tubular epithelium. Therefore, these additional biological functions need to be regarded when considering MDM2 inhibition therapy in patients with acute renal failure.

Since, podocytes strongly express MDM2, we hypothesized that blocking MDM2 during glomerular injury may enhance podocyte apoptosis, proteinuria and glomerulosclerosis. However, unexpectedly MDM2 blockade in early adriamycin nephropathy in Balb/c mice had the opposite effect and reduced intrarenal cytokine and chemokine expression, glomerular macrophage and T cell counts, plasma creatinine and BUN levels. In cultured podocytes exposed to adriamycin, MDM2 blockade did not enhance podocyte apoptosis but rather prevented aberrant nuclear divisions and death of aneuploid podocytes, i.e. mitotic catastrophe. Accordingly, MDM2 blockade induced p21 and prevented podocyte mitosis *in vivo* while TUNEL⁺ apoptotic podocytes were not detected. Thus, mitotic catastrophe is a previously unrecognized variant of podocyte loss where MDM2 promotes podocytes to complete the cell cycle, which in the absence of cytokinesis, leads to podocyte aneuploidy

and death. Furthermore, delayed MDM2 blockade also reduced plasma creatinine levels, BUN, tubular atrophy, interstitial leukocyte numbers and cytokine expression as well as interstitial fibrosis. Together, MDM2 blockade with nutlin-3a could be a novel therapeutic strategy to prevent renal inflammation, podocyte loss, glomerulosclerosis, proteinuria, and progressive kidney disease.

In conclusion, therapeutic MDM2 blockade may hold the risk of impaired epithelial healing in AKI. On the other hand it may delay or halt the progression of glomerular disorders to CKD by reducing renal inflammation and by directly protecting podocytes from cell death by mitotic catastrophe.

1. Introduction

1.1 Acute Kidney Injury

Acute kidney injury (AKI), formerly known as 'Acute renal failure', is a common and harmful condition occurring with high prevalence in hospitalized patients. The causes of AKI can be pre-renal (hypotension or shock), renal (acute interstitial nephritis, acute glomerular or vasculitic renal diseases; other non-specific conditions like ischemia or toxic injury) and post-renal (obstructive nephropathy). According to the Kidney Disease: Improving Global Outcomes (KDIGO), AKI is defined based on serum creatinine (Scr) and urine output as any of the following:

1. Increase in Scr by $\geq 0.3\text{mg/dl}$ ($\geq 26.5\mu\text{mol/dl}$) within 48hrs; or
2. Increase in Scr to ≥ 1.5 times baseline, which is known or presumed to have occurred within the prior 7 days; or
3. Urine volume $< 0.5\text{ ml/kg/h}$ for 6 hours.

The incidence of AKI in hospitalized patients is reported to be 2-7%, with around 5-10% more in ICU patients¹. Even though there are many advances in the knowledge and strategies to prevent AKI in recent years, the mortality rate remains high in patients of AKI; generally reported to be in the range of 30 to 70% and more than 50% in ICU patients¹. Renal ischemia/reperfusion injury (IRI) often contributes to AKI².

Renal IRI is caused by the impaired oxygen and nutrient supply to the kidney resulting in stress on the tubular epithelial cells. If the stress is severe, then death of these cells occurs either by apoptosis or necrosis resulting in functional impairment of kidney³. The pathophysiology of renal IRI is described in detail below.

1.1.1 Pathophysiology of renal ischemia/reperfusion injury (IRI)

The pathogenesis of IRI is complex. In simple words, ischemia/reperfusion is a pathological condition characterized by an initial restriction of blood supply to kidney followed by the restoration of perfusion and re-oxygenation. The imbalance between demand and supply of nutrients and oxygen results in hypoxia, and surprisingly restoration of the blood flow and re-oxygenation results in profound inflammatory response called reperfusion injury⁴.

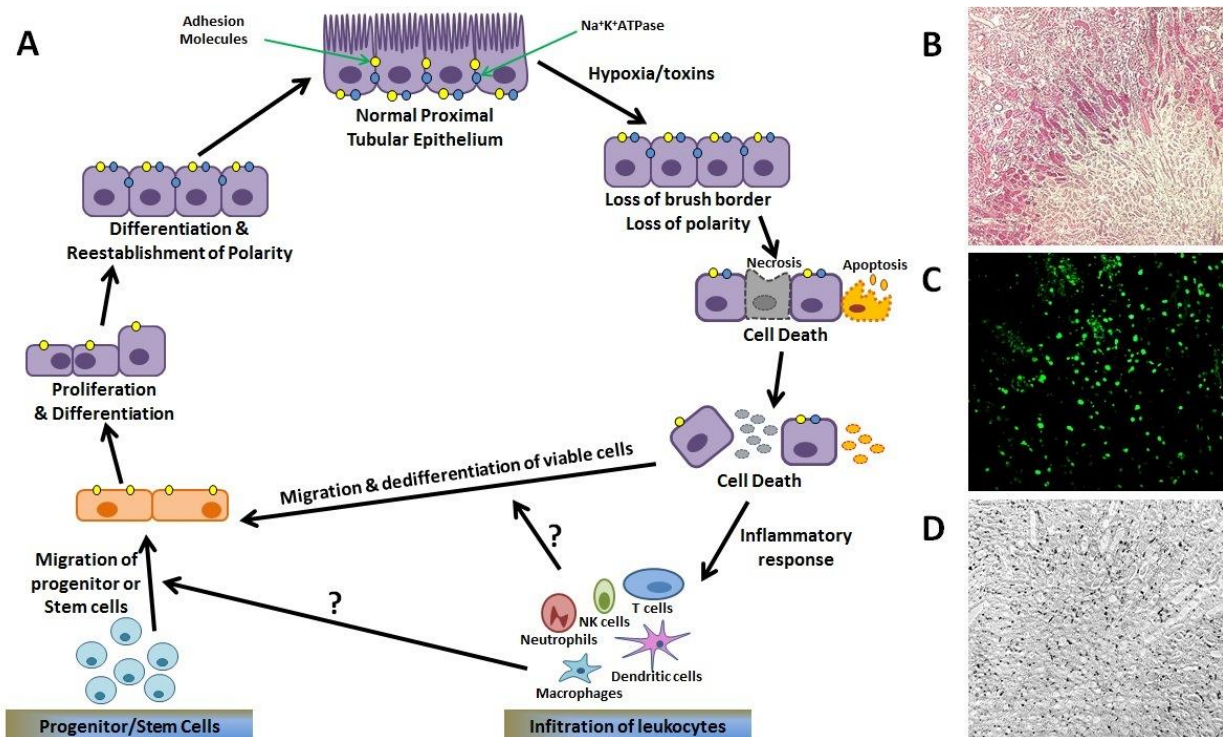


Figure 1 Pathophysiology of IRI A. The normal tubular epithelial cells lose their brush border and polarity upon ischemia reperfusion injury. If the hypoxic conditions remain for a long time, the cells die either by apoptosis or necrosis. This is followed by profound inflammatory response, in which the circulating leukocytes infiltrate into the kidney. Viable epithelial cells or the progenitor or stem cells then migrate and cover the denuded epithelial areas of the basement membrane. These cells then undergo dedifferentiation, proliferation to replace the lost epithelial cells. At last they differentiate to regain the previously lost polarity of the epithelium. (The image is adapted from Bonventre JV *et. al.*³ with modifications) B, C, D. The photographs show various processes occurring in the kidney after IR injury. B. Paraffin-Acid Schiff staining shows the necrosis of tubules. C. TUNEL staining shows the apoptosis of tubules D. Ki67 staining shows the repair process. Ki67 positive cells are enormously increased after the injury.

1.1.1.1 Injury

Epithelial cells in the S3 segment of the proximal tubule are the most affected cells after ischemic insult in the kidney³. Injury to the epithelium results in rapid loss of cytoskeletal integrity and cell polarity⁵. There is shedding of the proximal tubule brush border⁴; loss of polarity along with mislocalization of adhesion molecules as well as membrane proteins such as $\text{Na}^+\text{-K}^+\text{-ATPase}$ and $\beta\text{-integrins}$ ⁶; disruption of cell-cell interactions at adherent and tight junctions². There are also changes in actin localization from apical to lateral cell membrane⁶. Cells undergo apoptotic and necrotic cell death. Some literature describe that tubular cells undergo autophagy to maintain homeostasis and protect themselves against ischemic injury⁷.

When the ability of these cells to undergo autophagy is blocked, the cells accumulate malformed mitochondria and undergo apoptosis.

Injured tubular cells produce kidney injury molecule (KIM)-1 (mainly by proximal tubules) and neutrophils gelatinase-associated lipocalin (NGAL) (mainly by distal tubules). Presence of these proteins in urine has been found to be useful novel noninvasive biomarkers of AKI³.

Renal vasculature also plays an important role in the pathogenesis of IRI since it brings nutrients and oxygen to the epithelial cells. The integrity of vasculature is governed by the endothelium and an injury to endothelial cells as well as subsequent distortion of the peritubular capillary blood flow are characteristics of IRI⁵. The outer medulla of the kidney is at low oxygen tension owing to the countercurrent exchange properties of the vasa recta. Therefore, diminished or impaired blood flow to the outer medulla, due to arteriolar vasoconstriction, leads to death of proximal tubular cells during ischemia³.

Injured endothelial cells further contribute to pathology of ischemic AKI. There are enhanced interactions with the leukocytes due to increased expression of adhesion molecules like ICAM-1 and increased expression of counter receptors on leukocytes⁸. This leads to activation and transmigration of leukocytes, production of cytokines and profound inflammatory response which contributes to AKI³.

Regulation of tubular cell death

The cellular and molecular mechanisms that regulate tubular cell death and regeneration in AKI are not completely understood and remain under debate^{9,10}. A number of intracellular signaling cascades are activated and upregulated during and following a cell injury from ischemia, trauma, toxins, or infections. Ischemic renal injury has been traditionally associated with tubular cell necrosis. Early attempts at preventing and treating ischemic injury were primarily targeted at this "necrotic" phenotype and generally met with moderate success. However, recently apoptosis has emerged as a significant mode of cell death during ischemic renal injury^{11,12}.

p53 is the master regulator of cell cycle and apoptosis¹³. Once activated by a variety of stimuli, like ischemia, radiation etc., it induces cell cycle arrest or apoptosis in response to DNA damage. Several recent studies have shown that the expression of p53 increases in renal parenchymal cells during AKI and this has a detrimental impact on renal tubular regeneration^{9,14-16}.

Furthermore, *Linkermann et.al.* have provided an evidence for a programmed necrosis, termed as ‘necroptosis’, of tubular cells associated with renal IRI. They used necrostatin-1, a highly specific inhibitor of receptor-interacting protein (RIP) kinase 1 which mediates necroptosis and demonstrated that the kidneys treated with necrostatin-1 were protected from renal IRI. Suggesting that necroptosis, a novel form of programmed necrosis, has a functional relevance in pathophysiology of renal IRI and that necrostatin-1 has a potential to prevent or treat renal IRI^{17,18}.

1.1.1.2 Inflammation

Both the innate and adaptive immune responses contribute in the pathology of ischemic AKI. Innate immunity is activated in an antigen independent manner as soon as the injury happens. Infiltrating leukocytes viz. neutrophils, monocytes/macrophages, DCs, NK cells, and natural killer T (NKT) cells fabricate the innate component whereas the adaptive component is constructed by DC maturation and antigen presentation, T lymphocyte proliferation and activation, and T to B lymphocyte interactions.

Innate immunity

Innate immunity orchestrates the pro-inflammatory response during ischemic kidney injury. It is the immediate preprogrammed response to tissue injury which is composed of infiltrating cells (neutrophils) plasma proteins (complement) and physical barriers¹⁹. It has been found that Toll-Like Receptors (TLRs)²⁰ and the reactive oxygen species (ROS)²¹ are the initiators of the innate immune response after ischemic injury.

TLRs belong to the family of pattern recognition receptors (PPRs) which can recognize pathogen derived and non-pathogen derived immunostimulatory molecules²². The TLRs involved in the recognition of nucleic acids (TLR3, TLR7, TLR8 and TLR9) are localized within endolysosomal compartments, whereas other TLR family members (TLR1, TLR2, TLR4, TLR5 and TLR6) are found at the cell surface²³. Amongst all these receptors, TLR2/4 are known to mediate inflammatory responses in the ischemic kidney²⁴.

TLR2/TLR4 are present on both tubular epithelial cells as well as the immune cells. Their expression is increased in the kidney after injury suggesting their participation in the injury^{25,26}. They recognize some of the intracellular molecules that are released during renal

cell death, referred as danger associated molecular patterns (DAMPs) for e.g. histones²⁷, HMGB1²⁸, biglycans²⁹, hyaluronan³⁰, heat shock proteins³¹ etc. and thereby activate the sterile inflammatory response in the injured kidney. Moreover, hypoxia generated by ischemia reperfusion increases TLR4 activation³² and mice with TLR4 deletion are protected from ischemic kidney injury²⁶.

Stimulation of TLR2/4 results in activation of MyD88 dependent signaling pathway. This subsequently activates the transcription factors such as NF- κ B and AP-1 (activator protein-1) through the canonical IKK complex and the MAPK, ERK (extra cellular-signal-regulated kinase), JNK (c-jun N-terminal kinase) and p38 pathway respectively for the transcription of inflammatory cytokine genes³³. In the rested state, NF- κ B proteins are generally present in the cytoplasm in association with their inhibitory protein I κ B. After activation, the I κ B protein is phosphorylated, ubiquitylated and subsequently degraded by the proteasome, allowing NF- κ B complexes to translocate to the nucleus and bind its cognate DNA binding sites to regulate the transcription of a large number of target genes, including genes coding for cytokines, chemokines, stress-response proteins and anti-apoptotic proteins³⁴. Many preclinical studies have shown that inhibition of NF- κ B protected the kidneys from ischemic injury suggesting an important role of NF- κ B signaling in ischemic AKI^{35,36}.

Tubular cells

Tubular cells are not only the victim of the injury but also an active participator in the inflammatory response after the injury. They express the TLRs, complement and complement receptors. They are known to generate several pro inflammatory molecules including cytokines and chemokines such as TNF- α , IL-6, MCP-1, IL-18, TGF- β and RANTES, which then attract the inflammatory cells in the kidney³.

Neutrophils, Lymphocytes, and Macrophages

Neutrophils are referred as a first line of defense, meaning that they are the first defensive cell type to be recruited at the site of inflammation. In accordance with this, a robust influx of neutrophils is also observed in the kidneys after ischemia reperfusion. Upon activation, neutrophils produce number of cytotoxic substances including ROS molecules, such as superoxide anions, hypochloride, hydrogen peroxide etc³⁷. It has been noted that lowering the

infiltration of neutrophils in the injured kidneys, as found in *Icam-1*-deficient mice kidneys and using anti-neutrophils serum injections, protected the kidneys from ischemic renal injury⁸.

T cells are also reported to take part in the ischemic AKI by inducing infiltration of neutrophils in the injured ischemic kidneys. Both the Interferon gamma producing CD4+ T cells³⁸ and B cells are emerging as important contributors in ischemic renal injury. B cell deficiency also protects mice from renal ischemia reperfusion injury³⁹.

Macrophages infiltration occurs several hours after the renal injury. The role of macrophages in ischemic injury is very complex since macrophage activation can either be pro-inflammatory or anti-inflammatory depending on the macrophage phenotype⁴⁰. However, there are evidences suggesting little role of macrophages in tissue injury, although they may be involved in the repair⁴¹.

1.1.3 Repair

Some parts of the kidney have an extensive capacity to undergo regeneration or repair after injury, in contrast to other vital organs like heart or brain. Under normal circumstances the tubular cells divide at very slow rate but upon injury the speed of mitosis raises enormously⁴². Cell proliferation compensates for the loss of tubular cells by cell death.

There is an ongoing debate about whether the cells that replenish the epithelial cell population after injury originate from endogenous surviving epithelial cells, bone marrow stromal cells (BMSCs), or intra-renal progenitor cells. Studies document that the surviving epithelial cells after an ischemic injury spread, dedifferentiate, and migrate to cover the exposed areas of the basement membrane, and then proliferate to restore cell number^{43,44}. Even though some early studies predicted the involvement of bone marrow stromal cells in epithelial repair after injury^{45,46} recent literature rules out their participation in regeneration of post-ischemic kidneys^{44,47}.

To address the involvement of intra-renal progenitor cells in epithelial repair, genetic fate-mapping techniques were employed in transgenic mice and results demonstrated that surviving tubular cells after injury, and not the progenitor cells, participate in post-ischemic regeneration⁴⁴. In another study using the unbiased DNA analog-based approach, it has found that repair of injured proximal tubules does not involve specialized progenitors⁴⁸. However, a recent study from *Angelotti ML et. al.*, identified, with help of the sophisticated techniques

like Microarray and Flow Associated Cell Sorting (FACS), the new progenitor cells population (CD133⁺CD24⁺CD106⁻ cells), residing in proximal as well as in distal convoluted tubules. They have also demonstrated that these cells have the capacity to undergo proliferation and replace the injured tubular epithelial cells after AKI⁴⁹.

Cell cycle and repair

The re-entry of epithelial cells into the cell cycle after an injury has been viewed as a repair response to the loss of adjacent cells after an initial insult, but this has become more complicated with the upcoming literature. It has been observed that the inhibition of epithelial cell cycle, using p21 adenovirus or the drugs like roscovitine and olomoucine, has completely protected the mouse proximal tubular cells in culture from the cisplatin induced apoptosis⁵⁰. The pathophysiology of cisplatin nephrotoxicity is similar to IRI since, cisplatin also causes an extensive necrosis of the proximal tubular cells in the S3 segment⁵¹. It has also been noted that inhibition of cyclin dependent kinases 2/4/6 (CDK2/4/6), the key mediators of cell cycle checkpoint progression from G₁ to S phase, using a broad spectrum of small molecule CDK inhibitors has protected renal epithelial cells from cisplatin induced cell death both *in-vitro* and *in-vivo*⁵². Moreover, mice lacking p21^{CIP} CDK inhibitor exhibited exacerbated kidney ischemic injury, again emphasizing that the cell cycle inhibition protects kidney again IRI⁵³.

However, it should be noted that, the cell cycle arrest of epithelial cells in G₂/M phase induced progressive interstitial fibrosis in the kidney and also increased cell apoptosis⁵⁴. Further, inhibition of CDK2 does not only induce G₁ cell cycle arrest but also blocks the cells in G₂/M or an intra-S phase of the cell cycle⁵⁵. Therefore, even though the inhibition of CDK2 offers early protection from AKI, long term G₂/M arrest would likely be an undesirable long term effect. The more specific inhibitors of CDK are currently in pre-clinical studies to evaluate their efficacy and safety compared to the broad spectrum small molecule inhibitors of CDK.

1.2 Chronic Kidney Disease

Chronic Kidney Disease (CKD) is the gradual and progressive loss of kidney function leading to End stage renal disease (ESRD), which requires renal replacement therapy for survival. Its

Stage	Description	GFR ml/min/1.73m ²	Related Terms
1	Kidney damage with normal or increase in GFR	≥ 90	Albuminuria, Proteinuria, Hematuria
2	Kidney damage with mild decrease in GFR	60-89	Albuminuria, Proteinuria, Hematuria
3	Moderate decrease in GFR	30-59	Chronic renal insufficiency, early renal insufficiency
4	Severe decrease in GFR	15-29	Chronic renal insufficiency, early renal insufficiency, pre-ESRD
5	Kidney failure	<15 (or dialysis)	Renal failure, uremia, end-stage renal disease

Table 1 Severity of kidney disease (adopted and modified from Levey *et. al.*⁵⁶)

definition is based on the decline in glomerular filtration rate (GFR) and kidney damage with the increase in proteinuria (urine albumin/creatinine ratio). KDIGO defines CKD⁵⁶ as follows:

1. Kidney damage or GFR < 60 mL/min/1.73 m² for 3 months or more, irrespective of cause; or
2. Albumin-to-creatinine ratio > 30mg/g in two of the three spot urine specimens.

Kidney disease severity is classified into five stages according to the level of GFR (Table 1).

The CKD affects 14 to 15% of the adult US population and is projected to increase by 50% in the next 20 years⁵⁷. The causes of CKD are diabetes, obesity, hypertension, medications and infections. Amongst different forms of CKD, progressive glomerulosclerosis accounts for the vast majority of cases. Focal segmental glomerulosclerosis (FSGS) is one of the most common forms of acquired glomerular disease leading to ESRD. It accounts for 20% cases of the nephrotic syndrome in children and 40% of such cases in adults⁵⁸.

1.2.1 Focal Segmental Glomerulosclerosis

Focal segmental glomerulosclerosis (FSGS) is not a single disease but is a clinicopathological syndrome sharing a common glomerular lesion. It is mediated by diverse insults directed to or inherent within the podocyte. Hence also referred as a podocyte disease or a podocytopathy⁵⁹. An injury to podocytes leads to effacement of podocyte foot processes leading to proteinuria and glomerulosclerosis⁶⁰. In spite of the name the lesions of FSGS are not always focal, segmental or sclerotic.

1.2.2 Pathogenesis of FSGS

Loss of glomerular filtration barrier

Glomerular filtration barrier is responsible for regulating the efficient filtration of around 180 liters of blood every day in the kidney. Glomerular filtration barrier comprises of fenestrated glomerular endothelial cells (inner blood interface), glomerular basement membrane (GBM) (at the center), and highly differentiated and polarized epithelial cells called 'podocytes' (outer urinary interface)⁶¹ (Figure 2).

Podocytes

Podocytes are terminally differentiated glomerular visceral epithelial cells. They resemble to neurons in their large cell body and elongated cellular extensions, which are known as foot processes. These foot processes extend around the capillary loop to cover the GBM. They also interdigitate with neighboring podocytes by slit diaphragm⁶². A slit diaphragm is a zipper like structure which provides most important size-selective sieve of glomerular filtration barrier⁶². These terminally differentiated cells cannot undergo cell division and repair/regeneration, making podocyte depletion through detachment, apoptosis, or necrosis a critical mediator of glomerulosclerosis⁶³. This means, the structural and functional alterations in the podocyte and its slit diaphragm are important in the pathogenesis of FSGS and other glomerular diseases.

Several experimental models have addressed whether podocyte depletion or specific podocyte injury is sufficient to induce FSGS^{60,64,65}. The data from these studies suggests that the degree of podocyte depletion positively correlates with the severity of the disease. Loss of more than 20% podocytes leads to overt FSGS indicating the disease threshold.

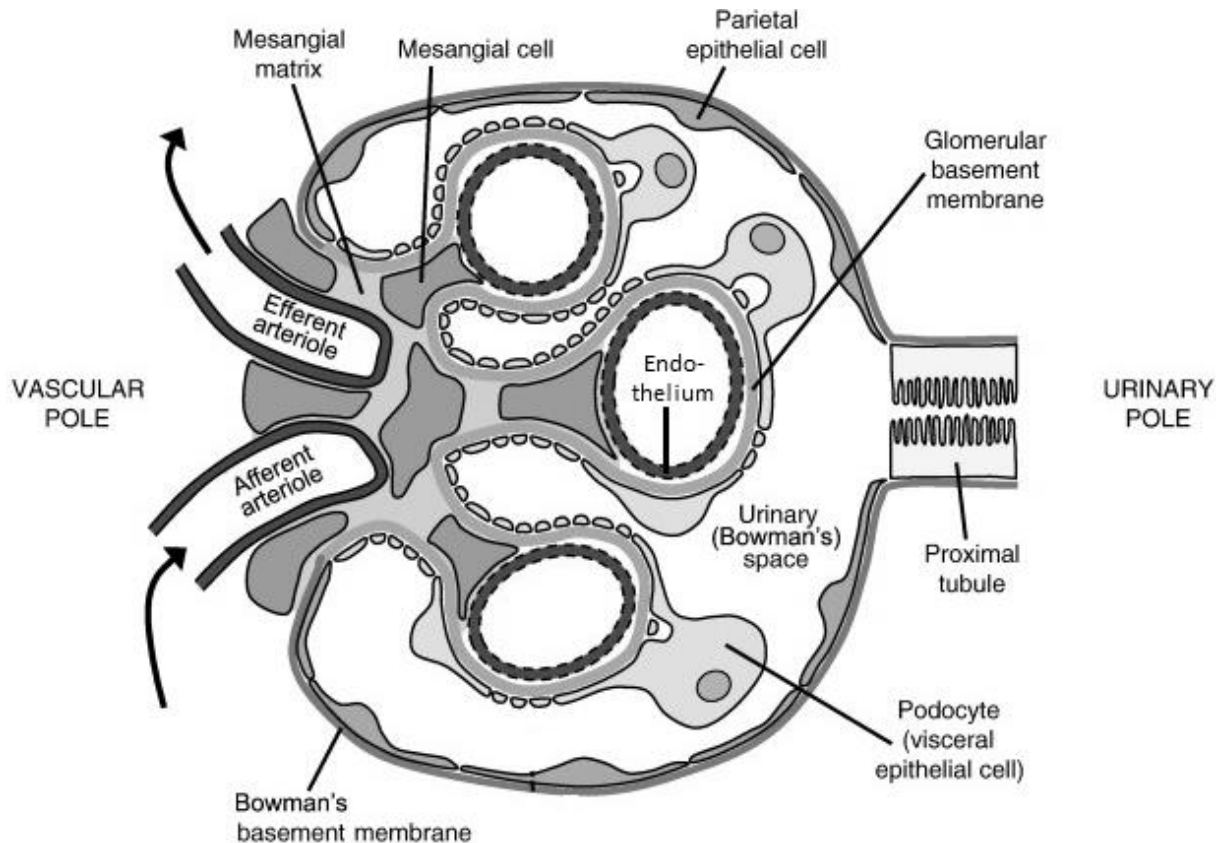


Figure 2 Schematic representations of glomerulus and glomerular cells The glomerular filtration barrier comprised of fenestrated glomerular endothelial cells, glomerular basement membrane and podocytes. The parietal epithelial cells are present along the Bowman's basement membrane. (The image was adapted and modified from Leeuwis J.W. *et. al.*⁶⁶)

Glomerular basement membrane (GBM)

The basement membrane of the glomerular capillaries (GBM) is much thicker than the basement membrane in other vascular beds⁶⁷. It is assembled through an interweaving of type IV collagen with laminins, nidogen, and sulfated proteoglycans. Mutations of the genes encoding these components of GBM cause glomerular disease in both humans and mice⁶⁸. For e.g. mutations in collagen chains leads to Alport's syndrome, a hereditary glomerulonephritis⁶⁹. Studies in *laminin β2*-knockout mice have revealed that proteinuria appeared before any structural alterations in podocytes were observed⁷⁰, suggesting that alterations in GBM may lead to proteinuric nephrotic syndrome. However, the loss of normal GBM structure might cause alterations in the functions of podocytes and endothelial cells leading to proteinuria and glomerulosclerosis⁷¹.

Glomerular endothelial cells and Glomerular Mesangium

The glomerular endothelial cells have a high density of fenestrae. The size of fenestrae is usually larger than the size of albumin, suggesting that the endothelial cells do not contribute to permselectivity of the glomerular filtration barrier. However, they do have charge-selective properties and the barrier probably begins at the endothelial level⁶⁷. Glomerular mesangium is composed of mesangial cells and the mesangial matrix, produced by mesangial cells. Primary function of mesangium is to maintain structure and function of glomerular filtration barrier, but their overall contribution to permselectivity is very less⁶⁷.

Parietal epithelial cells

So far the main focus of all the studies on glomerular disease was on the constituents of glomerular filtration barrier. However, in recent years, several studies have demonstrated that PECs are involved in the extracapillary proliferation, inflammation and in the development of FSGS⁷². *Smeets et. al.* have studied the development of FSGS in Thy-1.1 transgenic mice, which expresses the mouse Thy-1.1 antigen on podocytes. They observed that an injection of monoclonal antibody directed against the Thy-1.1 antigen have induced FSGS lesions with prominent epithelial cell hyperplasia⁷³.

Genetic susceptibility

Mutations in the genes which are involved in the nephrotic syndrome viz. NPHS1, NPHS2, ACTN4, CD2AP and WT1, TRPC6, LAMB2 (coding for proteins like nephrin, podocin, α -actinin-4, an adapter protein anchoring CD2 and others), have been found in two third of the patients with FSGS who present in the first year of life⁷⁴. It has been found that the mutations in nephrin and podocin are the most frequent causative mutations of FSGS compared to defects in other podocyte specific genes. Disruption or dysregulation of signaling through these genes leads to foot process effacement, loss of podocytes and glomerulosclerosis⁶¹.

Pathogenesis of glomerulosclerosis

Glomerulosclerosis is the scarring (sclerosis) of the glomeruli. It is caused by activation of the glomerular cells to produce scar material. This is stimulated by the factors which are either produced by these cells themselves or are brought to the glomerulus by circulating blood

which enters the glomerular filter⁷⁵. Podocyte loss through apoptosis or detachment into urinary space is a central determinant of progression to glomerulosclerosis^{76,77}. Accordingly, experiments have shown that replacement of podocytes (either recovery or repair) contributes to the regression of glomerulosclerosis^{78,79}.

There have been many evidences in recent years indicating that the epithelial cells lining the Bowman's capsule, called parietal epithelial cells, plays an important role in scarring. They undergo proliferation; produce extracellular matrix molecules like fibronectin, collagen as well as some other profibrotic growth factors⁸⁰. They also produce chemokines like MCP-1, MIP-1 and IL-8 and therefore direct the leukocyte infiltration in the injured glomerulus⁸¹.

1.2.3 Mechanisms of Podocyte death

How does the glomerular epithelial sheath compensate for podocyte injury? Generally, differentiated podocytes cannot complete mitotic cell divisions by cytokinesis because this would require to completely reorganizing their actin cytoskeleton which is not compatible with maintaining secondary foot processes and the slit membrane⁸². But, as a mechanism of compensatory growth, they can enter the S-phase of the cell cycle for enhanced DNA synthesis to undergo hypertrophy^{82,83}. The p53-dependent induction of cyclin kinase inhibitors such as p21 protects podocytes from passing the cell cycle restriction point of the G2/M phase which otherwise would lead to a process named "mitotic catastrophe"⁸⁴⁻⁸⁸. Mitotic catastrophe is defined as "cell death during mitosis" by an incomplete assembly of the chromosomes and the mitotic spindle in the pro-metaphase which then leads to aberrant chromosome segregation⁸⁷. Such cells die either immediately within mitosis or shortly after via apoptosis or necrosis⁸⁹. Morphologic features of mitotic catastrophe include multiple nuclei, micronuclei or irregularly shaped nuclei^{85,87}.

However, damaged podocytes also produce tumor necrosis factor (TNF)- α which triggers podocyte loss and progressive glomerulosclerosis by activating the extrinsic apoptosis pathway⁹⁰. Environmental factors that activate glomerular macrophages in-situ to secrete TNF- α enhance this mechanism⁹¹⁻⁹⁴ which can be blocked with etanercept to prevent TNF- α induced podocyte apoptosis and the progression of experimental CKD⁹⁰. Thus, the relative contribution of apoptosis versus mitotic death to podocyte loss is not known.

1.2.4 Inflammation in FSGS

An inflammatory response follows after tissue injury, irrespective of the underlying cause, leading to either tissue repair or progressive fibrosis with a loss of function⁹⁵. The earlier stages of FSGS are characterized by a glomerular damage in conjunction with heavy proteinuria which then extends to a prominent tubulointerstitial injury. The later phase is associated with tubular atrophy, vacuolization and fibrosis (Figure 3). There is a marked mononuclear inflammatory cell infiltration (neutrophils, macrophages, mast cells, lymphocytes and dendritic cells etc.) in either phase of the disease^{96,97} (Figure 4). Both renal and systemic levels of the inflammatory cytokines (IL-1, IL-6, IL-8, TNF- α , MCP-1 etc.) are also increased^{96,98}.

NF- κ B and FSGS

The NF- κ B transcription factors are one of the major regulators of the pro-inflammatory gene expression. Synthesis of cytokines like IL-1 β , IL-6, IL-18, and TNF- α is mediated by NF- κ B⁹⁹. The activation of NF- κ B has pathogenic roles *in vivo*. *Rangan GK et. al.* have demonstrated that the renal expression of NF- κ B increases progressively up to four weeks after adriamycin injections. They further demonstrate that this increase was correlated with the degree of proteinuria, inflammatory cells infiltrates and tubular atrophy¹⁰⁰. These authors along with many others have shown that inhibition of NF- κ B protected kidneys from adriamycin induced FSGS^{100,101}. It has also been observed that the renal cortical and tubular cell CC chemokines, including MCP-1, RANTES, and MIP-1 α were up-regulated via mediation of NF- κ B, and contributed to FSGS by attracting inflammatory cells into the interstitium¹⁰². Blockade of the CC chemokine receptor, CCR1 substantially reduced interstitial leukocyte accumulation and the subsequent renal fibrosis in murine model of FSGS⁹⁷. Therefore, in conclusion, the activation of NF- κ B has an important role in mediating interstitial monocyte infiltration and tubular injury in nonimmune proteinuric tubulointerstitial inflammation.

Leukocytes and FSGS

Several studies have demonstrated that the infiltrating leukocytes, mainly macrophages and T cells play a pivotal role in the pathogenesis of FSGS¹⁰³⁻¹⁰⁵. Macrophages have heterogeneous phenotypes; subpopulations of macrophages (M1), known as 'classical macrophages', have

pathogenic function in renal inflammation and other M2 macrophage subpopulation, known as 'alternative macrophages' have renoprotective function in resolution of inflammation and renal repair after injury¹⁰⁶.

To study the influence of macrophages on FSGS, Wang *et. al.* have isolated macrophages from spleens of Balb/c mice and transformed them into M1 and M2 phenotype by treatment with either LPS or IL-4, IL-13 respectively, before infusing them into mice with FSGS. They have observed that, mice infused with M1 macrophages exhibited aggravated FSGS whereas mice infused with M2 macrophages were protected from FSGS⁹⁴. In other independent studies, researchers have induced M2 macrophages *in-vivo* using cytokines like IL-25 and have shown that the phenotype change of macrophages from M1 to M2 protected the kidneys from adriamycin induced FSGS¹⁰³. It has also been observed that M2 macrophages induced the regulatory T cells in the lymph nodes draining the kidneys in adriamycin nephropathy (AN), which protected kidneys from FSGS¹⁰⁴. Further, Wang *et. al.* have recently found that these protective regulatory T cells in AN express CD39, an ecto-enzyme that degrades extracellular nucleotides, such as ATP, which is essential for the protective function of regulatory T cells during adriamycin induced FSGS¹⁰⁵.

Complement system and FSGS

The role of complement system in renal diseases has long been recognized. Complement system is critical in mediating not only host defense but also tissue injury, both in glomerulus and tubulointerstitium. Complement is activated as a result of proteinuria and contributes to fibrosis, scarring and progressive kidney disease. Irrespective of the pathways of complement activation in different diseases, the downstream injury is mainly mediated by C5 activation, a common mechanism in disease pathogenesis¹⁰⁷.

Several recent *in-vivo* studies have demonstrated that the intact alternative pathway of complement and its activation is critical for the progression of FSGS^{108,109}. They observed that mice deficient in complement component of alternative pathway for e.g C3, factor D are protected from adriamycin induced FSGS¹⁰⁹. Moreover, an inhibitory monoclonal antibody to factor B, another component of alternative pathway, delayed the development of adriamycin induced renal injury¹⁰⁸. On the other hand, mice deficient in C1q and CD59 complement components of the classical pathway, developed similar or aggravated disease compared to the wild-type mice¹⁰⁹.

1.2.5 Adriamycin nephropathy: a model of FSGS

Adriamycin nephropathy (AN) is a well-established animal model, which is analogous to human FSGS. This model has enabled a greater understanding of the processes underlying FSGS. The successful induction of this model depends on the species, strain, gender and age of the animals as well as on source and batch of adriamycin. The Balb/c mice are highly susceptible to AN whereas C57BL/6 mice are highly resistant. This strain specific susceptibility has been linked to the single gene locus with recessive inheritance on chromosome 16¹¹⁰. The susceptibility alleles at this locus are associated with blunted expression of protein arginine methyltransferase on chromosome 8, a protein implicated in cellular sensitivity to chemotherapeutic agents¹¹⁰.

Adriamycin, an anthracyclin antibiotic, is one of the most important anticancer agents. It is a DNA intercalating agent, which inhibits the enzyme topoisomerase II and thereby generates free radicals, which induce DNA damage and subsequent cell death¹¹¹. Studies have shown that adriamycin induces cell death by two mechanisms depending on the concentration used. For example, at high doses it induces cell death by apoptosis and at low doses by mitotic catastrophe¹¹², where cells with significant DNA damage undergo mitosis but are unable to complete it. Thus, when administered intravenously at an optimum concentration, adriamycin induces injury by direct toxic damage to the glomerulus. This direct damage to the kidney by adriamycin have been validated by clamping of a renal artery of one kidney before adriamycin injection. It was observed that, this procedure protected the clamped kidney from adriamycin induced FSGS¹¹³.

Adriamycin causes thinning of glomerular endothelium and podocyte effacement associated with loss of barrier to filtration of plasma proteins in urine (proteinuria), occurring as early as one week after adriamycin injection and becomes severe by four weeks¹¹⁴. The histological changes show podocyte fusion, focal segmental and global glomerulosclerosis¹¹⁵ (Figure 3A-3F), followed by tubulointerstitial injury (Figure 3H-3K). This is associated with a severe glomerular as well as tubulointerstitial inflammation as seen by marked increase in T and B lymphocytes and macrophages in the kidneys^{110,115} (Figure 4). Adriamycin is known to activate NF- κ B through I κ B specific kinase (IKK) complex which regulates the pro-inflammatory gene expression¹¹⁶.

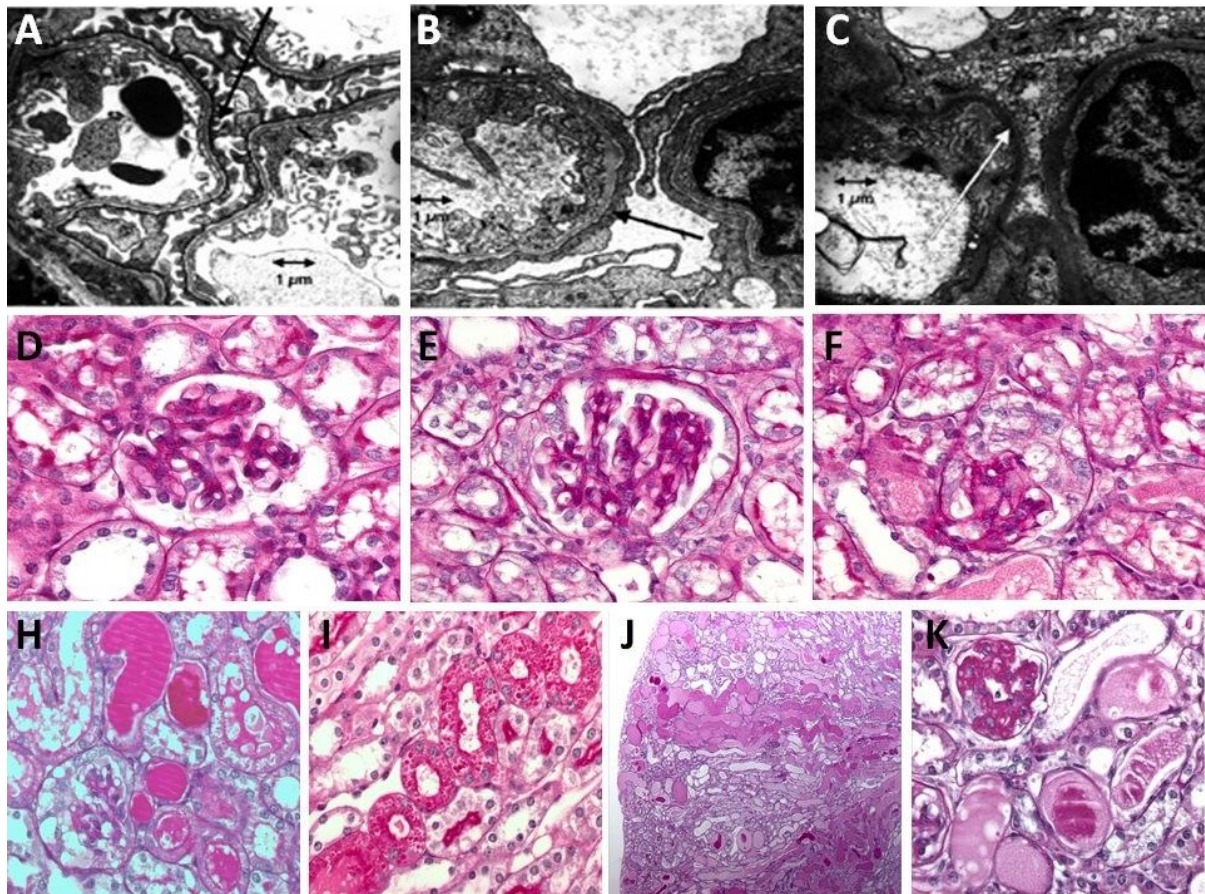


Figure 3 Pathogenesis of FSGS A,B,C: Electron micrographs of glomeruli. A. Podocyte foot processes are normal in control mice. B. Two weeks after adriamycin injection they become fused. C. Six weeks after adriamycin injection they disappear. Black arrow represents foot processes and white arrows represent denuded basement membrane. (These images are adapted from Lee WV et. al.¹¹⁰). D,E,F : PAS staining of glomerular lesions. D. Control mouse showing no lesions. E. Glomeruli showing segmental lesions. F. Glomeruli showing global lesions. H & I. PAS staining of tubular injury. Tubules get damaged as early as week 2 after adriamycin injection. H. Damages tubular containing either urine or protein casts. I. A damaged nephron from a damaged glomerulus. J & K. PAS staining of tubular injury. Tubular atrophy and increased protein or urine casts occur in the kidney four weeks after adriamycin injection. J. Lower magnification image representing the extent of tubular damage with proteinuria at week 4. K. Higher magnification image showing a globally sclerosed glomerulus surrounded by a necrotic tubule also containing protein or urine casts.

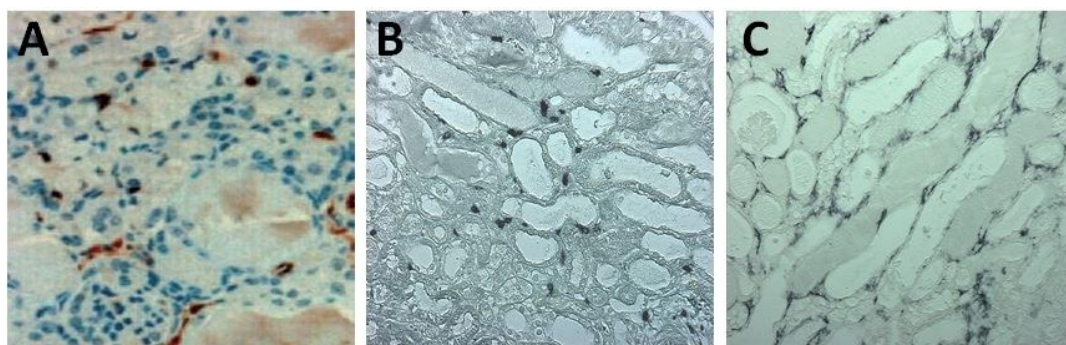


Figure 4 Inflammation in FSGS Adriamycin treated kidney shows accumulation of A. CD45+ Leukocytes (image taken from Vielhauer V. et. al.⁹⁷) B. CD3+ T lymphocytes C. F4/80 Macrophages after adriamycin injections.

Pros and cons of AN as an experimental model of CKD

AN has several strengths as an model of CKD, viz¹¹⁰.

1. It is highly reproducible and robust model of renal injury, with severe degree of tissue injury associated with acceptable mortality (< 5%) and morbidity (weight loss).
2. The timing of the injury is consistent and predictable making it a best suited model to study the interventions which either protect or worsen the kidney injury.
3. The nature of injury is exactly similar to the chronic proteinuric renal disease in humans.

There are also limitations to use this model, viz¹¹⁰.

1. Adriamycin has a narrow therapeutic index whereby doses as little as $\pm 0.5\text{mg/kg}$ results in either no injury or toxicity leading to death.
2. Batch-to-batch variability occurs whereby certain batches of adriamycin cause less severe injury than others.

1.3. Murine Double Minute (MDM)-2

Murine double minute (MDM)-2 is an intracellular protein with oncoprotein functions. It was originally identified in a spontaneously transformed mouse Balb/c cell line (T3T-DM)¹¹⁷. Later it was shown to interact with p53 and inhibit its transcription¹¹⁸. Since then MDM2 has evolved as a potential target for anticancer therapy.

MDM2 is considered to be a valuable for a variety of reasons:

1. MDM2 is an E3 ubiquitin ligase that negatively regulates p53 mainly by ubiquitin-mediated degradation, thereby suppressing coordinated cell cycle arrest or apoptosis and promoting cell survival and growth¹¹⁹.
2. Cell type-specific deletion of MDM2 recovers p53 and induces cell type-specific cell death¹²⁰.
3. MDM2 is strongly expressed in many malignancies with wild-type p53 as an alternate mechanism to disrupt the p53 pathway in early cancer development^{121,122}.

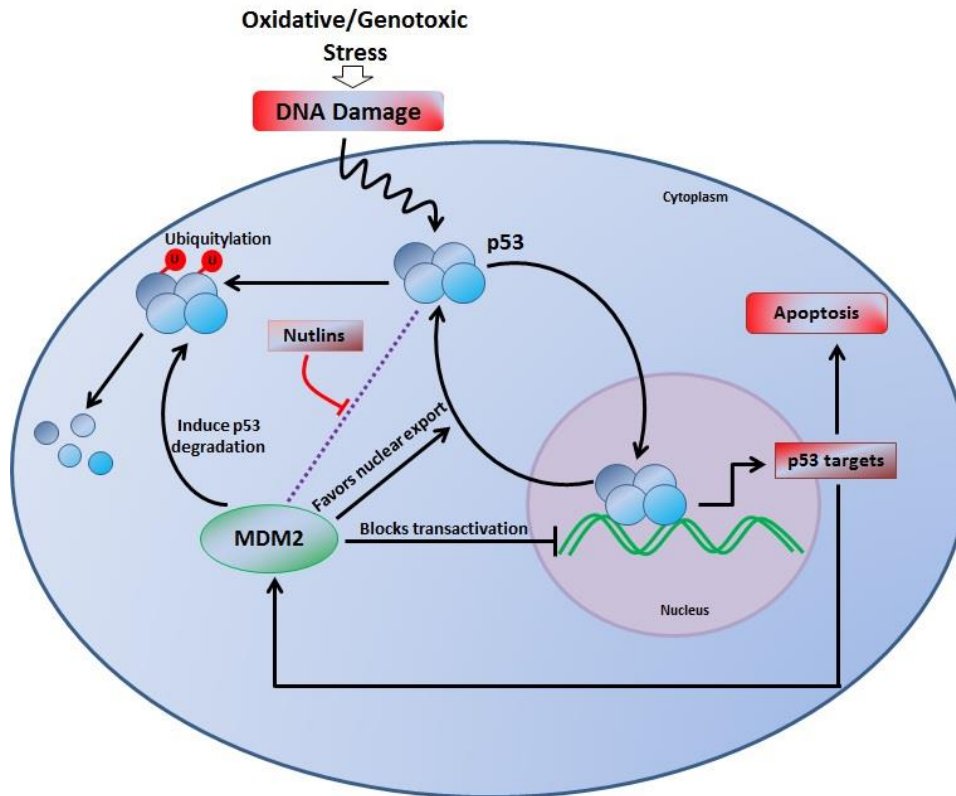


Figure 5 Regulation of p53 by MDM2 p53 and MDM2 form an auto-regulatory feedback loop. p53 expression is increased upon DNA damage by oxidative or genotoxic stress, which in turn increase the expression of MDM2. MDM2 negatively regulates p53 in at least three different ways, i.e. (1) MDM2 functions as the E3 ubiquitin ligase promoting ubiquitin-dependent proteosomal degradation of p53, (2) MDM2 facilitates nuclear export of p53 into the cell cytoplasm, moving p53 away from its site of action and (3) MDM2 interacts with p53 transcription activation domain, thus inhibiting p53 transcriptional activity.

4. MDM2 overexpression is linked to gain-of-function mutations in many tumors¹¹⁹.
5. MDM2 blockade with suitable antagonists was shown to block tumor growth in a number of animal models¹²³.

As such a clinical trial is currently ongoing to study the effects of the MDM2 antagonist RO5503781, in advanced malignancies other than leukemia (www.clinicaltrials.gov).

MDM2 has emerged as a valuable therapeutic target mainly because of the auto-regulatory feedback loop between p53 and MDM2 in various tumor cells¹²³. However, recent data have shown that MDM2 has a number of p53-independent effects¹²⁴. The p53 dependent and p53 independent actions of MDM2 are discussed below.

1.3.1 The classical p53-dependent role of MDM2 on cell cycle control

MDM2 is an oncoprotein, which negatively regulates tumor suppressor protein p53. p53 is one of the central regulators of cell cycle. It is activated upon cellular or genotoxic stress leading to quiescence, senescence or death of cells with DNA damage, therefore avoiding aberrant mitosis and carcinogenesis. Once activated p53 accumulates in the nucleus and being a transcription factor, it activates many genes specific for above mentioned functions of p53. At the same time, p53 also stimulates the expression of MDM2¹²⁵.

Activated MDM2 inhibits functions of p53 by three main pathways¹²⁵: (Figure 5)

1. It blocks transcriptional activity of p53
2. It favors nuclear export of p53
3. Being an E3 ubiquitin ligase, it stimulates degradation of p53

This is how MDM2 and p53 form a tightly regulated negative feedback loop in which activated p53 up-regulates MDM2 expression which in turn will target p53 for degradation¹²⁵⁻¹²⁷.

This regulation of p53 by MDM2 in normal tissues is very essential, since p53 over-expression results in dramatic apoptosis in multiple organs¹²⁸. Moreover, MDM2 deficiency leads to p53-driven, uncontrolled cell death already during embryonic development. This phenotype can be entirely rescued by concomitant deletion of p53¹²⁹. On the other side, MDM2 gene duplication or hyperactivation eliminates p53-mediated growth control of cells with significant DNA damage, which supports tumorigenesis¹²⁷. Upon genotoxic or cytotoxic stress p53 and MDM2 are activated by phosphorylation and acetylation on specific sites resulting in their dissociation, p53 stabilization and consequent transcriptional up-regulation of p53 target genes leading to cell cycle arrest, DNA repair or apoptosis¹³⁰.

The interactions between MDM2 and p53 are affected by several other factors as well. For example, DNA damage activates ARF which binds to MDM2 and inhibits MDM2-mediated ubiquitination and degradation of p53, leading to stabilization of p53¹³¹. Some ribosomal proteins induced after ribosomal stress acts in the same manner¹³².

Interestingly, MDM2 can also promote p53 mRNA translation thereby acting as a p53 enhancer rather than p53 inhibitor¹³³.

1.3.2 p53-independent roles of MDM2 in carcinogenesis

There is growing evidence that MDM2 has a number of p53-independent functions in cell cycle regulation, differentiation, transcription, or DNA synthesis^{124,126}. Many of these p53-independent MDM2 roles foster cell transformation and tumorigenesis. MDM2 has been found to be overexpressed in tumors expressing both wild type and mutated p53^{121,127}. This suggests that up-regulated MDM2 on its own has an additional growth advantages independent of p53.

For example, estrogen-induced breast cancer cell proliferation requires a p53-independent MDM2-mediated pathway to activate cell proliferation and p53 is not the key target of MDM2¹³⁴. MDM2 also interacts with Rb, E2F1, MTBP, Smads etc. that play a key role in cell cycle regulation and seem to contribute to MDM2's oncogenic effects independently of p53^{124,126}. Furthermore, p53 is also not required for MDM2 to promote the translation of the anti-apoptotic protein XIAP which accumulates in cancer cells and supports their resistance to radiation therapy¹³⁵. Interestingly, there is a report, which demonstrates tumor suppressive properties of MDM2. They document that the *p53/Mdm2*-double deficient mice had shorter tumor latency compared to *p53*-null mice with MDM2 expression retained¹³⁶.

MDM2 promotes cancer cell mobility via protein-protein interaction with non-metastatic cells 2 protein (NME2). MDM2 overexpression suppresses NME2-mediated inhibition of cell motility¹³⁷. MDM2 is also known to negatively regulate IGF1-R which protects cells from DNA-damage-induced apoptosis thus allowing transformed cells to undergo apoptosis, independent of p53¹³⁸.

Together, p53-dependent and -independent effects of MDM2 mostly promote the proliferation of cells with DNA damage, tumor growth, and metastasis.

1.3.3 Inhibitors of p53-MDM2 interactions

Restoring p53 activity by inhibiting the interaction between p53 and MDM2 represents an attractive approach for cancer therapy. Two classes of MDM2 antagonists have been reported, low molecular weight compounds and small peptides. To date, the most studied chemotypes amongst the low molecular weight compounds have been cis-imidazolines (e.g., nutlins), benzodiazepines (BDPs) and spiro-oxindoles¹³⁹. The cis-imidazolines (nutlins-1, 2 and 3) are the first to be reported as potent and selective small molecular inhibitors of p53-MDM2

interaction¹³⁹. Nutlin-3 is the most potent amongst all. It is a racemic mixture of nutlin-3a (active enantiomer) and nutlin-3b (inactive enantiomer).

The crystal structure based analysis revealed that a relatively deep p53 binding pocket is present on the surface of MDM2 and nutlins bind to this pocket competing with p53 and thus inhibiting MDM2 mediated degradation of p53¹⁴⁰. Among all of the available inhibitors of p53-MDM2 interactions only nutlin-3 and MI-219 have excellent pharmacokinetic profile. A detailed analysis of pharmacokinetics of nutlin-3a has been performed in mice after both intravenous and oral administration. This study demonstrated that nutlin-3a shows rapid absorption, high bioavailability and saturable elimination kinetics¹⁴¹.

1.3.4 Toxicity of MDM2 inhibitors to normal tissue

One critical concern in the development of MDM2 inhibitors is their potential toxicity to normal tissues. This concern was intensified after the study which showed that p53-MDM2 interactions are important in normal cells as well. Moreover, p53 activation in the absence of the MDM2 gene causes severe toxicity to radiosensitive normal adult mouse tissues, leading to rapid animal death¹²⁸. However, nutlin-3a and MI-219 showed little toxicity to animals at therapeutically efficacious dose regimen¹⁴².

1.4. Role of proliferation in kidney injury and repair

1.4.1 Role of proliferation in AKI

As mentioned earlier cell proliferation balances the loss of tubular cells by cell death after acute kidney injury (Figure 1A, 1D). Upon injury tubular cells start dividing at increased rate to replace the damaged tissue⁴². Thus, a rapid proliferative response ultimately leading to restoration of normal structure and function of the nephron is the cellular hallmark of kidney repair⁴⁴. The origin of the cells that replace the injured tubular epithelia is not known, though several reports suggest the intra-renal origin^{44,143}.

Humphreys et. al. had generated transgenic mice, using genetic fate mapping technique, in which 94%–95% of tubular epithelial cells, but no interstitial cells, were labeled with either b-galactosidase (lacZ) or red fluorescent protein (RFP). They observed that, two days after IRI, 50.5% of outer medullary epithelial cells co-express Ki-67 and RFP, indicating that differentiated epithelial cells that survived injury undergo proliferative expansion⁴⁴. They also

observed that after complete recovery, 66.9% of epithelial cells had incorporated BrdU, compared to only 3.5% of cells in the uninjured kidney⁴⁴. In a very similar approach, *Lin et al.* have produced transgenic mice that expressed enhanced GFP (EGFP) specifically and permanently in mature renal tubular epithelial cells. They also observed that, following IRI, EGFP-positive cells showed incorporation of BrdU and expression of vimentin¹⁴³. Both of these studies strongly support the idea that the surviving tubular epithelial cells after the injury undergo proliferation or regeneration to replace the injured tubular epithelial cells after AKI in the adult mammalian kidney.

Before confirmation of the above described mechanism of renal repair, several lines of reports suggested that the bone marrow derived cells or hematopoietic stem cells differentiate into tubular epithelial cells and undergo proliferation to replace the injured tubular epithelial cells^{45,46}. *Lin et al.* transplanted hematopoietic stem cells that express beta galactosidase constitutively from male mice into female mice which underwent IRI. Four weeks after HSC transplantation, beta-galactosidase-positive cells (male origin) were detected in renal tubules of the recipients by X-Gal staining (female mice)⁴⁶. In another study, *Kale et al.* demonstrated that $\text{Lin}^- \text{Sca-1}^+$ cells from the adult mouse bone marrow are mobilized into the circulation by transient renal ischemia and home specifically to injured regions of the renal tubule. There they differentiate into tubular epithelial cells and proliferate to replace the injured epithelial cells. Post-recovery analyses in these mice revealed that majority of the new cells in the necrotic tubules are derived from $\text{Lin}^- \text{Sca-1}^+$ cells⁴⁵. Even though the current literature rules out the direct involvement of these cells in renal regeneration, it is noteworthy that there are some paracrine interactions between these cells and renal epithelial cells which in turn stimulate renal cell proliferation and thus regeneration after injury¹⁴⁴.

There are also evidences for the involvement of renal progenitor cells in the tubular regeneration¹⁴⁵. *Maeshima et al.* have demonstrated that the BrdU label retaining cells (LRC) undergo asymmetrical cell division after kidney injury and most of them become positive for proliferating cell nuclear antigen (PCNA), whilst the PCNA-positive but BrdU-negative tubular cells are rarely observed, suggesting that cells proliferating during tubular regeneration are essentially derived from LRC¹⁴⁵. In a recent study, *Angelotti ML et al.* have demonstrated that a new renal progenitor cell type, characterized as $\text{CD133}^+ \text{CD24}^+ \text{CD106}^-$, have the capacity to undergo proliferation and replace the injured tubular epithelial cells after AKI⁴⁹. These reports suggest that renal progenitor cells actively proliferate and eventually differentiate into epithelial cell, during tubular regeneration.

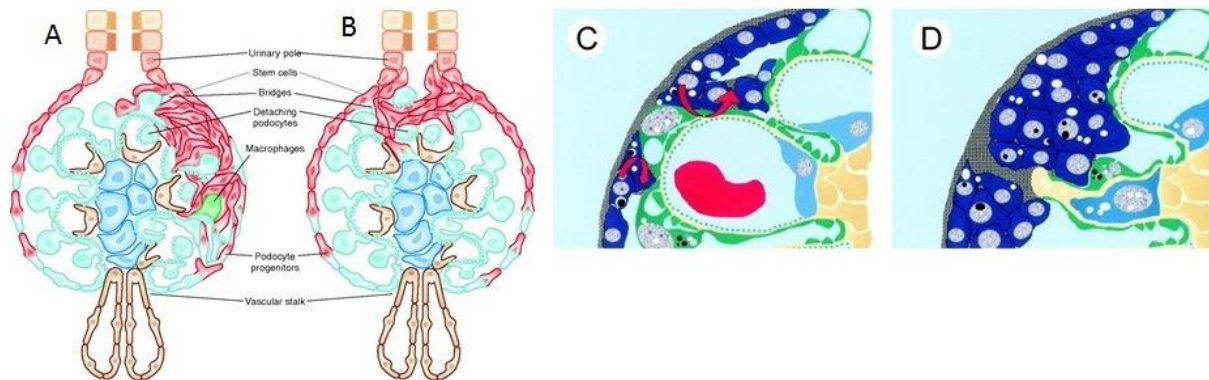


Figure 6 Role of proliferation in glomerulosclerosis A,B. Aberrant proliferation of glomerular epithelial stem cells generates hyperplastic lesions. A. After massive podocyte injury, glomerular epithelial stem cells (red) generate cell bridges with the glomerular tuft in several areas of the glomerulus to quickly replace lost podocytes (light blue). However, numerous areas of podocyte injury distort glomerular structural integrity, thus altering the polarity of glomerular epithelial stem cell division and initiating their abnormal proliferation and the development of extracapillary hyperplastic lesions as well as crescents. Macrophages (green) can also be included within the lesions. Similar processes might occur in crescentic glomerulonephritis and collapsing glomerulopathy. B. Replacement of podocytes under physiologic conditions follows a gradient, with neopodocytes progressively added at the vascular stalk. Thus, the tip podocytes represent the “oldest” podocytes of the glomerular tuft, which suggests they might be more susceptible to injury related to heavy proteinuria. Glomerular epithelial stem cells may also proliferate and migrate from the urinary pole of the Bowman's capsule toward the tuft in an attempt to replace the podocytes lost in response to heavy proteinuria, and generate the tip lesion. (The images were adapted from Lasagni L *et. al.*¹⁴⁶). C,D. Aberrant proliferation of parietal epithelial cells generate hyperplastic lesions. C. Proliferation of PEC adjacent to the bridging podocytes, filling up Bowman's space, giving the appearance of a cellular FSGS lesion. D. The proliferating PEC in Bowman's space produces ECM (gray) that eventually forms tuft adhesions. (The images were adapted from Smeets B *et. al.*⁷³).

1.4.2 Role of proliferation in CKD

The outcome of glomerular disorders depends on a balance between injury and regeneration executed by renal progenitors, bone marrow-derived stem cells, mesenchymal stem cells as well as parietal epithelial cells^{146,147}. Although primary injury to each of the somatic cell types in the glomerular tuft associates with some form of glomerular disease, injury to endothelial and mesangial cells repair by proliferation of adjacent cells¹⁴⁶.

On the other hand, as mentioned earlier podocytes are highly differentiated cells that cannot divide, which explains why podocyte injury results in focal or global glomerulosclerosis. Data from experimental models demonstrate that podocyte repopulation contributes to the regression of glomerulosclerosis⁷⁸. Since resident podocytes do not divide, this suggests that new podocytes are derived by regeneration from glomerular epithelial stem cells. A large body of evidence has recently suggested that parietal epithelial cells represent a reservoir of renal progenitors in adult human kidney which generate novel podocytes during childhood and adolescence, and can regenerate injured podocytes¹⁴⁷.

However, this regenerative process is often inadequate because of inefficient proliferative responses by glomerular epithelial stem cells or renal progenitors with aging or in the setting of focal segmental glomerulosclerosis, resulting in inadequate or no repair of podocytes after injury and subsequent glomerulosclerosis¹⁴⁶ (Figure 6A,6B). Alternatively, an abnormal proliferative response of these cells to podocyte injury can generate hyperplastic glomerular lesions as observed in crescentic glomerulonephritis, collapsing glomerulopathy and other types of glomerular disorders^{146,147} (Figure 6C, 6D).

The later phenomenon has been investigated in detail by *Smeets et. al.*. They studied the development of FSGS in Thy-1.1 transgenic mice. Injection of anti-Thy-1.1 monoclonal antibody to these mice induced acute albuminuria and FSGS lesions. They found that at day 3 after the anti-Thy-1.1 mAb injection, podocyte became hypertrophic and they formed bridges to PEC and against denuded segments of Bowman's capsule. Further, at day 6 they observed a marked proliferation in the bowman's space. These proliferating cells were negative for desmin and all podocyte markers, but stained positive for CD10, and thus confirmed to be PECs. Moreover, the staining properties of the early adhesions were found to be identical to that of Bowman's capsule, suggesting that the ECM in the adhesions was produced by PECs⁷³. Therefore, it had been confirmed that the PECs proliferate and produce ECM and contribute to the development of glomerulosclerosis.

In summary, proliferation of renal cells (both tubular and glomerular) is essential process for renal repair after injury. Therefore it is necessary to investigate the processes, molecules, pathways which promote the recovery/repair or which suppress the injury. MDM2, an oncoprotein, participates in cell proliferation by keeping p53 under control. It has been found to be overexpressed in the cancer tissue. So far, the involvement of MDM2 in renal injury and repair has not been studied in detail. The scope of the thesis is to study the roles of MDM2 in renal injury and repair.

2. Hypotheses

Based on the above literature, it was hypothesized that MDM2 plays an important role in both acute as well as chronic renal injury.

Acute kidney injury

It was hypothesized that the regulatory role of MDM2 on p53 is mandatory for limiting p53-dependent tubular cell apoptosis and for promoting tubular cell regeneration during AKI. As such the assumption was that therapeutic MDM2 inhibition, with nutlin-3a, will aggravate acute tubular necrosis and impair tubular regeneration in AKI, a theoretical concern that have been addressed by studying the effects of the MDM2 antagonist nutlin-3a in a model of murine postischemic AKI.

Chronic kidney disease

Podocytes strongly express MDM2. Therefore, it was hypothesized that MDM2 is essential for podocyte survival and it also promotes the abnormal healing response that contribute to glomerulosclerosis after podocyte injury. This has been addressed by studying the effects of the MDM2 antagonist, nutlin-3a, in a murine model of adriamycin induced focal segmental glomerulosclerosis. The assumption was that MDM2 inhibition will aggravate AN by enhancing podocyte apoptosis.

3. Material and Methods

3.1 Instruments and Chemicals

3.1.1 Instruments

Balance:

Analytic Balance, BP 110 S

Sartorius, Göttingen, Germany

Mettler PJ 3000

Mettler-Toledo, Greifensee, Switzerland

Cell Incubators:

Type B5060 EC-CO₂

Heraeus Sepatech, München, Germany

Centrifuges:

Heraeus, Minifuge T

VWR International, Darmstadt, Germany

Heraeus, Biofuge primo

Kendro Laboratory Products GmbH, Hanau, Germany

Heraeus, Sepatech Biofuge A

Heraeus Sepatech, München, Germany

ELISA-Reader:

Tecan, GENios Plus

Tecan, Crailsheim, Germany

Fluorescence Microscopes:

Leica DC 300F

Leica Microsystems, Cambridge, UK

Olympus BX50

Olympus Microscopy, Hamburg, Germany

Spectrophotometer:

Beckman DU® 530

Beckman Coulter, Fullerton, CA, USA

TaqMan Sequence DetectionSystem:

ABI prism [™] 7700 sequence PE Biosystems, Weiterstadt, Germany
detector

Other Equipments:

Nanodrop	PEQLAB Biotechnology GMBH, Erlangen, Germany
Cryostat RM2155	Leica Microsystems, Bensheim, Germany
Cryostat CM 3000	Leica Microsystems, Bensheim, Germany
Homogenizer ULTRA-TURRAX T25	IKA GmbH, Staufen, Germany
Microtome HM 340E	Microm, Heidelberg, Germany
pH meter WTW	WTW GmbH, Weilheim, Germany
Thermomixer 5436	Eppendorf, Hamburg, Germany
Vortex Genie 2 [™]	Bender & Hobein AG, Zürich, Switzerland
Water bath HI 1210	Leica Microsystems, Bensheim, Germany

3.1.2 Chemicals and reagents

RNeasy Mini Kit	Qiagen GmbH, Hilden, Germany
RT-PCR primers	PE Biosystems, Weiterstadt, Germany

Cell culture:

DMEM-medium	Biochrom KG, Berlin, Germany
RPMI-1640 medium	GIBCO/Invitrogen, Paisley, Scotland, UK
FSC	Biochrom KG, Berlin, Germany
Dulbecco's PBS (1×)	PAA Laboratories GmbH, Cölbe, Germany
Trypsine/EDTA (1×)	PAA Laboratories GmbH, Cölbe, Germany

Penicillin/Streptomycin (100×) PAA Laboratories GmbH, Cölbe, Germany

Antibodies:

MDM2	Abcam, Cambridge, UK
p-MDM2	Cell signaling, Danvers, MA
p53	Santa Cruz Biotechnology, Santa Cruz, CA
p-p53	Cell signaling, Danvers, MA
p21	Santa Cruz Biotechnology, Santa Cruz, CA
NF-κB p65	Cell signaling, Danvers, MA
NF-κB p-p65	Cell signaling, Danvers, MA
p42/44 MAPK	Cell signaling, Danvers, MA
p-p42/44 MAPK	Cell signaling, Danvers, MA
p38 MAPK	Cell signaling, Danvers, MA
p-p38 MAPK	Cell signaling, Danvers, MA
H3	Cell signaling, Danvers, MA
p-H3	
IκB	Cell signaling, Danvers, MA
p-IκB	Cell signaling, Danvers, MA
p52	Cell signaling, Danvers, MA
HRP linked Anti-Rabbit secondary Ab	Cell signaling, Danvers, MA
HRP linked Anti-Mouse secondary Ab	Cell signaling, Danvers, MA
HRP linked Anti-Goat secondary Ab	Dianova, Hamburg, Germany
β-Actin	Cell signaling, Danvers, MA
α-tubulin	Cell signaling, Danvers, MA

Tamm–Horsfall protein	Santa Cruz Biotechnology, Santa Cruz, CA
Lotus tetragonolobus lectin	Vector Labs, Burlingame, CA
rat anti-mouse neutrophils	Serotec, Oxford, UK
CD3+	AbD Serotec, Düsseldorf, Germany
F4/80+	AbD Serotec, Düsseldorf, Germany
Claudin	Bioworld technology, CB8 7SY England
Nephrin	Acris Antibodies GmbH, Herford, Germany
Ki-67	Dako Deutschland GmbH, Hamburg, Germany
α -SMA	Dako Deutschland GmbH, Hamburg, Germany

Elisa Kits:

mouse IL-6	R &D Systems, Minneapolis, MN, USA
mouse TNF- α	Biologend, San Diego, CA
mouse Albumin	Bethyl Laboratories, TX, USA
Creatinine FS	DiaSys Diagnostic System, GmbH, Holzheim, Germany
Urea FS	DiaSys Diagnostic System, GmbH, Holzheim, Germany

Chemicals:

Acetone	Merck, Darmstadt, Germany
AEC Substrate Packing	Biogenex, San Ramon, USA
Bovines Serum Albumin	Roche Diagnostics, Mannheim, Germany
Skim milk powder	Merck, Darmstadt, Germany
DEPC	Fluka, Buchs, Switzerland
DMSO	Merck, Darmstadt, Germany

Diluent C for PKH26 dye	Sigma-Aldrich Chemicals, Germany
EDTA	Calbiochem, SanDiego, USA
30% Acrylamide	Carl Roth GmbH, Karlsruhe, Germany
TEMED	Santa Cruz Biotechnology, Santa Cruz, CA
Eosin	Sigma, Deisenhofen, Germany
Ethanol	Merck, Darmstadt, Germany
Formalin	Merck, Darmstadt, Germany
Hydroxyethyl cellulose	Sigma-Aldrich, Steinheim, Germany
HCl (5N)	Merck, Darmstadt, Germany
Isopropanol	Merck, Darmstadt, Germany
Calcium chloride	Merck, Darmstadt, Germany
Calcium dihydrogenphosphate	Merck, Darmstadt, Germany
Calcium hydroxide	Merck, Darmstadt, Germany
MACS-Buffer	Miltenyl Biotec, Bergisch Gladbach, Germany
Beta mercaptoethanol	Roth, Karlsruhe, Germany
Sodium acetate	Merck, Darmstadt, Germany
Sodium chloride	Merck, Darmstadt, Germany
Sodium citrate	Merck, Darmstadt, Germany
Sodium dihydrogenphosphate	Merck, Darmstadt, Germany
Penicillin	Sigma, Deisenhofen, Germany
Roti-Aqua-Phenol	Carl Roth GmbH, Karlsruhe, Germany
Streptomycin	Sigma, Deisenhofen, Germany
Tissue Freezing Medium	Leica, Nussloch, Germany
Trypan Blue	Sigma, Deisenhofen, Germany
Oxygenated water	DAKO, Hamburg, Germany
Xylol	Merck, Darmstadt, Germany

Miscellaneous:

Cell death detection (TUNEL) kit	Roche, Mannheim, Germany
Microbeads	Miltenyl Biotech, Germany
Cell Titer 96 Proliferation Assay	Promega, Mannheim, Germany
LS+/VS+ Positive selection columns	Miltenyl Biotec, Bergish Gladbach, Germany
Preseparation Filters	Miltenyl Biotec, Bergish Gladbach, Germany
Super Frost® Plus microscope slides	Menzel-Gläser, Braunschweig, Germany
Needles	BD Drogheda, Ireland
Pipette's tip 1-1000µL	Eppendorf, Hamburg, Germany
Syringes	Becton Dickinson GmbH, Heidelberg, Germany
Plastic histocassettes	NeoLab, Heidelberg, Germany
Tissue culture dishes Ø 100x20mm	TPP, Trasadingen, Switzerland
Tissue culture dishes Ø 150x20mm	TPP, Trasadingen, Switzerland
Tissue culture dishes Ø 35x10mm	Becton Dickinson, Franklin Lakes, NJ, USA
Tissue culture flasks 150 cm ²	TPP, Trasadingen, Switzerland
Tubes 15 and 50 mL	TPP, Trasadingen, Switzerland
Tubes 1.5 and 2 mL	TPP, Trasadingen, Switzerland

All other reagents were of analytical grade and are commercially available from Invitrogen, SIGMA or ROTH.

3.2 Experimental procedures

3.2.1 Animals

C57BL/6 wild-type mice and *p53*-deficient C57BL/6 mice were obtained from Taconic (Ry, Denmark) and Blab/c mice were obtained from Charles River (Sulzfeld, Germany). All mice were kept under normal housing conditions under a 12-h light and dark cycle. Water and standard chow (Ssniff, Soest, Germany) were available ad libitum for the complete duration

of the study. Cages, bedding, nestles, food, and water were sterilized by autoclaving before use.

3.2.2 Animal models

Ischemia Reperfusion induced Acute Renal Failure

Renal ischemia–reperfusion was performed under general anesthesia. The left or both renal pedicles were clamped for either 45 or 30 min, respectively, with microaneurysm clamps (Medicon, Tuttlingen, Germany) via 1-cm flank incisions. Body temperature was constantly measured with a rectal probe and maintained at 36–37°C throughout the procedure by placing the mice on a heating pad (Figure 7). After clamp removal, the kidney was inspected for restoration of blood flow closing the wound with standard sutures. To maintain fluid balance, all mice were supplemented with 0.5 ml of normal saline.

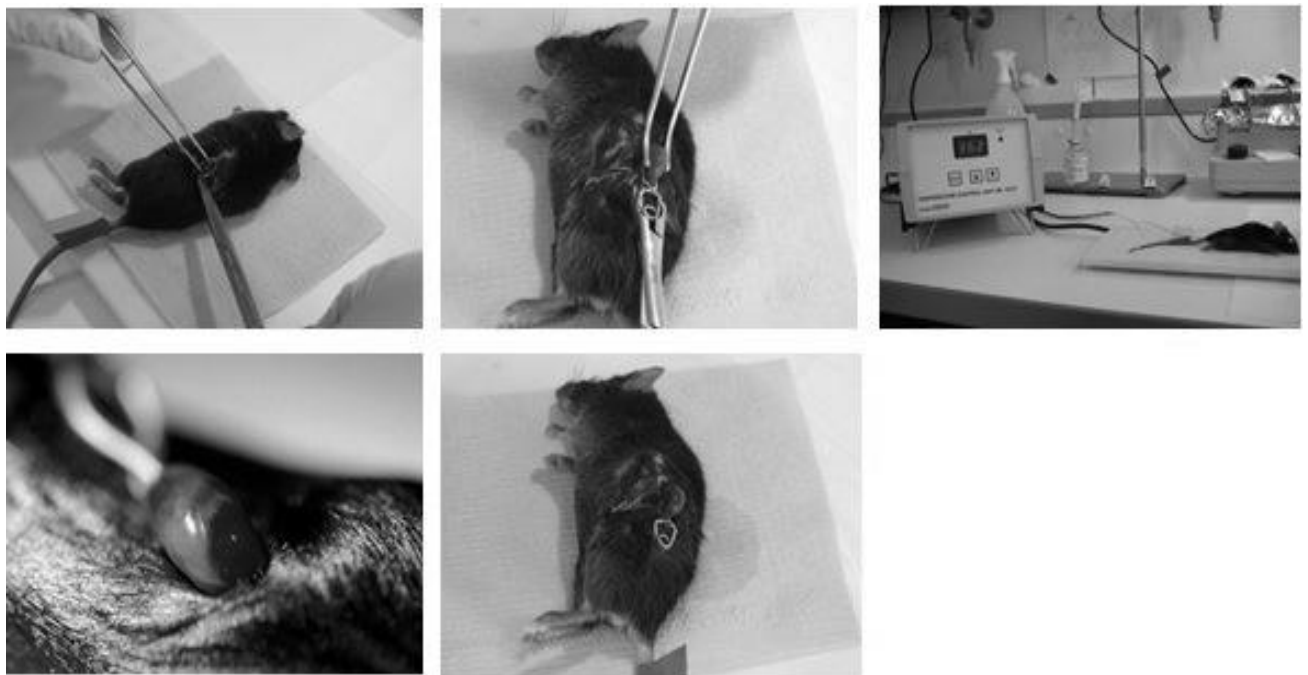


Figure 7 Ischemia reperfusion surgery on C57Bl6 mice

Adriamycin induced Focal Segmental Glomerulosclerosis

To induce progressive glomerulosclerosis and tubulointerstitial inflammation in mice adriamycin (Pharmacia & Upjohn, Erlangen, Germany) was injected intravenously at day 0

and day 14 at a dose of 13mg/kg body weight. AN is characterized by persistent proteinuria throughout the study period of 4 weeks, associated with chronic glomerular and tubulointerstitial lesions as seen in human FSGS.

Mice from both the studies received intra-peritoneal injections with either 20 mg/kg of the MDM2 inhibitor nutlin-3a (Axxora, Lörrach, Germany) in 50% dimethyl sulfoxide (vehicle) or vehicle only. Five to eight mice per group were examined in each experiment. At the end of each experiment plasma and urine samples were collected before sacrifice by cervical dislocation and then afterwards kidney tissues was harvested. The harvested kidney tissues are divided into three parts each. One part was immediately flash frozen in liquid nitrogen and then further stored at -80°C for protein isolation and cryo sections, second part was collected in RNA later solution (Ambion, CA, USA) and stored at -20°C for RNA isolation and third part of the kidney was kept in formalin to fix the tissue before embedding in paraffin for histological analysis.

All experimental procedures were performed according to the German animal care and ethics legislation and had been approved by the local government authorities.

3.2.3 Experimental design

Study 1: Ischemic renal failure

Groups of C57Bl6 wild type mice (n=6) received single nutlin-3a injection 24 h before bilateral renal artery clamping for 45 min. Control mice received vehicle. All mice were then sacrificed 24 h after the IR surgery. Next groups of C57Bl6 wild type mice (n=6) received nutlin-3a injection 24 h before bilateral renal artery clamping for 30 min. They received additional nutlin-3a injections at day +1 and +3 after the IR surgery. Control mice received vehicle. These mice were sacrificed at day +5 after IR surgery.

In another set of experiment, groups of mice (n=6) received a single nutlin-3a injection 24 h before unilateral renal artery clamping; others received three injections on the days -1, +2, and +3 after the IR surgery. All mice were sacrificed at day +5 after IR surgery. Similar set of experiments were performed in *p53*-deficient mice (Figure 8).

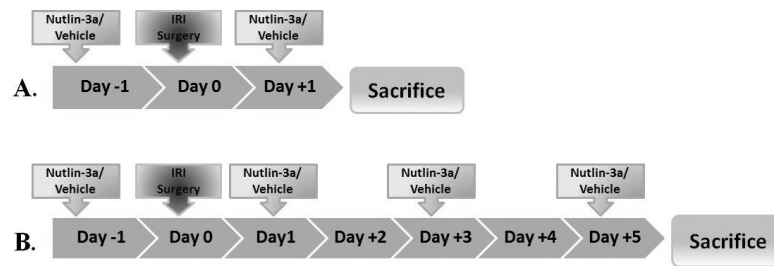


Figure 8 Schematics of experiment design for Ischemic reperfusion induced acute renal failure

Study 2: Adriamycin nephropathy

To study the role of MDM2 in glomerular injury in adriamycin induced FSGS, groups of Balb/c mice received single intravenous injections of adriamycin 13mg/kg at day 0 (week 0) and either nutlin-3a or vehicle at day 8, 10, 12 before sacrifice at day 14 (week 2).

Another groups of Balb/c mice received two intravenous injections of adriamycin 13mg/kg at day 0 and day 14 (week2) and either nutlin-3a or vehicle on alternate days after the second adriamycin injection (week 2) till they were sacrificed at day 28 (week 4) for studying the role of MDM2 in tubulointerstitial injury in FSGS (Figure 9).

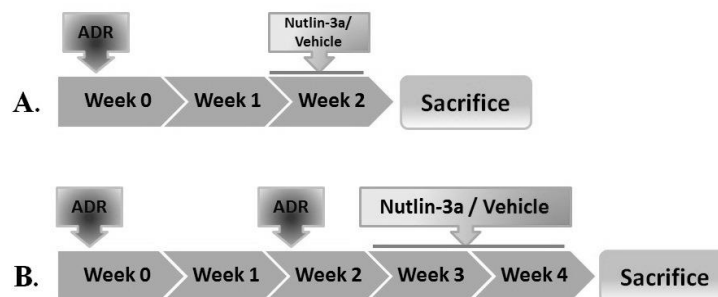


Figure 9 Schematics of experiment design for adriamycin induced chronic renal failure

3.3 Blood and urine sample collection

Blood samples were collected by retro-orbital bleeding technique, under isoflurane anesthesia, in microcentrifuge tubes containing EDTA (10µl of 0.5 M solution per 200µl of blood).

Collected blood samples were centrifuged at 8000 rpm for 5 min and plasma was separated and stored at -20⁰C until used for analysis.

Urine samples were collected at the end of the study and are stored at -20°C until used for further biochemical analysis.

3.4 Urinary albumin to creatinine ratio

3.4.1 Urinary albumin

Urinary albumin levels were determined using albumin Elisa kit from Bethyl laboratories following manufacturer's instructions. Generally albumin levels in urine samples from FSGS mice were quite high, so urine samples were diluted 1000 to 1500 times with water before estimation. In short, capture antibody (Anti-Mouse albumin, 1:100 dilution) was coated on polyethylene flat bottom 96 well plates (Nunc plates) using carbonate-bicarbonate (pH 9.6) coating buffer. After overnight incubation of the capture antibody at 4°C , plate was washed 3 times with wash buffer (Tris NaCl with Tween 20) and blocked with blocking solution (Tris, NaCl with 1% BSA, pH 8) at room temperature for 1 hour. After blocking was over the plate was washed 3 to 5 times with wash buffer and then diluted samples/standards were added in respective wells and further incubated for 1 hour. After incubation was over each well was washed 5 times with wash buffer and diluted HRP-conjugated detection antibody (using the suggested dilution) was added and the plate was incubated in dark for further 1 hour. After HRP-conjugate incubation was over each well was washed 5 to 7 times with wash buffer and TMB reagent (freshly prepared by mixing equal volumes of two substrate reagents) was added and incubated in dark till color reaction was completed followed by addition of stop solution (2 M H_2SO_4). The absorbance was read at 450 nm within 10 min of stop solution addition. The albumin content in each sample was determined using the equation of regression line generated by plotting absorbance of different standards against their known concentrations.

3.4.2 Urinary creatinine, plasma creatinine and plasma BUN

Urinary creatinine and plasma creatinine levels were measured using Jaffe's enzymatic reaction using a Creatinine FS kit (DiaSys Diagnostic system, GmBH, Holzheim, Germany). Urine samples were diluted 10 times with distilled water whereas plasma samples were used undiluted. Different dilutions of standard were prepared using the stock provided with the kit. Working monoreagent was prepared by mixing 4 part of reagent 1 (R1) and 1 part of reagent 2 (R2) provided with the kit. Then, 10 μl of each of the diluted samples and standards were

added to a 96 well plate with flat bottom (Nunc maxisorb plate). The monoreagent (200 μ l) was added to each well and the reaction mixture was incubated for one minute before measuring the absorbance at 492 nm immediately after and 1 (A1) and 2 (A2) min of addition using elisa plate reader. The change in absorbance (ΔA) was calculated as $\Delta A = [(A2 - A1) \text{ sample or standard}] - [(A2 - A1) \text{ blank}]$. And creatinine content of samples was calculated as:

$$\text{Creatinine (mg/dl)} = \Delta A \text{ sample} / \Delta A \text{ standard} * \text{Concentration of standard (mg/dl)}$$

Plasma BUN levels were measured using an enzymatic reaction using a Urea FS kit (DiaSys Diagnostic system, GmbH, Holzheim, Germany). Different dilutions of standard were prepared using the stock provided with the kit. Working monoreagent was prepared by mixing 4 part of reagent 1 (R1) and 1 part of reagent 2 (R2) provided with the kit. Then, 2 μ l of each of the sample and standards were added to a 96 well plate with flat bottom (Nunc maxisorb plate). The monoreagent (200 μ l) was added to each well and the reaction mixture was incubated for one minute before measuring the absorbance at 360 nm immediately after and 1 (A1) and 2 (A2) min of addition using elisa plate reader. The change in absorbance (ΔA) was calculated as $\Delta A = [(A1 - A2) \text{ sample or standard}] - [(A1 - A2) \text{ blank}]$. And BUN content of samples was calculated as:

$$\text{BUN (mg/dl)} = \Delta A \text{ sample} / \Delta A \text{ standard} * \text{Concentration of standard (mg/dl)} * 0.467$$

Urinary albumin to creatinine ratio was calculated after converting values for albumin and creatinine to similar units (mg/dl). Albumin content for each sample calculated (mg/dl) was divided by creatinine content (mg/dl) for the same sample.

3.5 Cytokines Elisa

All cytokine levels in supernatant collected from *in-vitro* cells stimulations were estimated using ELISA kits following the manufacturer's instructions. In brief, The NUNC ELISA plate wells were captured overnight at 4°C with the capture antibody in coating buffer. Next day the plates were washed 3 times with the washing buffer as given in protocol for 3 times and blocked with the blocking solution or assay diluent for 1 hour or as specified. Again the washings were repeated 3 times followed by addition of standards; samples and sample diluent (blank) into the wells of tap dried plate and incubated at RT for 2 hours. This was followed by washings for 5 times or as specified. Then HRP/AP conjugated secondary

antibody diluted in assay diluent was added. Incubate the plate as specified. The wells were washed again for 5-7 times or as specified and incubated with the 100 µl of substrate A and B (1:1 mixture) for 25-30 min in dark to develop colour. The reaction was stopped by addition of 100 µl 1 M H₂SO₄. The reading of the absorbance was taken at 450 nm and the reference wavelength was 620 nm using a spectrophotometer (TECAN-Genios Plus).

3.6 Immunostaining and Confocal imaging

For immunohistological studies middle part of kidney from each mouse were fixed in formalin (10 % in PBS or Saline) over night and processed using tissue processors (Leica) and paraffin blocks were prepared. 2µm thick paraffin-embedded sections were cut. De-paraffinization was carried out using xylene (3 * 5 min) followed by re-hydration, which was carried out by incubating the sections in 100% absolute ethanol (3 * 3 min), 95% ethanol (2 * 3 min) and 70% ethanol (1 * 3 min) followed by washing with PBS (2 * 5 min). Blocking endogenous peroxidase was carried out by incubating sections in H₂O₂ and methanol mixture (20 ml of 30% H₂O₂ in 180ml of methanol) for 20 min in dark followed by washing in PBS (2* 5min). For unmasking of antigen sections were dipped in antigen unmasking solution (3 ml of antigen unmasking solution + 300 ml of distilled water) and cooked in microwave for total of 10 min (4*2.5 min, every 2.5 min water level was checked and made up to the initial levels with distilled water every time). After microwave cooking sections were cooled to room temperature for 20 min and washed with PBS. Blocking endogenous biotin was carried out by incubating sections with one drop of Avidin (Vector) for 15 min followed by incubation with Biotin (Vector) for further 15 min. After the incubation was over sections were washed with PBS (2* 5 min).

Sections were incubated with different primary antibodies either for 1 hour at room temperature or overnight at 4⁰C in a wet chamber followed by wash with PBS (2* 5 min). After washing sections were incubated with biotinylated secondary antibodies (1:300, dilution in PBS) for 30 min followed by wash with PBS (2* 5 min). Substrate solution (ABC solution, Vector) was added and sections were incubated for 30 min at room temperature in a wet chamber followed by wash with PBS (1* 5 min). Tris (1* 5 min) and sections were stained for DAB followed by counter staining with methyl green (Fluka). Then sections were washed with alcohol (96 %) to remove excess stain and xylene. Sections were dried and mounted with VectaMount (Vector).

The primary antibodies used in the study are mentioned above. For each immunostaining negative controls staining was performed by incubation with a respective isotype antibody instead of primary antibody.

For Confocal imaging, the sections, prepared as described above, were incubated with the following primary antibodies: pig anti-mouse nephrin (1:100, Acris Antibodies, Herford, Germany), rabbit anti-mouse WT1 (1:25, Santa Cruz Biotechnology, Santa Cruz, CA) and rabbit anti-mouse MDM2 (1:100, Abcam, Cambridge, UK) and Biotinylated lotus tetragonolobus lectin (Vector Labs, CA, USA) for 1 h in PBS or 0.1% milk solution in room temperature. After washing, the sections were incubated with secondary antibodies guinea pig Alexa Fluor 488 (1:100, Invitrogen, Carlsbad, CA) or rabbit Cy3 (1:200, Jackson ImmunoResearch Laboratories, West Grove, PA) for 30 minutes at room temperature. Stainings were evaluated using confocal microscopy with LSM 510 microscope and LSM software (Carl Zeiss AG).

3.7 Periodic acid Schiff staining

Formalin-fixed tissues were processed using tissue processors (Leica) and paraffin blocks were prepared. 2 µm thick paraffin-embedded sections were cut. De-paraffinization was carried out using xylene (3 * 5 min) followed by re-hydration by incubating the sections in 100% absolute ethanol (3 * 3 min), 95% ethanol (2 * 3 min) and 70% ethanol (1 * 3 min) followed by washing with distilled water (2 * 5 min). Re-hydrated sections were incubated with Periodic acid (2 % in distilled water) for 5 min followed by washing with distilled water (1 * 5 min). Then sections were incubated with Schiff solution for 20 min at room temperature followed by washing with tap water (1 * 7 min) and counter staining with Hematoxylin solution (1 * 2 min). This was followed by washing with tap water (1 * 5 min) and finally sections were dipped in alcohol 90% and dried and closed with cover slips.

3.8 Histopathological evaluations

3.8.1 PAS staining

Postischemic tubular injury was scored by assessing the percentage of tubules in the corticomedullary junction that displayed cell necrosis, loss of brush border, cast formation, and tubular dilatation as follows:

<u>Score</u>	<u>Injury level</u>
0	None
1	≤ 10%
2	21 % to 40 %
3	41 % to 60 %
4	61 % to 80 %
5	81 % to 100 %

All sections were quantified in each group and were expressed as mean ± SEM.

Glomerular sclerotic lesions were assessed using a semi quantitative score by a blinded observer as follows, after assessing 50 glomeruli from each section:

<u>Score</u>	<u>Lesion in Glomeruli</u>
No lesion	None
Segmental Lesion	≤ 50 %
Global Lesion	≥ 50 %

All sections were quantified in each group and were expressed as percentage of glomeruli with each score (mean ± SEM).

3.8.2 *Mac2 staining*

Number of infiltrated macrophages in glomeruli as well as in interstitium were counted in sections stained with Mac2 (pan marker for macrophage) antibodies. Mac2 positive cells were counted manually in 15 glomeruli or 15 non-overlapping high power fields interstitium for each section and were presented as mean ± standard error of mean for respective groups.

3.8.3 *Ki67 staining*

Number of proliferating cells within glomeruli and tubules were evaluated using Ki 67 staining. For quantification Ki67 positive cells were counted manually in 25 glomeruli in each section and for proliferating tubular cells, 10 h.p.f. from each section was calculated and presented as mean ± SEM for respective groups.

3.8.4 SMA- α staining

For tissue fibrosis assessment sections were stained with SMA- α anti-body. Adobe photoshop software was used to quantify the percentage SMA- α positive area from each section. The data is presented as mean \pm SEM for respective groups.

3.8.5 TUNEL staining

A terminal deoxynucleotidyl transferase dUTP nick end labeling (TUNEL) assay was performed to quantify apoptotic tubular epithelial cells. Paraffin sections of kidney were stained with *In situ* Cell death detection kit (Roche, Mannheim, Germany) according to the manufacturer's instruction. The TUNEL positive cells were counted using adobe photoshop software. The data is presented as mean \pm SEM for respective groups.

3.9 RNA analysis

3.9.1 RNA isolation

A part of kidney from each mouse was preserved in RNA-later immediately after kidney isolation and stored at -20°C until processed for RNA isolation. RNA isolation was carried out using RNA isolation kit from Ambion (Ambion, CA, USA). In short, tissues (30 mg) preserved in RNA-later were homogenized using blade homogenizer for 30 seconds at 4 in lysis buffer (600 μl) containing β -mercaptoethanol (10 $\mu\text{l}/\text{ml}$). The homogenate was centrifuged at 6000 rpm for 5 min and 350 μl of supernatant was transferred to fresh DEPC-treated tube. To this equal amount (350 μl) of 70 % ethanol was added and mixed gently. This whole mixture was then loaded on RNA column and processed for RNA isolation as per the manufacturer's instruction. Isolated RNA measured, checked for purity as follows and was stored at -80°C .

3.9.2 RNA quantification and purity check

The isolated RNA samples were quantified using Nano drop (PEQLAB Biotechnology GMBH, Erlangen, Germany). The ratio of optical densities at 260 nm and 280 nm is an indicator for RNA purity (indicative of protein contamination in the RNA samples). Only samples with a ratio of 1.8 or more were considered to be of acceptable quality.

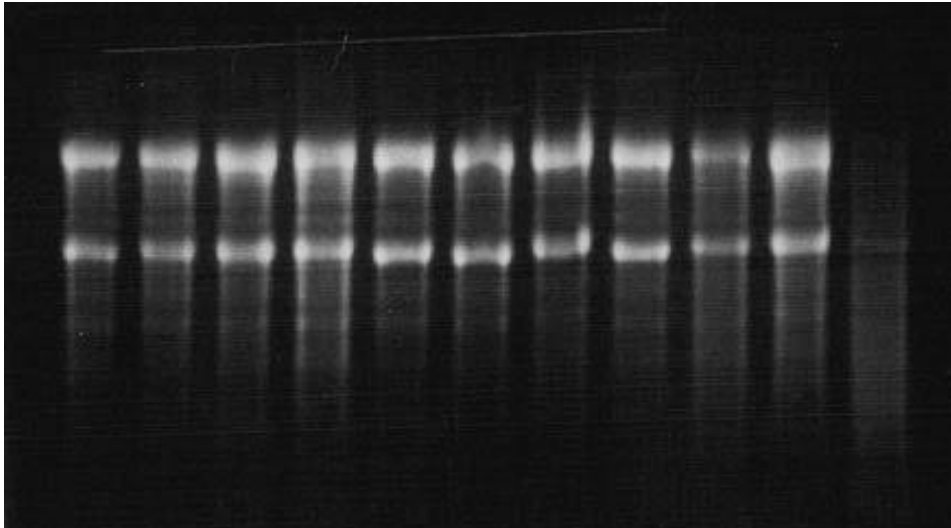


Figure 10 RNA integrity check

3.9.3 RNA integrity check

Further quality check (if necessary) was performed using a denaturing RNA gel. In short 2 % Agarose gel with Ethidium-bromide was casted, RNA samples were mixed with RNA loading buffer (4:1 ratio) (Sigma Aldrich, Germany) and were loaded on the gel. Electrophoresis was carried out at constant volt (70-100 V) using MOBS running buffer for 1 hour and the gel was read on a gel documentation apparatus under UV lamp. RNA samples showing a single bright band were considered to be of good quality. Loss of RNA integrity could be detected as smear formation in the agarose gel (Figure 10).

3.9.4 cDNA synthesis and real-time RT-PCR (SYBR Green)

The isolated RNA samples were quantified and processed for cDNA conversion using reverse transcriptase II (Invitrogen, Karlsruhe, Germany). RNA samples were diluted in DEPC treated tubes with water to get final concentration of 2 μg / 30 μl , to this diluted RNA samples 13.9 μl of master mix* was added, all tubes were incubated at 42⁰C for 1 hour and 30 min on thermal shaker. Upon completion of incubation cDNA samples were stored at -20⁰C until used for RT-PCR analysis using SYBR green. The cDNA samples prepared as described above were diluted 1:10 a dilution for the real-time RT-PCR. 2 μl of diluted cDNA samples were mixed with SYBR green master mix (10 μl), forward primer, specific for gene of interest (0.6 μl), reverse primer specific for gene of interest (0.6 μl), Taq polymerase (0.16 μl) and distilled water (6.64 μl). The real-time RT-PCR was performed using Light Cycler480.

*The master mix was prepared by mixing 9 μ l of 5x buffer (Invitrogen, Karlsruhe, Germany), 1 μ l of 25 mM dNTP mixture (Amersham Pharmacia Biotech, Freiburg, Germany), 2 μ l of 0.1 M DTT (Invitrogen, Karlsruhe, Germany), 1 μ l of 40U/ μ l RNAsin (Promega, Mannheim, Germany), 0.5 μ l of Hexanucleotide (Roche, Mannheim, Germany), 1 μ l of Superscript (Invitrogen, Karlsruhe, Germany) or ddH₂O in the case of the control cDNA (RT minus).

3.9.5 Real time PCR

Pre-incubation was carried out for 5 minutes at 95⁰C so as to activate the polymerase and complete de-naturation of cDNA samples. Then the cDNA was amplified for 40 cycles, each comprising of 15 seconds incubation at 95⁰C and 45 seconds incubation at 60⁰C. For melting curve initial 95⁰C for 5 seconds followed by 65⁰C for 1 min with continuous heating was used. The RT-PCR for the reference genes (18S rRNA) was carried out under similar conditions. The CT values were calculated using the Light Cycler480 and the results were normalized with respective reference gene expression for each sample. In all cases controls consisting of ddH₂O were negative for target or reference genes. All designed SYBR green primers for all genes evaluated were obtained from Metabion (Metabion, Martinsried, Germany).

3.9.6 Oligonucleotide primers used for SYBR-Green RT-PCR

The following oligonucleotide primers were used in the study.

Gene	Sequence
18s	Forward: GCAATTATTCCTCCATGAACG
	Reverse: AGGGCCTCACTAAACCATCC
Ccl2	Forward: CCTGCTGTTCACAGTTGCC
	Reverse: ATTGGGATCATCTTGCTGGT
Cxcl10	Forward: GGCTGGTCACCTTTCAGAAG
	Reverse: ATGGATGGACAGCAGAGAGC
IL-6	Forward: TGATGCACTTGCAGAAAACA
	Reverse: ACCAGAGGAAATTTCAATAGGC

Nphs1	Forward:	TTAGCAGACACGGACACAGG
(Nephrin)	Reverse:	CTCTTTCTACCGCCTCAACG
Nphs2	Forward:	TGACGTTCCCTTTTTCCATC
(Podocin)	Reverse:	CAGGAAGCAGATGTCCCAGT
Nos2	Forward:	TTCTGTGCTGTCCCAGTGAG
(iNos)	Reverse:	TGAAGAAAACCCCTTGTGCT
Tnf- α	Forward:	CCACCACGCTCTTCTGTCTAC
	Reverse:	AGGGTCTGGGCCATAGAACT
MDM2	Forward:	TGTGAAGGAGCACAGGAAAA
	Reverse:	TCCTTCAGATCACTCCCACC
CXCL2	Forward:	CGGTCAAAAAGTTTGCCTTG
	Reverse:	TCCAGGTCAGTTAGCCTTGC
BAX	Forward:	GATCAGCTCGGGCACTTTAG
	Reverse:	TTGCTGATGGCAACTTCAAC
BAD	Forward:	GTACGAACTGTGGCGACTCC
	Reverse:	GAGCAACATTCATCAGCAGG
BAK1	Forward:	AGACCTCCTCTGTGTCCTGG
	Reverse:	AAAATGGCATCTGGACAAGG
BID	Forward:	GTGTAGCTCCAAGCACTGCC
	Reverse:	GCAAACCTTTGCCTTAGCC
NOXA	Forward:	ACTTTGTCTCCAATCCTCCG
	Reverse:	GAAGTCGCAAAAGAGCAGGA
PUMA	Forward:	CACCTAGTTGGGCTCCATTT
	Reverse:	ACCTCAACGCGCAGTACG

Table 2 Oligonucleotide primer sequences used in the study

3.10 Protein isolation and western blotting

3.10.1 Protein isolation

Proteins from kidney tissue and cells from cell culture were extracted using RIPA buffer (Sigma, Germany) containing protease inhibitors (Roche, Germany). In brief, part of the kidney tissue stored at -80°C was homogenized using blade homogenizer for 30 seconds at 4 in RIPA buffer (500 μl) containing protease inhibitor. For cell culture experiments, after stimulations were over, cells were washed with PBS and then lysed in the RIPA buffer containing protease inhibitors. The lysates was then maintained at constant agitation for two hours at 4°C . The samples were then centrifuged for 20 min at 12000rpm at 4°C . Then the supernatant (proteins) was separated in new tube, pallet was discarded. Protein estimation was done using Barford's assay.

3.10.2 Western blotting

After determination of protein concentrations, 50 μg of the protein was mixed with 5x SDS loading buffer (100 mM Tris-HCl, 4% SDS, 20% glycerol, and 0.2% bromophenol blue) for Western blot analysis. Samples were heated at 95°C for 5 min. Proteins were separated by SDS PAGE and then transferred to a polyvinylidene difluoride (PVDF) membrane. Nonspecific binding to the membrane was blocked for 1hr at room temperature with 5% milk in Tris-buffered saline buffer (20 mM Tris-HCl, 150 mM NaCl, and 0.1% Tween 20). The membranes were then incubated overnight at 4°C with primary antibodies. After washing, the membrane was incubated with respective secondary antibodies in Tris buffered saline buffer. The signals were visualized by an enhanced chemiluminescence system (Amersham, Buckinghamshire, UK).

3.11 Magnetic cell sorting technique for isolation of renal cells

In brief, kidneys were finely minced and digested for 30 min at 37°C with 1 mg/ml collagenase D (Roche, Mannheim, Germany) and 0.1 mg/ml deoxyribonuclease type I (Sigma-Aldrich, Steinheim, Germany) in Hank's balanced salt solution. The digested tissues were washed and filtered through a 30- μm nylon mesh filter to remove debris and cell segments. Renal CD45+CD11c+ cells were isolated using microbead-conjugated antibodies

(Miltenyi Biotech, Bergisch-Gladbach, Germany). Magnetic bead separation was done according to the manufacturer's instructions.

3.12 Electrophoretic mobility shift assay

Electrophoretic mobility shift assay was performed using a LightShift Chemiluminescent EMSA Kit (Thermo Scientific, Rockford, IL). Following quantification of protein amounts by Bradford assay, 2 µg of nuclear extracts were analyzed for their binding activity to an IL-6-derived κB sequence–containing biotin end–labeled oligonucleotide probe. 50-biotin end-labeled NF-κB oligonucleotides 50-AAATGTGG GATTTTCCCATGAGTCTC-30 and its reverse counterpart (Metabion) were annealed for the duplex probe. Binding reaction and electrophoresis on 6% native polyacrylamide gel were performed according to the manufacturer's protocol and transferred on a nylon membrane. For oligonucleotide competitions, we added 20 ng of specific oligonucleotide competitor before adding the probe. The biotin end-labeled DNA is detected using the Streptavidin horse radish peroxidase conjugate and the chemiluminescent substrate.

3.13 *In-vitro* methods

3.13.1 Cell culture

The mouse embryonic fibroblasts (MEFs) deficient either for *p53* or *p53/Mdm2* were kindly provided by Dr. G Lozano, University of Houston, TX and The murine macrophage cell line J774 were purchased from American Type Culture Collection, Rockville, MD, USA. To obtain CD133+CD24+ cells, total renal cells depleted for CD45 and CD31 were treated with a magnetic separation for CD133. The purified cell fractions consisted of >98% of CD133+CD24+ cells. Expression of WT1, nephrin, and CD133 was checked to evaluate the purity of podocyte cultures. Cells were plated in VRAD medium containing DMEM-F12 (Sigma) supplemented with 10% FBS, vitamin D3 100 nM (Sigma), and all-trans retinoic acid (100 µM; Sigma). MEFs were maintained in Dulbecco's modified Eagle's medium (DMEM) (GIBCO/Invitrogen, Carlsbad, CA, USA) and J774 cells were maintained in RPMI medium (GIBCO/Invitrogen, Carlsbad, CA, USA). Both media were supplemented with 10% fetal bovine serum and 1% penicillin/streptomycin. Cells were grown under standard conditions (in an incubator set at 37°C supplied with 5 % CO₂/air). Trypsin was used for splitting the cells.

Cells were counted using Neubauers' chamber and desired number of cells were used for experiments.

3.13.2 Cell freezing and thawing

At earlier passages large amounts of cells were grown under standard culture conditions and were frozen for future use. Cells to be frozen were detached from the culture plates and were spun down under sterile conditions for 3 min at 1000 RPM. The cell pellet was maintained on ice and carefully re-suspended in cold freezing medium (90 % respective culture medium and 10 % DMSO) by pipetting the suspension repeatedly up and down. 1.5 ml aliquots were quickly dispensed into freezing vials (4°C). The cells were slowly frozen at -20°C for 1 h and then at -80°C overnight. The next day, all aliquots were transferred to liquid nitrogen.

In order to thaw cells a frozen vial was removed from liquid nitrogen and put in a water bath at 37°C. The cells were then dispensed in 5 ml of warm complete growth medium and spun down at 1000 RPM for 5-7 min. Then the old medium was removed and the cells were re-suspended in fresh medium and transferred to new culture plate. The medium was changed once more after 24 h.

3.13.3 Stimulation experiments

For cell stimulation experiments, the cells were seeded at a density of 5×10^5 cells/well in six-well plates in DMEM and grown overnight to confluence. Cells were treated with 5 µg/ml ultrapure LPS (InvivoGen, San Diego, CA) and incubated at 37°C, 5% CO₂ for 0.5–18 h. Total cell protein was extracted for western blot analysis and supernatants were collected for IL-6 or TNF-α ELISA. Nuclear proteins were isolated by using high-salt extraction.

3.13.4 In-vitro assessment of podocyte death

To analyze cell death, cells were treated for 24 hours with adriamycin 0.2 µg/ml plus nutlin-3a 10µM (Sigma) and harvested for propidium iodide (PI)/annexin V staining. Apoptotic cells were identified by double supravital staining with PI and recombinant APC-conjugated annexin V following the manufacturer's instructions (BD Biosciences, San Diego, CA). Data acquisition was performed using LSRII flow cytometer (BD Biosciences) and data were analyzed with FlowJo software (Tree Star, Inc. Ashland, OR).

3.14 Statistical analysis

Data are presented as mean \pm SEM. For multiple comparison of groups one way ANOVA was used followed by post-hoc Bonferroni`s test, using SigmaStat (Jandel Scientific, Erkarath, Germany). Paired Student`s t-test was used for the comparison of single groups. A value of $p < 0.05$ was considered to indicate statistical significance.

4. Results

4.1 Part I MDM2 inhibition in ischemia reperfusion induced acute kidney injury

4.1.1 MDM2 expression in the healthy and postischemic kidney

To start out, MDM2 mRNA expression screen in solid organs of healthy adult C57BL/6 mice was performed. The highest MDM2 mRNA expression levels were found in muscle and heart, whereas the renal MDM2 mRNA levels were more in the range of lung, colon, urinary bladder, and brain (Figure 11A). Immunostaining localized MDM2 to the cytoplasm of epithelial cells in proximal and distal tubuli, and probably to podocytes inside glomeruli (Figure 11B). Next, the MDM2 expression in postischemic and sham kidneys 1 and 5 days after renal pedicle clamping was determined by western blot analysis. MDM2 protein levels were reduced in both kidneys, postischemic and sham-operated, at day 1 but MDM2 levels recovered in sham kidneys at day 5 (Figure 11C). Furthermore, p53 protein expression was strongly induced in postischemic kidneys at 24h and remains elevated at day 5 after ischemia–reperfusion. Together, inside the kidney MDM2 is mainly expressed by (tubular) epithelial cells.

4.1.2 MDM2 blockade prevents early postischemic AKI

To address a putative functional contribution of MDM2 to AKI, MDM2 function was blocked using nutlin-3a, a small-molecule MDM2 antagonist that inhibits MDM2-mediated degradation of p53 leading to cell cycle arrest and apoptosis in various cancer cells¹⁴². The hypothesis was that nutlin-3a treatment would elicit a similar effect in AKI, i.e., foster p53-mediated tubular cell apoptosis, a process that should aggravate the early phase of postischemic injury. However, MDM2 blockade with nutlin-3a rather significantly reduced serum creatinine levels at 24 h after bilateral renal artery clamping as compared with vehicle-treated C57BL/6 mice (Figure 12A). This protective effect was associated with less tubular injury in postischemic kidneys at 24h also after unilateral renal artery clamping (Figures 12B and C), and immunostaining for either brush border lectin or Tamm–Horsfall protein revealed that this protective effect applied to proximal and distal tubules, respectively (Figure 13). In AKI, loss of intact tubules involves both tubular cell necrosis and apoptosis¹⁴⁸. Interestingly,

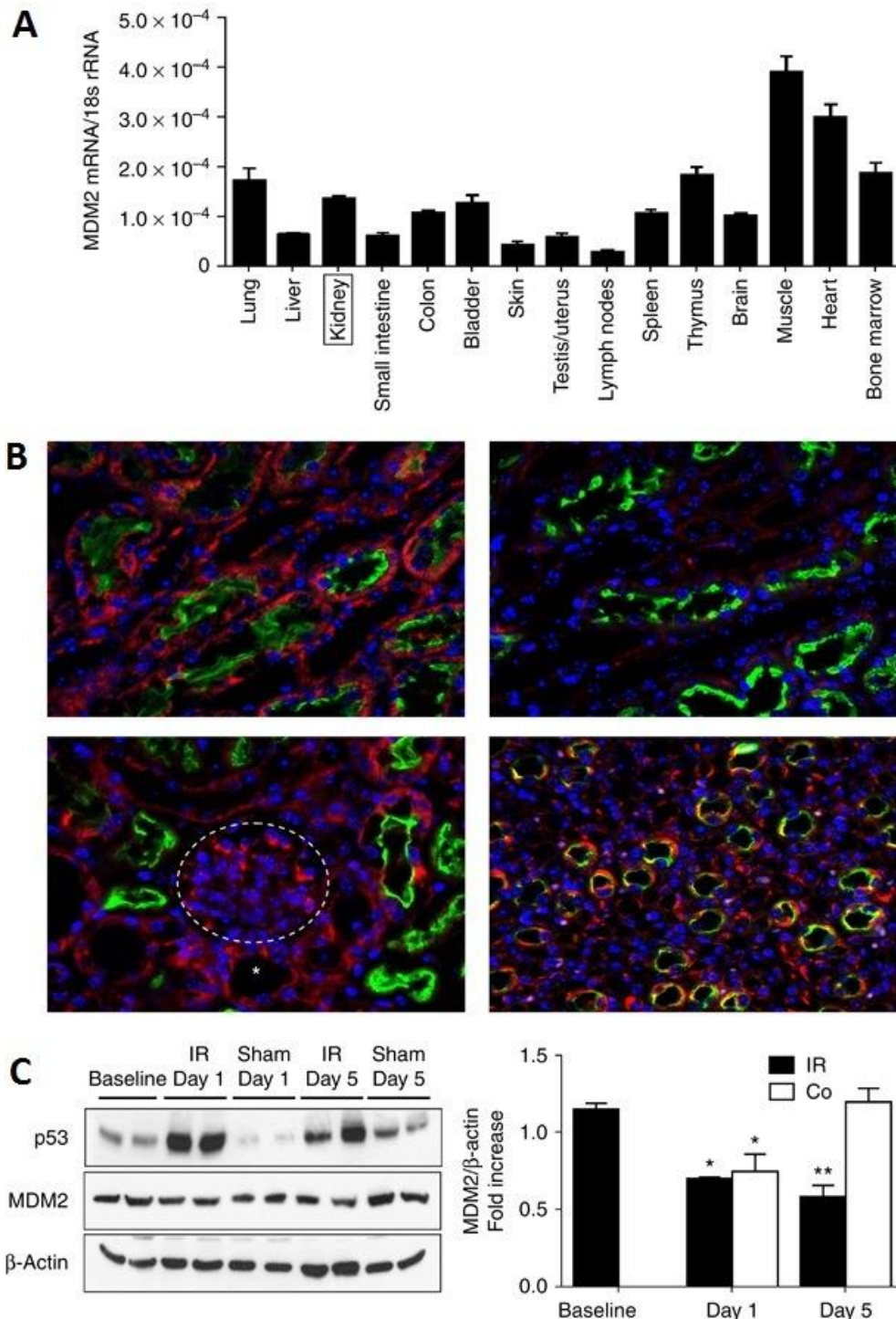


Figure 11 Renal murine double minute-2 (MDM2) expression A. Total mRNA was isolated from different organs of adult C57BL/6 mice and MDM2 mRNA expression levels were quantified by reverse transcription-polymerase chain reaction. Data are expressed as ratio of MDM2 mRNA to the respective 18s rRNA level in mean \pm s.e.m. from samples of five mice. B. MDM2 immunostaining (red) was performed on paraffin-embedded kidney samples of adult C57BL/6 mice. Lotus tetragonolobus lectin stains the brush border of proximal tubuli in green. 4,6-Diamidino-2-phenylindole stains nuclei in blue. Note the cytoplasmic staining pattern of MDM2 in proximal and distal tubuli in cortex (upper left) and medulla (lower right), which is absent in negative control stains (upper right). Few resident glomerular cells express MDM2 (lower left). Original magnification \times 400. C. The expression of MDM2 and p53 in ischemic-reperfusion (IR) and contralateral (Co) kidneys at 1 day and 5 days was determined by western blot analysis. β -Actin staining is shown as loading control. The graph on the right shows a quantitative analysis of several blots. * $P < 0.05$, ** $P < 0.01$ vs. baseline.

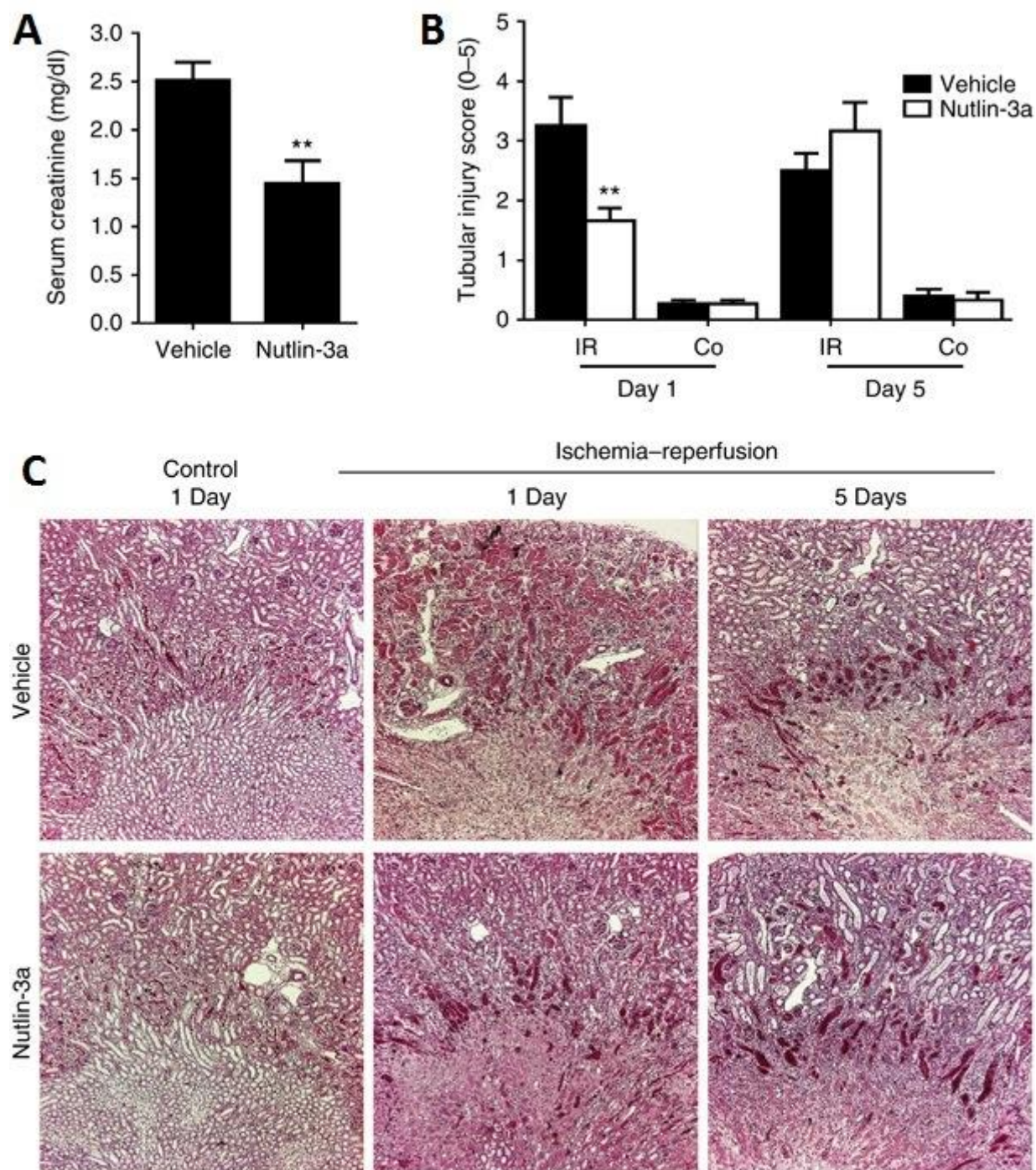


Figure 12 MDM2 blockade and postischemic acute kidney injury A. Serum creatinine levels were determined 24 h after bilateral renal artery clamping. Data are mean±s.e.m. from six mice in each group. B. Tubular injury was quantified on periodic acid–Schiff (PAS)-stained renal section at day 1 and 5 after unilateral renal artery clamping as described in methods. IR, ischemia–reperfusion kidney; Co, contralateral kidney. ** $P < 0.01$ nutlin-3a- vs. vehicle-treated mice. C. Representative images from PAS stains of all groups are shown at original magnification of $\times 100$.

MDM2 blockade significantly reduced the numbers of terminal deoxytransferase uridine triphosphate nick end labeling (TUNEL)-positive tubular cells (Figure 14). These results were

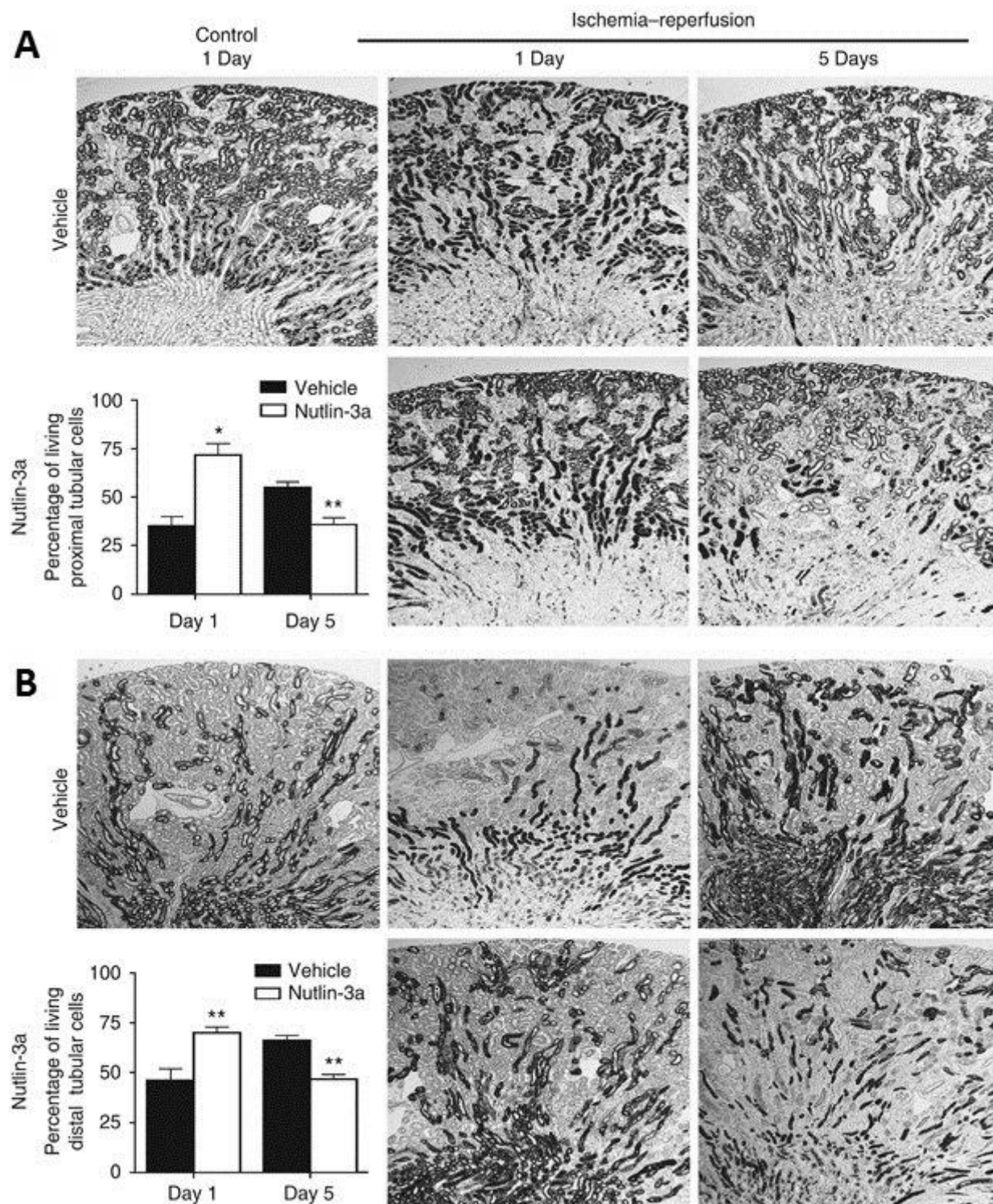


Figure 13 Postischemic injury of proximal and distal tubuli Lotus tetragonolobus lectin staining identified proximal tubuli (A) and Tamm–Horsfall protein staining identified distal tubuli (B) in postischemic kidneys. The quantitative assessment of tubuli with intact staining patterns is shown for each staining. Data are mean±s.e.m. from six mice in each group. * $P < 0.05$, ** $P < 0.01$ nutlin-3a- vs. vehicle-treated mice. All images are shown at original magnification of $\times 100$.

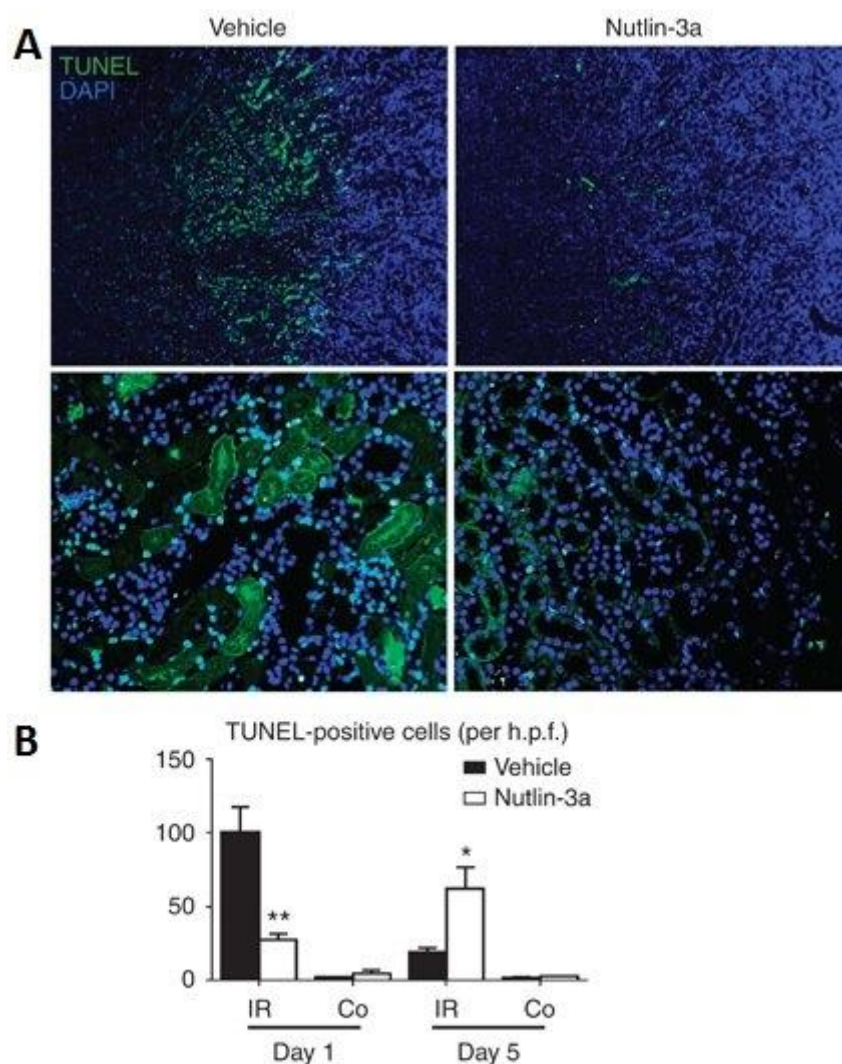


Figure 14 Renal cell apoptosis after renal ischemia–reperfusion A. TUNEL staining (green) identified apoptotic renal cells in postischemic kidneys. DAPI staining of cell nuclei is shown in blue. Original magnification of upper panel $\times 100$, lower panel $\times 400$. B. The quantitative assessment of TUNEL-positive cells per high-power field (h.p.f.) is shown as mean \pm s.e.m. from six mice in each group. * $P < 0.05$, ** $P < 0.01$ nutlin-3a- vs. vehicle-treated mice. Co, contralateral kidney; DAPI, 4,6-diamidino-2-phenylindole; IR, ischemia–reperfusion kidney; TUNEL, terminal deoxynucleotidyl transferase dUTP nick end labeling.

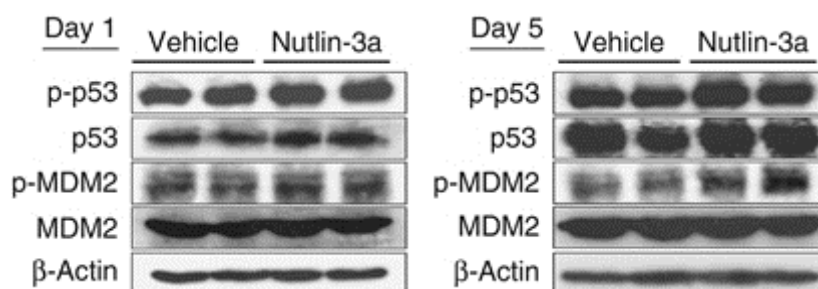


Figure 15 MDM2 and p53 protein expression in postischemic kidneys Total proteins were extracted from kidneys of vehicle- and nutlin-3a-treated C57BL/6 mice at day 1 and day 5 after renal artery clamping as indicated. β -Actin expression is shown as a loading control.

unexpected since the anticipation was that MDM2 blockade would enhance tubular cell apoptosis by promoting p53 activation in AKI¹⁴⁻¹⁶.

To verify the potential of nutlin-3a to activate p53 in vivo, western blots was performed from the kidney protein isolates for total p53 and for phosphorylated, i.e. activated, p53. As expected, nutlin-3a treatment slightly increased the protein levels of p53 at 24h after renal artery clamping (Figure 15), presumably by inhibiting MDM2-mediated p53 degradation. Furthermore, nutlin-3a treatment slightly increased the protein levels of activated p53 and also the expression of p53-dependent apoptotic genes (Figures 15 and 16A), whereas the levels of MDM2 and phosphorylated MDM2 remained unaffected by nutlin-3a treatment (Figure 15).

Together, MDM2 blockade with nutlin-3a stabilizes and activates p53 in the postischemic kidney. As p53 activation is known to contribute to postischemic tubular cell apoptosis and AKI, it has been assumed that the protective effect of MDM2 blockade on early AKI is mediated via another, p53-independent, pathomechanism of AKI.

4.1.3 MDM2 promotes postischemic renal inflammation in a p53-independent manner

To verify p53-independent effects of MDM2 blockade in early AKI, the same set of experiments were performed in *p53*-deficient mice (Figure 17). A comparison of AKI 24h after renal artery clamping revealed no difference in the renal phenotype of *wild-type* or *p53*-deficient mice with nutlin-3a treatment as evidenced by the tubular injury score or the percentages of lectin or Tamm–Horsfall protein–positive proximal and distal tubuli, respectively (Figure 17). Moreover, the numbers of infiltrating neutrophils, F4/80 macrophages, or CD3 T cells were not affected by the p53 genotype.

In analyzing other disease pathomechanism of AKI that could involve MDM2 in a p53-independent manner, postischemic renal inflammation was evaluated. Oxidative stress and cell necrosis are important stimuli of sterile inflammation, and inflammatory cytokines and infiltrating immune cells contribute to postischemic tissue injury^{20,149}. Ischemia–reperfusion strongly induced intrarenal mRNA expression of several pro-inflammatory mediators such as CXCL2, CCL2, interleukin (IL)-6, and the proapoptotic cytokine tumor necrosis factor (TNF)- α within 24h, an effect that was suppressed by MDM2 blockade (Figure 18A). Whereas IL-6 expression derived from different types of resident immune cells and renal parenchymal cells, MDM2 blockade suppressed the induction of TNF- α , CXCL2, and CCL2 mainly in intrarenal CD11c-positive dendritic cells (Figure 18B).

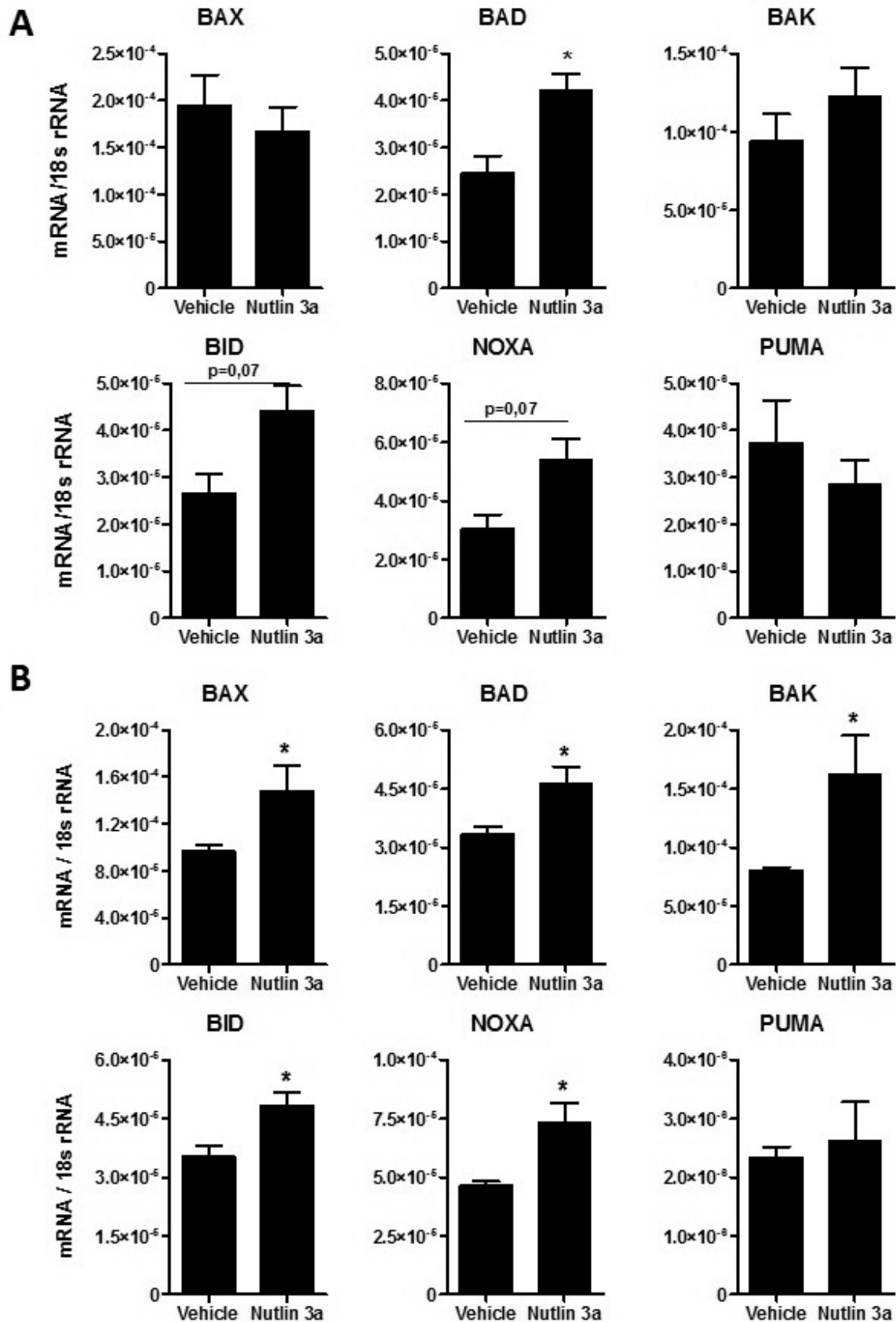


Figure 16 Nutlin-3a induces proapoptotic p53 target genes in postischemic kidneys Total RNA was extracted from postischemic kidneys after renal artery clamping (A) at day 1 (B) at day 5. The mRNA expression levels were determined for the indicated genes by real-time polymerase chain reaction. Data are expressed as mean of the ratio vs. the respective 18s rRNA level \pm s.e.m. * $P < 0.05$ vs. vehicle-treated mice.

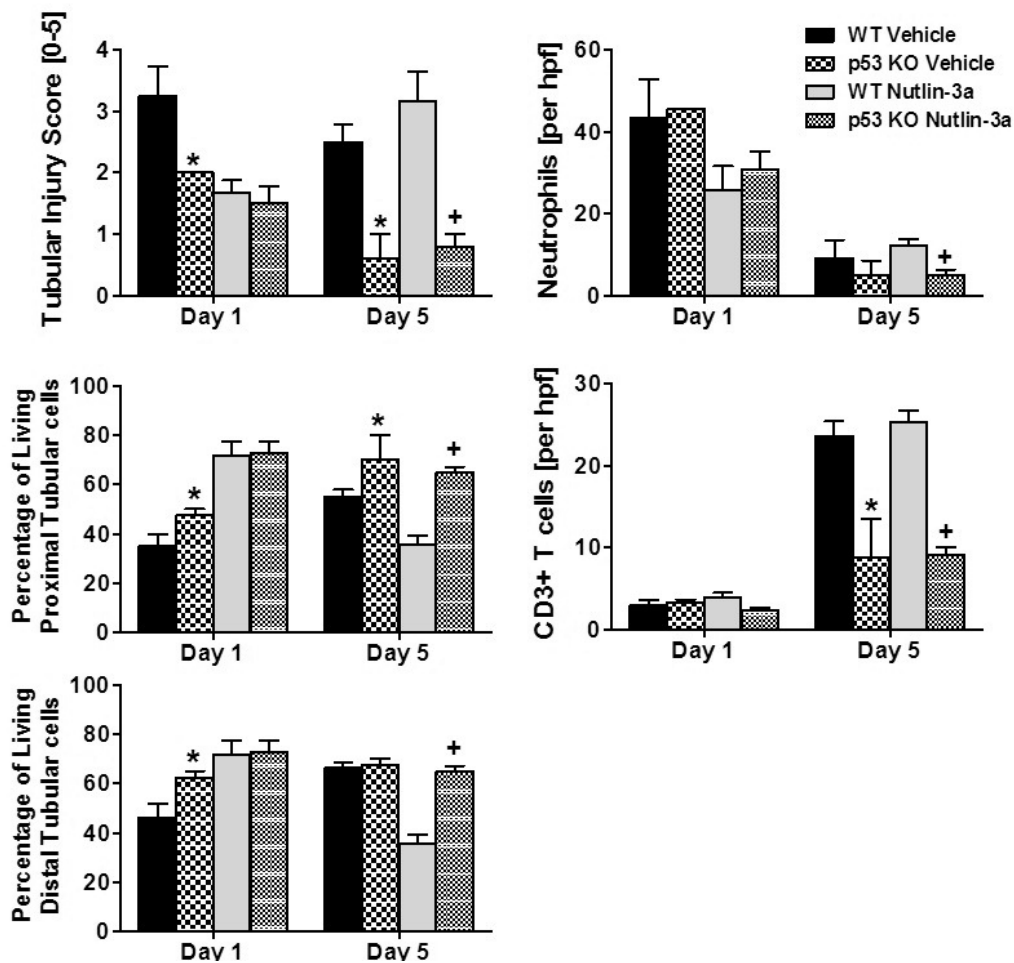


Figure 17 MDM2 blockade and acute kidney injury in wild-type (WT) and p53-deficient mice Left column: Tubular injury was quantified on periodic acid–Schiff (PAS)-stained (upper graph), *Lotus tetragonolobus* lectin-stained (middle graph), and Tamm–Horsfall protein-stained sections (lower graph) of postischemic kidneys at day 1 and 5 after unilateral renal artery clamping as described in methods. p53 KO=p53-deficient mice. Right column: The same sections were stained for neutrophils (upper graph), CD3+ T cells (middle graph), and F4/80+ macrophages (lower graph). Neutrophils and T cells were quantified per high-power field (h.p.f.) and expressed as mean±s.e.m. of 15 h.p.f. Macrophages were quantified by assessing the percentage of staining-positive area via digital morphometry and are expressed as mean±s.e.m. of 15 h.p.f. * $P < 0.05$ vs. wild-type vehicle treated mice, + $P < 0.05$ vs. wild-type nutlin-3a treated mice.

Accordingly, the numbers of infiltrating neutrophils (but not of F4/80+ macrophages or CD3+ T cells) were significantly reduced after 24h in postischemic kidneys of nutlin-3a-treated wild-type mice (Figure 19). There were no significant changes in MDM2 mRNA expressions in renal cells. The given knowledge about MDM2 inhibition by nutlin-3a rather suggests proapoptotic–antiproliferative effects that rule out the assumption of tissue protection during AKI. Together, MDM2 blockade ameliorates postischemic AKI by suppressing the sterile inflammatory response inside the kidney in a p53-independent manner.

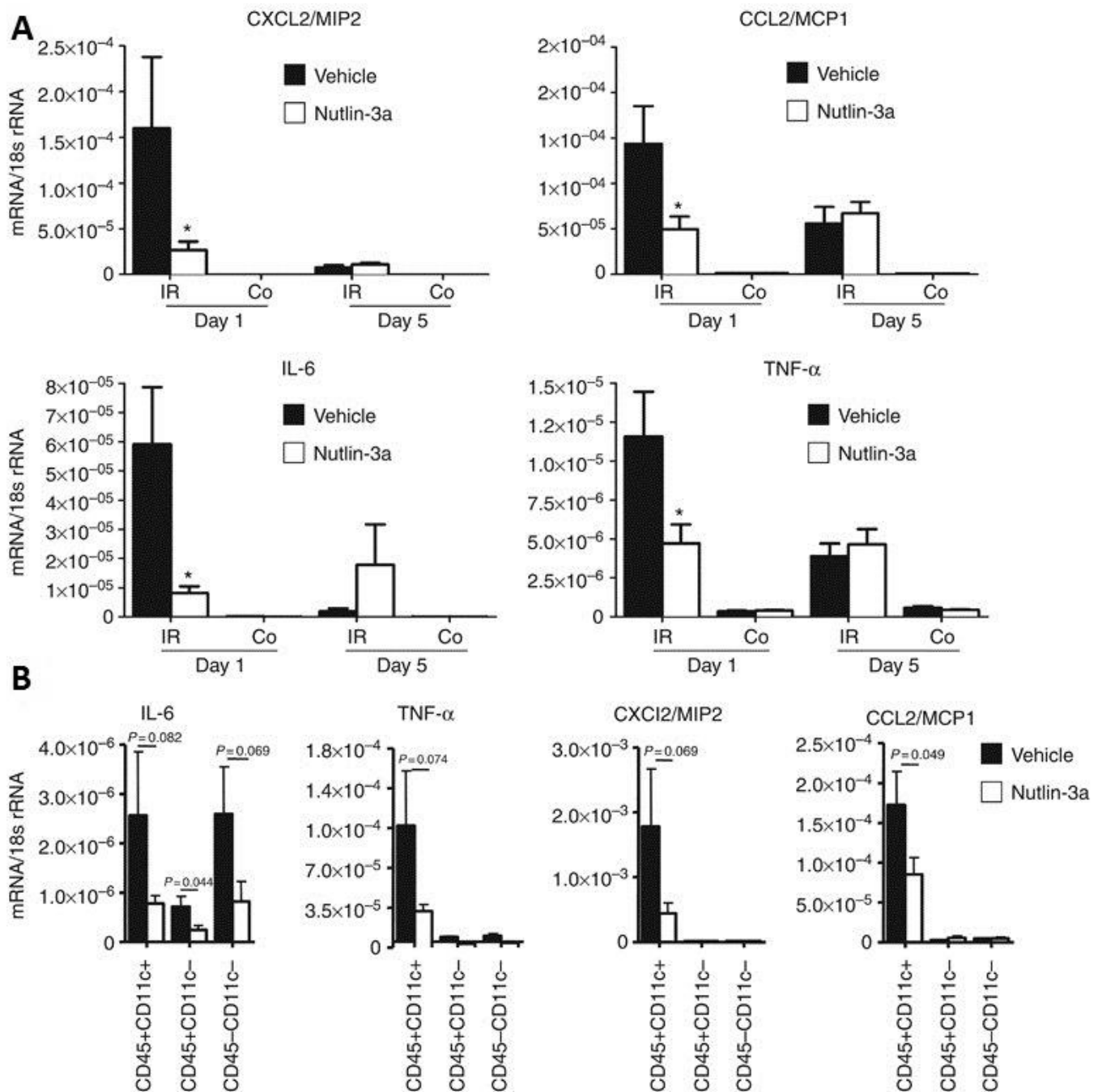


Figure 18 MDM2 blockade and inflammatory mediator expression in postischemic kidneys A. Total mRNA was prepared from vehicle- (black bars) or nutlin-3a-treated (white bars) C57BL/6 mice at day 1 or 5 after unilateral renal artery clamping as indicated. * $P < 0.05$ vs. vehicle-treated mice. B. CD45⁺ leukocytes and CD45⁻ renal parenchymal cells were separated from postischemic kidneys of both treatment groups 24 h after renal artery clamping by magnetic bead isolation as described in Materials and Methods. The CD45⁺ cell population was further separated into CD11c⁺ ‘dendritic cells’ and CD11c⁻ other leukocytes. The mRNA expression levels were determined for the indicated cytokines and chemokines by real-time polymerase chain reaction and are expressed as mean of the ratio vs. the respective 18s rRNA level \pm s.e.m. P -levels for the comparison of nutlin-3 vs. vehicle treatment are as indicated. Co, contralateral ‘sham’ kidney; IL, interleukin; IR, clamped kidney; TNF, tumor necrosis factor.

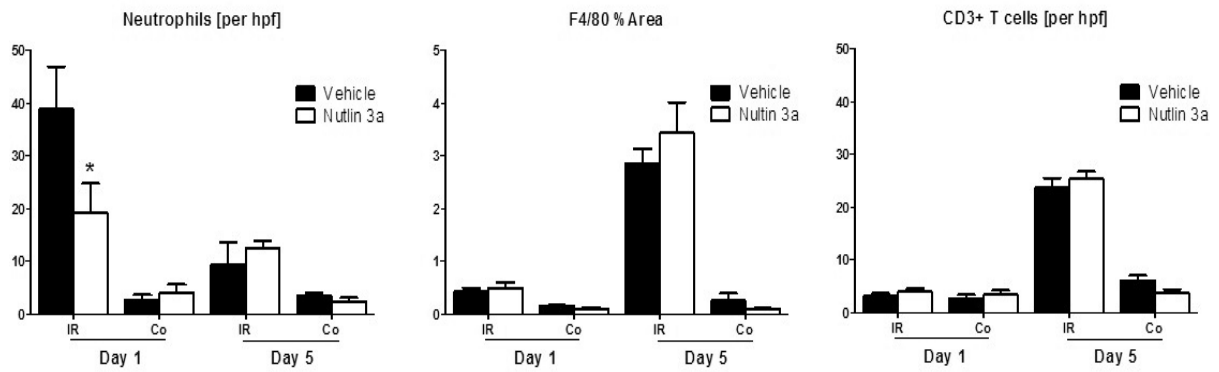


Figure 19 MDM2 blockade and leukocyte infiltrates in postischemic kidneys Renal sections from postischemic (IR) and contralateral kidneys (Co) were stained for different leukocyte markers as described in methods. Neutrophils and CD3+ T cells were counted per h.p.f. F4/80 positive macrophages were quantified by digital morphometry and data are expressed as percentage of h.p.f. Data are means \pm SEM of 15 h.p.f. from at least 6 mice in each group. * $p < 0.05$ versus vehicle-treated mice of the respective time point.

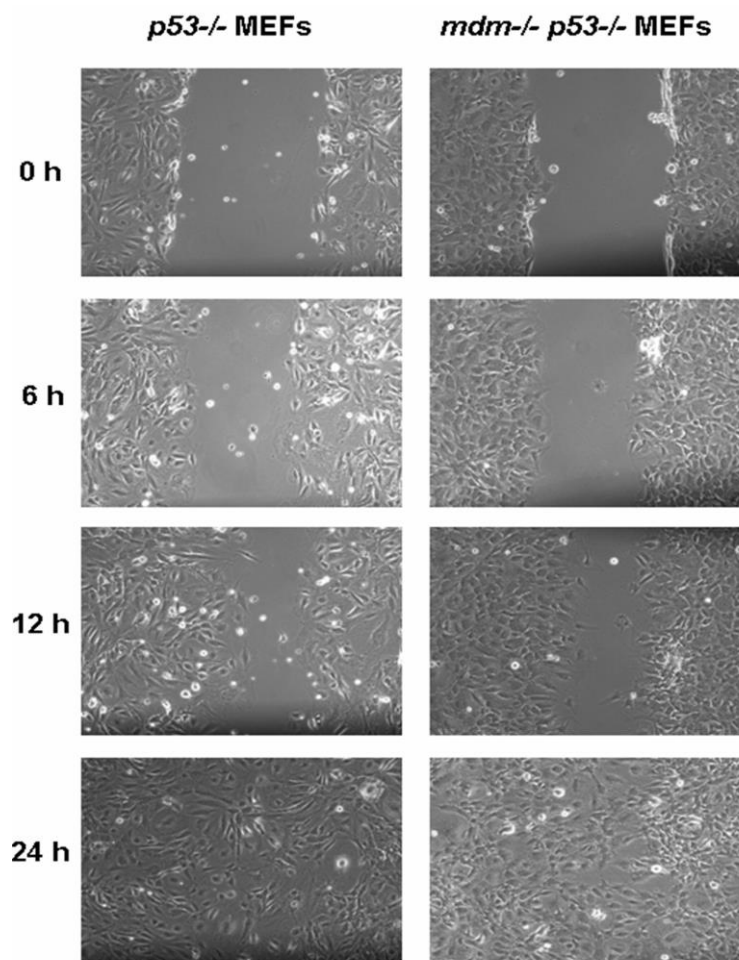


Figure 20 Scratch Assay A scratch of similar size was made into monolayers of *p53*-deficient and *p53/Mdm2*-double deficient MEFs. The images illustrate that the MDM2 genotype did not affect the time that was necessary to close the gap.

4.1.4 MDM2 is required for NF- κ B target gene transcription

How MDM2 can affect the expression of pro-inflammatory cytokines? To answer this question, *p53*-deficient and *p53/Mdm2* double-deficient mouse embryonic fibroblasts (MEFs) were used as a reliable and validated experimental system to identify *p53*-independent effects of MDM2¹²⁹. Because postischemic renal inflammation is largely mediated via MyD88 and TLR4²⁶, the TLR4/MyD88 agonist lipopolysaccharide (LPS) was used to activate the cells and cytokine production was measured after 18 h by enzyme-linked immunosorbent assay. Lack of MDM2 completely prevented LPS-induced TNF- α production and strongly reduced IL-6 release by *p53*-deficient MEFs (Figure 21A). Theoretically, the difference in cytokine production could be secondary to different cell survival or cell growth of the two cell lines. This was ruled out by comparing cell viability and scratch-induced wound healing of cell monolayers. Both cell lines grew at the same rate and healed scratch wounds within the same time interval (Figure 20). Thus, MDM2 is required for TLR-induced cytokine production, an effect that obviously does not require *p53*.

To further explore the molecular mechanism by which MDM2 promotes cytokine induction, the signaling events occurring after TLR4 activation were investigated by western blot analysis, namely the expression levels of nuclear factor (NF)- κ B p65, I κ B α , p38 mitogen-activated protein kinase (MAPK), p44/42 MAPK, and their phosphorylated forms. To verify the results, a similar set of experiments was performed in J774 macrophages treated with MDM2 inhibitor or vehicle. There were no significant differences found between the two genotypes of MEF, or between nutlin-3a-treated and untreated macrophages, that could explain the lack of LPS-induced cytokine induction in *p53/Mdm2* double-deficient MEFs (Figure 21B, Figure 22). Thus, MDM2 should modulate TLR-induced cytokine expression beyond the level of NF- κ B signaling.

Therefore, whether MDM2 modulates the capacity of NF- κ B to interact with the promoter region of its target genes, namely the binding activity of NF- κ B to the κ B site of the IL-6 promoter was determined. This was tested by gel-shift analysis of nuclear extracts that were prepared 1h after LPS stimulation in both types of cells. Lack of MDM2 significantly impaired LPS-induced NF- κ B binding activity to the IL-6 promoter (Figure 21C). NF- κ B activation by LPS in the *p53*-deficient and *p53/Mdm2*-double deficient MEFs was also examined by using NF- κ B-luciferase reporter assay and showed lower level of activation of NF- κ B in the cells lacking MDM2 (Figure 22).

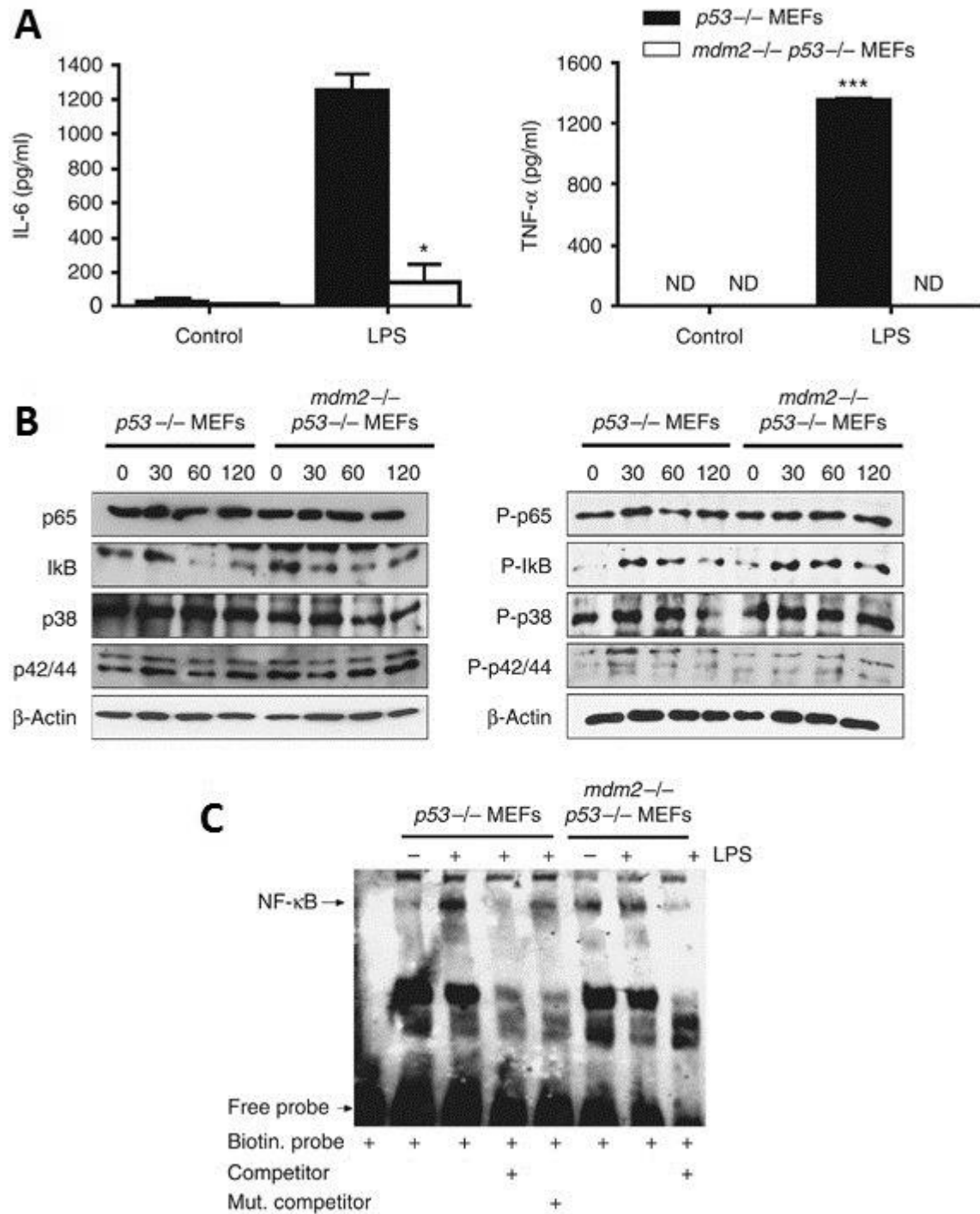


Figure 21 *In-vitro* studies with *p53*- and *p53/Mdm2*-deficient mouse embryonic fibroblasts A. Mouse embryonic fibroblasts (MEF) either deficient for *p53* or *p53/Mdm2* were stimulated with 5 μg/ml LPS, and IL-6 and TNF-α levels in the supernatants were measured after 18 h. B. Effect of LPS stimulation of TLR4 on different signaling pathways in both cell lines after 0.5, 1, and 3 h. The graph shows western blots for the respective TLR signaling proteins. β-Actin is shown as loading control. C. LPS-induced NF-κB binding to IL-6 promoter region DNA was studied in both cell lines by electrophoretic mobility shift assay. Binding site-specific competitor DNA and nonspecific noncompeting DNA were used to document NF-κB's interaction with the sequence-specific binding site. The data are representative of three independent experiments. IL, interleukin; LPS, lipopolysaccharide; MDM2, murine double minute-2; ND, not determined; NF-κB, nuclear factor-κB; TLR, Toll-like receptor.

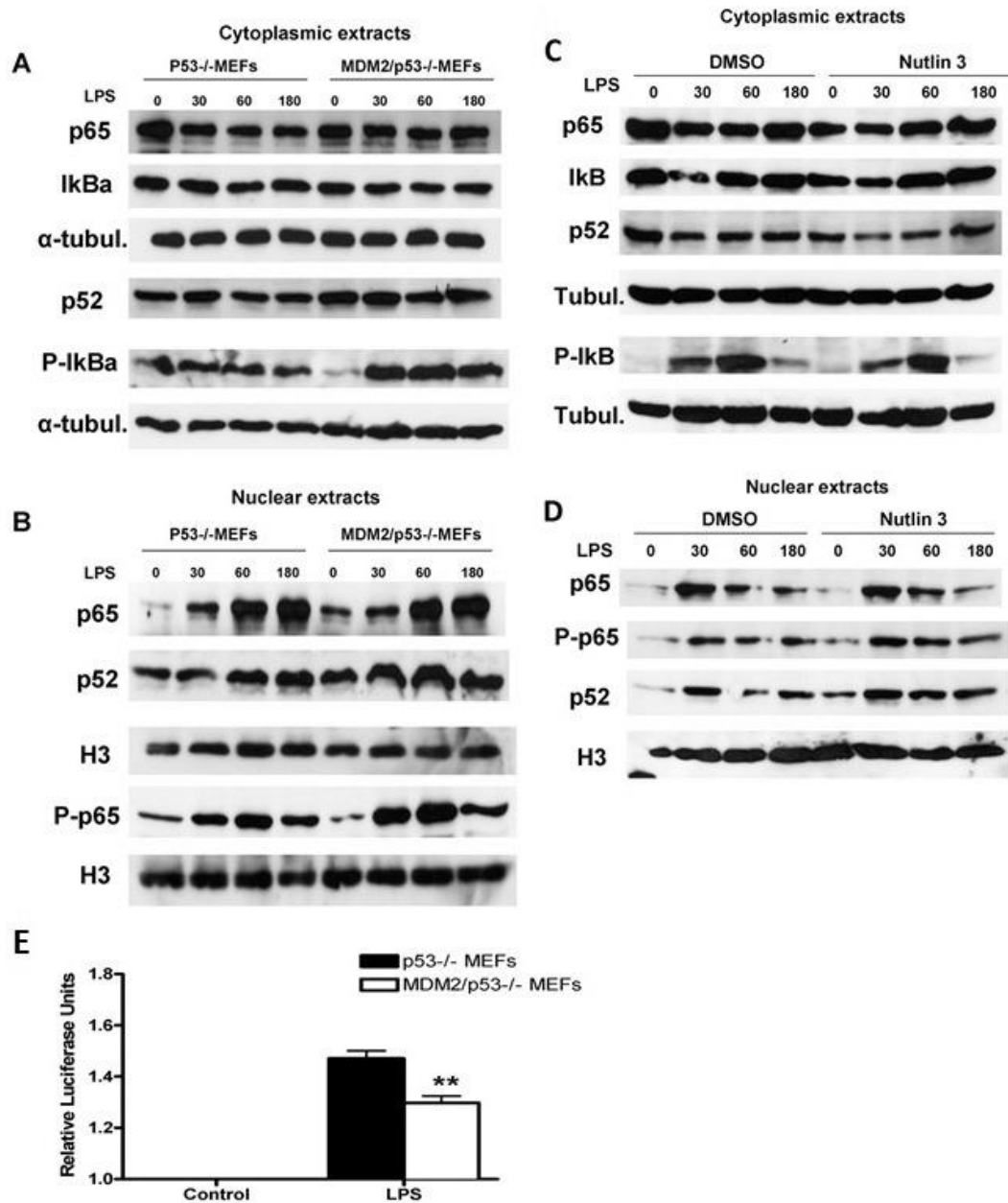


Figure 22 Effect of LPS stimulation on p53^{-/-} and MDM2/p53^{-/-} MEFs as well as on J774 macrophages treated with or without nutlin-3a and NF-κB luciferase activity. A,B. NF-κB signaling pathway in p53^{-/-} and MDM2/p53^{-/-} MEFs after 0, 5, 1, and 3 hours of LPS stimulation in cytoplasmic and nuclear protein extracts. C,D. NF-κB signaling pathway in J774 cells pretreated with nutlin-3a or DMSO after 0.5, 1, and 3 hours of LPS stimulation in cytoplasmic and nuclear protein extracts. Data were western blots for the respective NF-κB signaling proteins. α-tubulin and histone 3 are shown as loading controls for cytoplasmic and nuclear extracts respectively. Data are representative of three independent experiments. E. The p53-deficient and p53/Mdm2-double deficient cells were cotransfected with pNF-κB-luc and Renilla reporter vectors. 24 hours posttransfection the cells were treated with 1 μg/ml LPS or vehicle for 5 hours and processed using the dual luciferase reporter system (Promega). Activities of firefly and Renilla luciferases were measured by luminometer. Firefly luciferase activity was divided by Renilla luciferase activity to correct for differences in transfection efficiencies. Experiments were done in triplicates.

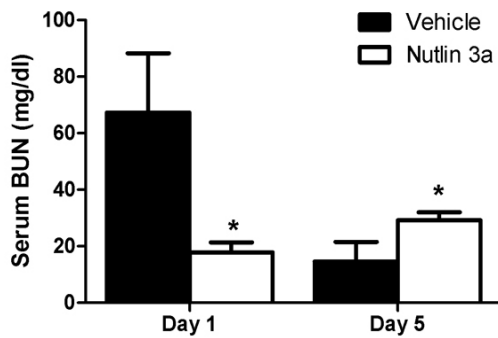


Figure 23 MDM2 blockade and postischemic AKI Serum BUN levels were determined at day 1 and day 5 after bilateral renal artery clamping for 30min. Data are means \pm SEM from 5 mice in each group

Together, MDM2 has a p53-independent function in facilitating the binding of NF- κ B to the promoter of its target genes, an effect that promotes TLR-induced expression of pro-inflammatory cytokines or chemokines and that appears to contribute to postischemic renal inflammation and AKI.

4.1.5 MDM2 drives tubular regeneration

Postischemic renal inflammation and tubular damage is transient and followed by tubular regeneration, which is similar to epithelial regeneration in other organs including dermal wound healing¹⁵⁰. Tubular regeneration involves and requires the proliferation of surviving tubular cells or tubular progenitors in each single nephron to restore the nephron's physiological functions. To address whether MDM2 does also modulate this phase of AKI, both renal arteries were clamped for 30 min and serum blood urea nitrogen was monitored, with or without nutlin-3a treatment. Nutlin-3a protected renal function at the early phase but aggravated it at later phase of tubular regeneration (Figure 23). Furthermore, the postischemic and contralateral kidneys were studied at day 5 after unilateral renal artery clamping for 45 min. Although MDM2 blockade had significantly reduced AKI at day 1 after ischemia–reperfusion, the tubular injury was rather aggravated at day 5 as compared with vehicle-treated wild-type mice (Figures 12B, 12C and 14). MDM2 blockade increased the numbers of TUNEL-positive cells in postischemic kidneys at day 5 (Figure 14B), indicating that MDM2 blockade enhanced tubular cell apoptosis in the regeneration phase of AKI. In fact, MDM2 blockade induced the intrarenal mRNA expression levels of several proapoptotic p53 target genes such as BAX, BAD, BAK, BID, and NOXA at day 5 after renal artery clamping (Figure 16B).

This effect was consistent with the initial hypothesis and also MDM2 blockade increased the intrarenal protein levels of p53 and activated p53 at day 5 (Figure 15), therefore the putative dependency of the proapoptotic effect of MDM2 blockade on p53 was questioned. Consistent with this concept, *p53*-deficient mice were found to be entirely protected from nutlin-3a-mediated aggravation of tubular injury and to have less renal immune cell infiltrates at day 5 as compared with wild-type mice (Figure 17). Furthermore, lack of MDM2 had no effect on the healing of scratched monolayers of *p53*-deficient MEFs (Figure 20).

In summary, MDM2 blockade with nutlin-3a suppresses the early postischemic renal inflammation by inhibiting the p53-independent effects of MDM2 on NF- κ B signaling. In contrast, nutlin-3a aggravates AKI in the healing phase by inhibiting the suppressive effect of MDM2 on p53-mediated cell cycle arrest and apoptosis.

The conclusion is MDM2 has a dual role in postischemic AKI as it mediates both renal inflammation and epithelial regeneration.

4.2 Part II MDM2 inhibition in adriamycin induced focal segmental glomerulosclerosis

4.2.1 MDM2 is expressed in glomerular epithelial cells in healthy & AN kidney

Confocal microscopy of Balb/c mouse kidneys localized MDM2 mostly to the perinuclear cytoplasm of podocytes as indicated by costaining with nephrin (Figure 24A). Podocyte foot processes that cover the circumference of the glomerular capillaries were MDM2 negative which excludes any direct contribution of MDM2 to the slit membrane or to the distal cytoskeleton of secondary foot processes (Figure 24A). Claudin-1 positive PECs also displayed a positive cytoplasmatic staining signal which, however, was less prominent (Figure 24B). Proximal and distal tubules were also strongly positive for MDM2 (Figure 24C). MDM2 staining patterns did not change throughout the course of AN (Figures 25 and 26). Western blotting confirmed that renal MDM2 expression was not regulated throughout AN, while p53 was induced with time (Figure 24D).

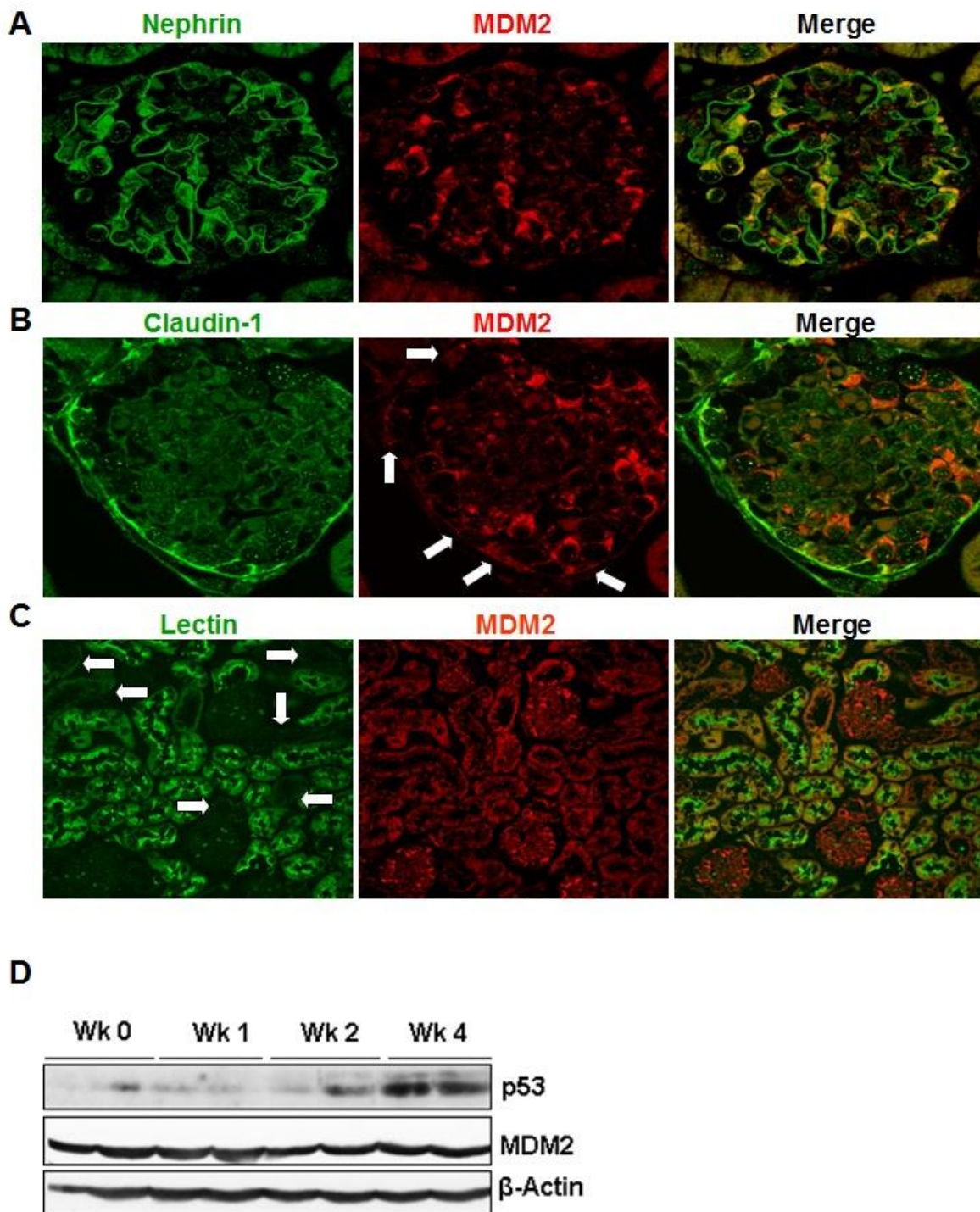


Figure 24 MDM2 expression in Balb/c mice A-C: MDM2 immunostaining (red) was assessed by confocal microscopy. A: In glomeruli the expression mostly co-localized with nephrin (green) which mark podocytes. B: Weaker MDM2 positivity is present also in parietal epithelial cells co-stained with claudin-1 (green) as indicated by white arrows. Original magnification 400x. C: In the tubulointerstitial compartment MDM2 staining localized to lectin positive proximal tubules as well as to lectin negative distal tubules (latter marked by white arrows). Original magnification 200x. D: The expression of p53 and MDM2 during the course of AN was determined by western blot. β -actin is shown as loading control.

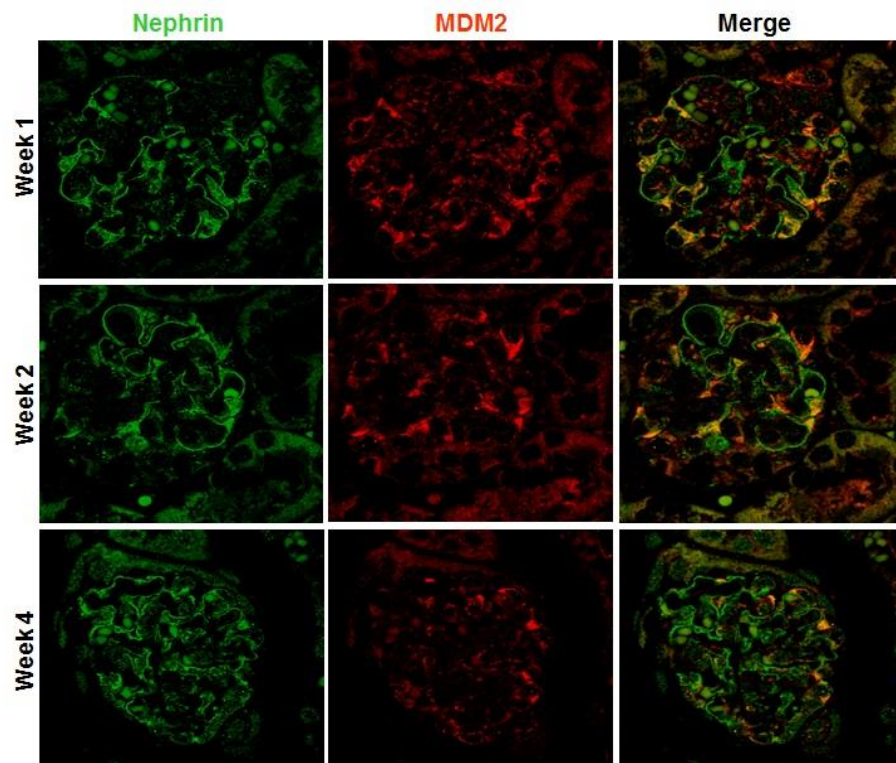


Figure 25 MDM2 expression in glomerulus throughout the course of AN MDM2 immunostaining (red) was assessed by confocal microscopy. In glomeruli the expression mostly colocalized with nephrin (green) which mark podocytes. Original magnification 400x.

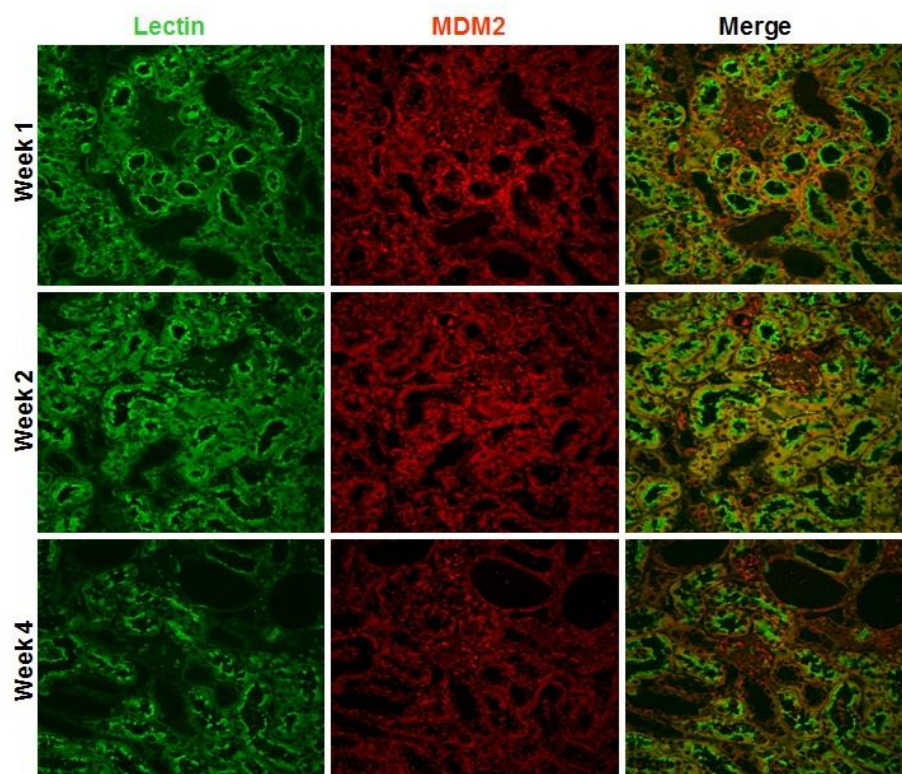


Figure 26 MDM2 expression in tubular compartment throughout the course of AN In the tubulointerstitial compartment MDM2 staining (red) localized to lectin positive proximal tubules (green) as well as to lectin negative distal tubules. Original magnification 200x.

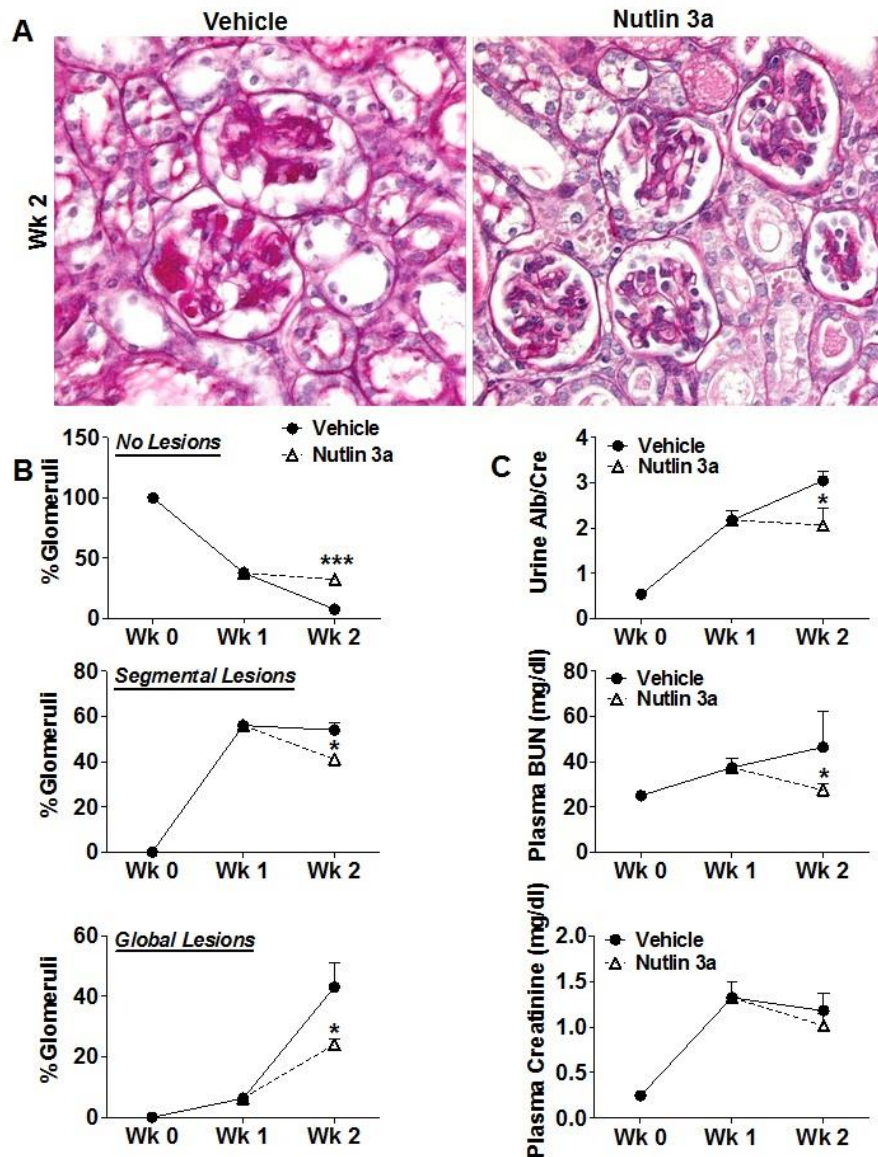


Figure 27 MDM2 blockade and glomerular disease in early AN A: Representative images of glomeruli from PAS stains of all groups are shown at a magnification of 200x. B: Glomerular lesions were quantified on PAS-stained renal sections as described in the text. C. Proteinuria, plasma creatinine and plasma BUN were determined at week 1 and week 2. Data are means \pm SEM. * $p < 0.05$ nutlin-3a- versus vehicle-treated mice at week 2.

Together, MDM2 is predominantly expressed in the monolayer of renal epithelial cells along the nephron, including podocytes, PECs, and tubular epithelia but its expression is not regulated during the progression of AN.

4.2.2 MDM2 blockade prevents glomerular pathology and renal dysfunction

The small molecule MDM2 antagonist nutlin-3a was used to determine the functional role of MDM2 during early and advanced AN. The first injection of adriamycin induced proteinuria

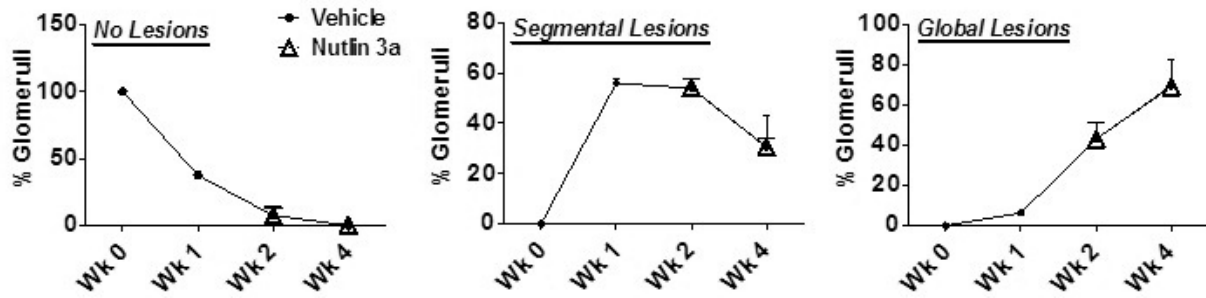


Figure 28 Semi-quantitative assessments of glomerular lesions Using these criteria Balb/c mice with AN displayed a progressive decrease in the numbers of glomeruli with no lesions in favor of progressively increasing numbers of glomeruli with global lesions. Treatment with nutlin-3a from week 2-4 had no significant effect on these measures. Data are mean \pm SEM for each time point.

and segmental lesions with tuft adhesions to Bowman's capsule which was associated with a rise in serum creatinine and BUN levels as markers of an impaired excretory renal function (Figures 27A-27C). Global glomerular lesions developed only after week 1 (Figure 27B and 28). At the end of week 1 one group of mice with AN received nutlin-3a and another group received vehicle. At the end of week 2 vehicle-treated mice had diffuse lesions (means affecting almost all glomeruli), of which around 50% displayed global lesions (means more than half of the glomerular tuft injured) (Figure 27B). This was associated with a further increase of proteinuria and BUN levels compared to week 1 (Figure 27C). Nutlin-3a treatment significantly reduced this progression of glomerular injury in terms of all of these structural parameters as well as BUN levels (Figures 27A-27C).

Thus, MDM2 expression in glomerular epithelial cells contributes to the progression of glomerular pathology, proteinuria, and renal failure in early AN.

4.2.3 MDM2 blockade prevents glomerular inflammation and podocyte loss

Human and experimental FSGS is driven by the loss of podocytes^{61,110} hence, we quantified podocytes by co-staining for WT-1 and nephrin (Figure 29A). Healthy mice had an average of 15 WT-1/nephrin+ cells per glomerulus which decreased to around 8 and 6 at week 1 and 2 after injection, respectively (Figure 29B). Nutlin-3a treatment starting from the end of week 1 significantly increased the number of podocytes as compared to vehicle-treated mice at the end of week 2 (Figures 29A and 29B), a result consistent with nutlin-3a's effect on proteinuria (Figure 27C).

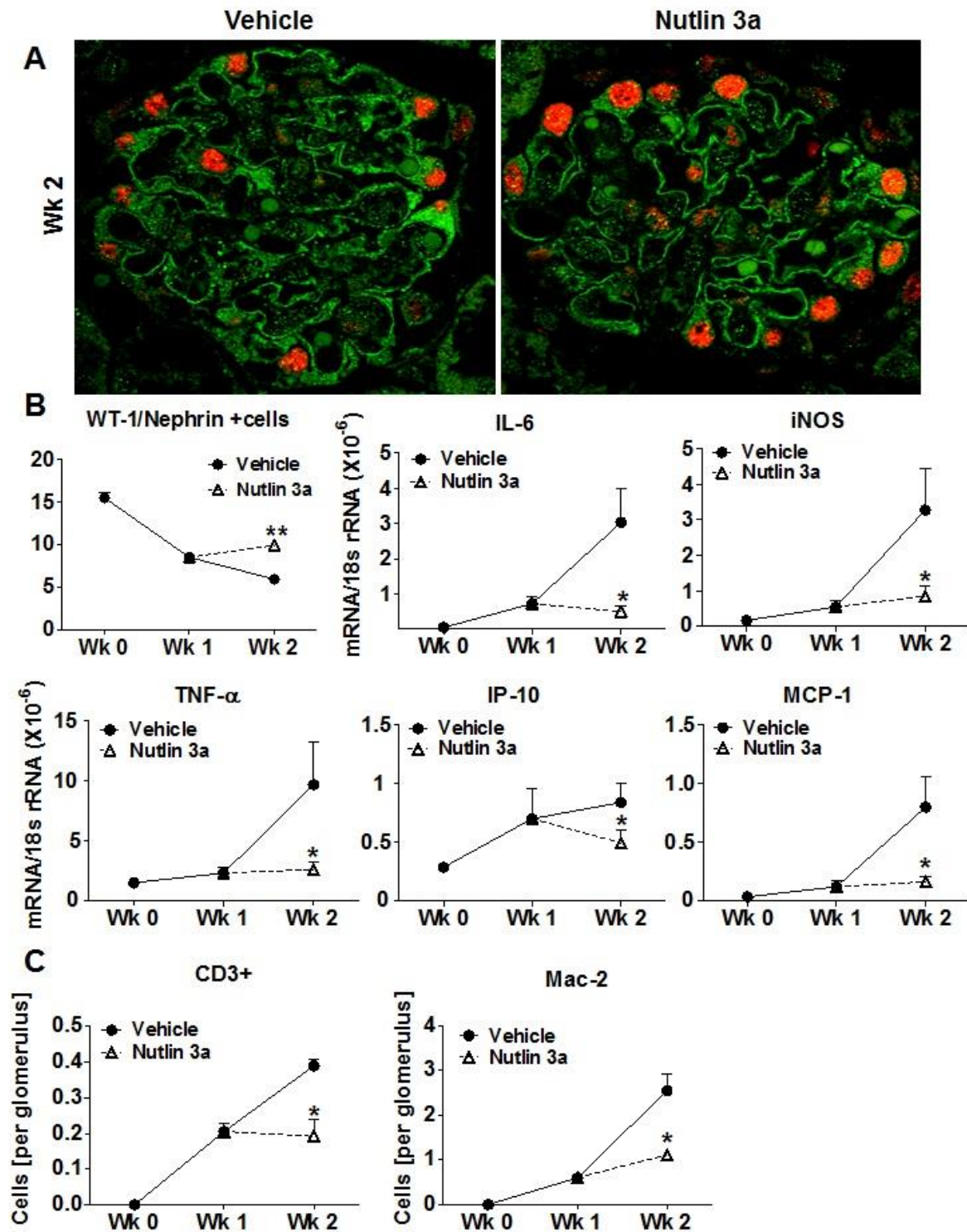


Figure 29 MDM2 blockade reduces podocytes injury and glomerular inflammation A: WT-1/nephrin co-staining was used to quantify differentiated podocytes in kidneys of vehicle- and nutlin-3a- treated kidneys. Original magnification 400x. B: Numbers of nephrin/WT-1 double-positive cells were quantified in both groups. B: Total mRNA was prepared from vehicle- and nutlin-3a- treated kidneys. The mRNA expression levels were determined for the indicated cytokines and chemokines by real-time PCR and expressed as mean of the ratio versus the respective 18s rRNA level. C: Renal sections from vehicle- and nutlin-3a- treated kidneys were stained for different leukocyte markers as described in methods. CD3+ T cells and Mac-2+ cells were counted per glomerulus. All data are means \pm SEM. * $p < 0.05$, ** $p < 0.01$ versus vehicle group.

Total kidney mRNA expression of IL-6, TNF- α , iNOS, CCL2, and IP-10/CXCL10 increased from week 1 to week 2 of AN (Figure 29B). Nutlin-3a treatment from the end of week 1 entirely prevented this induction of all of these pro-inflammatory mediators (Figure 29B). CCL2 and IP-10/CXCL10 are known to mediate macrophage and T cell recruitment into the kidney¹⁵¹, therefore, we assessed the numbers of glomerular macrophages and T cells by immunostaining. Nutlin-3a significantly reduced the numbers of intraglomerular Mac2+ macrophages and CD3+ T cells as compared to vehicle-treated mice with AN (Figure 29C) suggesting that MDM2 blockade can potently block glomerular inflammation.

Thus, MDM2 blockade prevents glomerular inflammation and podocyte loss in early AN.

4.2.4 Nutlin-3a prevents adriamycin-induced podocyte death by mitotic catastrophe

To see, whether MDM2 blockade with nutlin-3a had direct or indirect effects on podocyte death in AN, the effects of MDM2 blockade with nutlin-3a on adriamycin-induced podocyte death were studied *in-vitro*. CD133+/CD24+ renal progenitor cells were differentiated into mature podocytes before exposing them to adriamycin in the presence of either nutlin-3a or vehicle. Cell death was analyzed by propidium iodine (PI) and annexin V staining per flow cytometry. Adriamycin increased the numbers of PI positive podocytes, an effect that was significantly reduced by nutlin-3a (Figure 30A and 30B). Immunostaining of the mitotic spindle with tubulin and for cell cycle metaphase with histone-3 phosphorylated at serine 10 confirmed that adriamycin induced aberrant mitotic spindles and abnormal nuclear shapes (Figure 30C). Together, MDM2 enhances adriamycin-induced podocyte death by pushing podocytes to complete mitosis which can destroy podocytes through mitotic catastrophe. This process can be prevented by nutlin-3a. (*The presented in-vitro experiments were carried out in collaboration with University of Florence, Italy.*)

4.2.5 Effect of MDM2 blockade on p21 expression and podocyte mitosis in AN

To assess this phenomenon also *in-vivo*, we performed immunostaining for histone H3 phosphorylated at serine 10 (H3-P) and the podocyte marker podocin. H3-P marks the prophase of nuclear division and, therefore, displays cells that are about to complete mitosis. H3-P/podocin positivity was absent in healthy mouse kidneys (Figure 30D). AN in Balb/c mice was associated with the presence of some H3-P positive podocytes and their number was

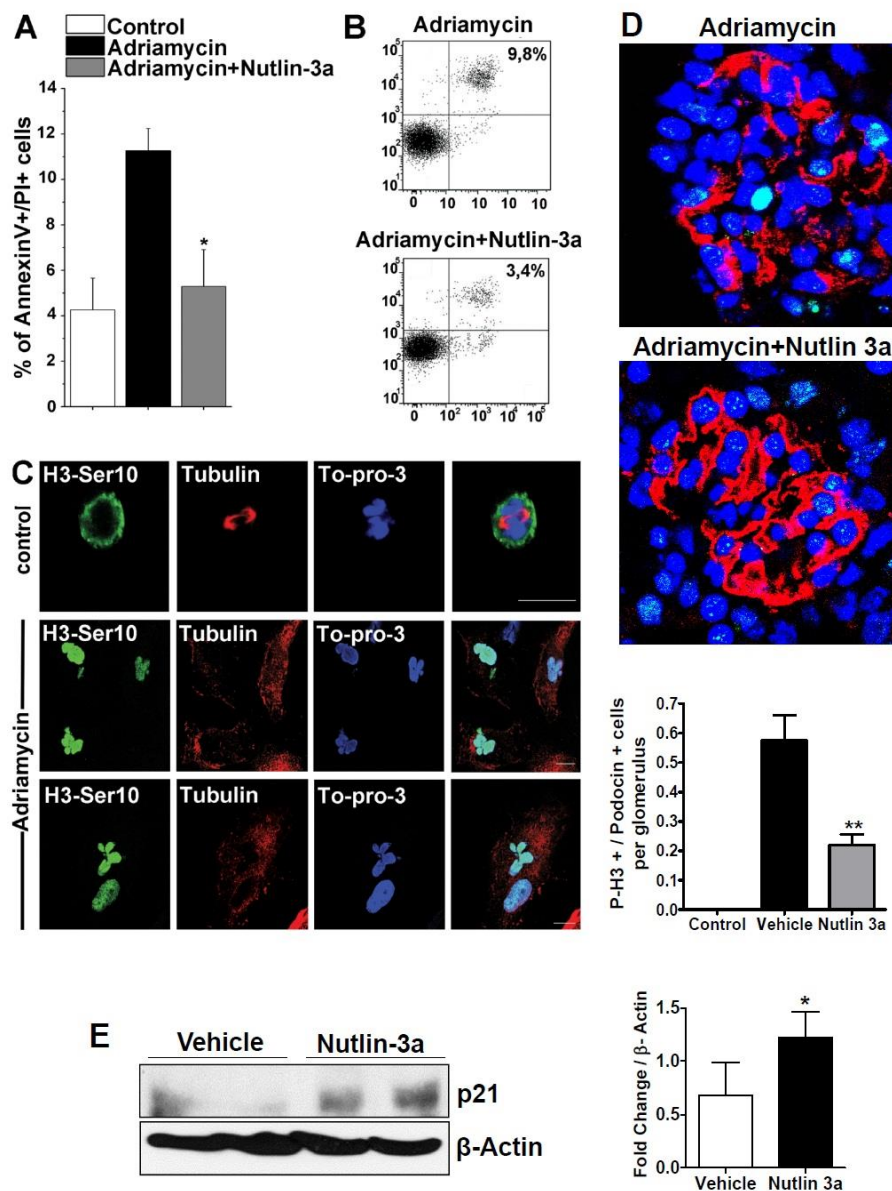


Figure 30 Nutlin-3a affects adriamycin-induced podocyte death *in-vitro* Podocytes were generated, cultured in VRADD medium, and exposed to adriamycin (ADR) as described in methods. A and B: Flow cytometry analysis of cultured podocytes for propidium iodide (PI) and annexin V 24 hours after stimulation. Data represent means \pm SD of 4 identical experiments (A) and representative dot blots are shown (B). * $p < 0.05$ versus the ADR (+vehicle) group. C: Immunostaining of podocytes for histone 3 phosphorylated at the serine 10 residue (H3-Ser10) serves as a marker for cells within the metaphase in green. Tubulin staining marks the mitotic spindle in red. To-pro-3 marks the chromatin inside the nucleus in blue. Note that immature podocytes proliferate by forming normal mitotic spindles and appropriate chromosomal alignment in the metaphase plate in between the spindles (control). Mature podocytes do not proliferate any more in culture but adriamycin induced mitotic events with abnormal assembly of the mitotic spindles with abnormal nuclear as an indicator of aberrant chromosomal division and mitotic catastrophe leading to cell death. Original magnification of x1000. D: Immunostaining for podocin (red), H3-Ser10 (yellow) double positive cells in renal sections of Balb/c mice with AN. To-pro-3 marks the chromatin inside the nucleus in blue at an original magnification of x400). Data in the graph are expressed as mean \pm SEM. ** $p < 0.01$ nutlin-3a- versus vehicle-treated mice at week 2. E: Western blot for p21 on mouse kidney isolates harvested from nutlin-3a and vehicle treated Balb/c mice at 2 weeks. Note that p21 expression is stronger upon nutlin-3a treatment. Quantification of p21 bands versus β -actin is shown on the right.

significantly reduced in nutlin-3a-treated mice (Figure 30D). By contrast, TUNEL positive podocytes could not be detected (not shown). This finding correlated with an increase of intrarenal p21 expression (Figure 30E), a cyclin-dependent kinase inhibitor mediating the p53-dependent G1 phase cell cycle arrest. Thus, MDM2 blockade with nutlin-3a prevents podocyte loss in AN by reducing podocyte mitosis, a process that is associated with podocyte depletion, proteinuria, and FSGS.

4.2.6 Delayed MDM2 blockade prevents the progression of AN

Progression of sclerosis of a single glomerulus involves the loss of the associated tubules so that eventually the entire nephron degenerates, a process involving its removal by phagocytes and replacement by fibrous tissue¹⁵². Therefore, progressive glomerulosclerosis is associated with tubular atrophy as well as a progressive inflammatory response and fibrosis of the tubulointerstitial compartment^{152,153}. The same applies for the later phase of adriamycin-induced glomerulosclerosis. In order to study how MDM2 blockade affects this phase of AN, mice with AN at 2 weeks after the first injection of adriamycin were randomized for treatment with either nutlin-3a or vehicle for 14 days and renal function and tubulointerstitial pathology were assessed at the end of week 4. MDM2 blockade significantly reduced plasma creatinine levels and BUN as compared to vehicle-treated mice; this was associated with significantly less tubular atrophy (Figures 31A and 31B). By contrast, proteinuria and glomerular damage were not all affected by nutlin-3a. This suggests that in advanced AN, MDM2 blockade prevents renal dysfunction mainly by preventing progression of tubular atrophy.

4.2.7 Delayed MDM2 blockade prevents AN-related tubulointerstitial inflammation

MDM2 blockade in early AN suppressed inflammation but not a proliferative epithelial response inside the glomerulus as evaluated by the numbers of Ki-67+ glomerular cells (Figure 32A). MDM2 blockade obviously also did not suppress tubular cell proliferation in the later phase as evaluated by the numbers of Ki-67+ tubular cells (Figure 32B). Therefore, it was speculated that MDM2 blockade improved the tubulointerstitial damage of advanced AN rather by suppressing renal inflammation. In fact, real time PCR of total kidney mRNA revealed that nutlin-3a treatment from week 2 to 4 significantly reduced the intrarenal mRNA expression of TNF- α , iNOS, CCL2, and IP-10/CXCL10 (Figure 33A). This was associated

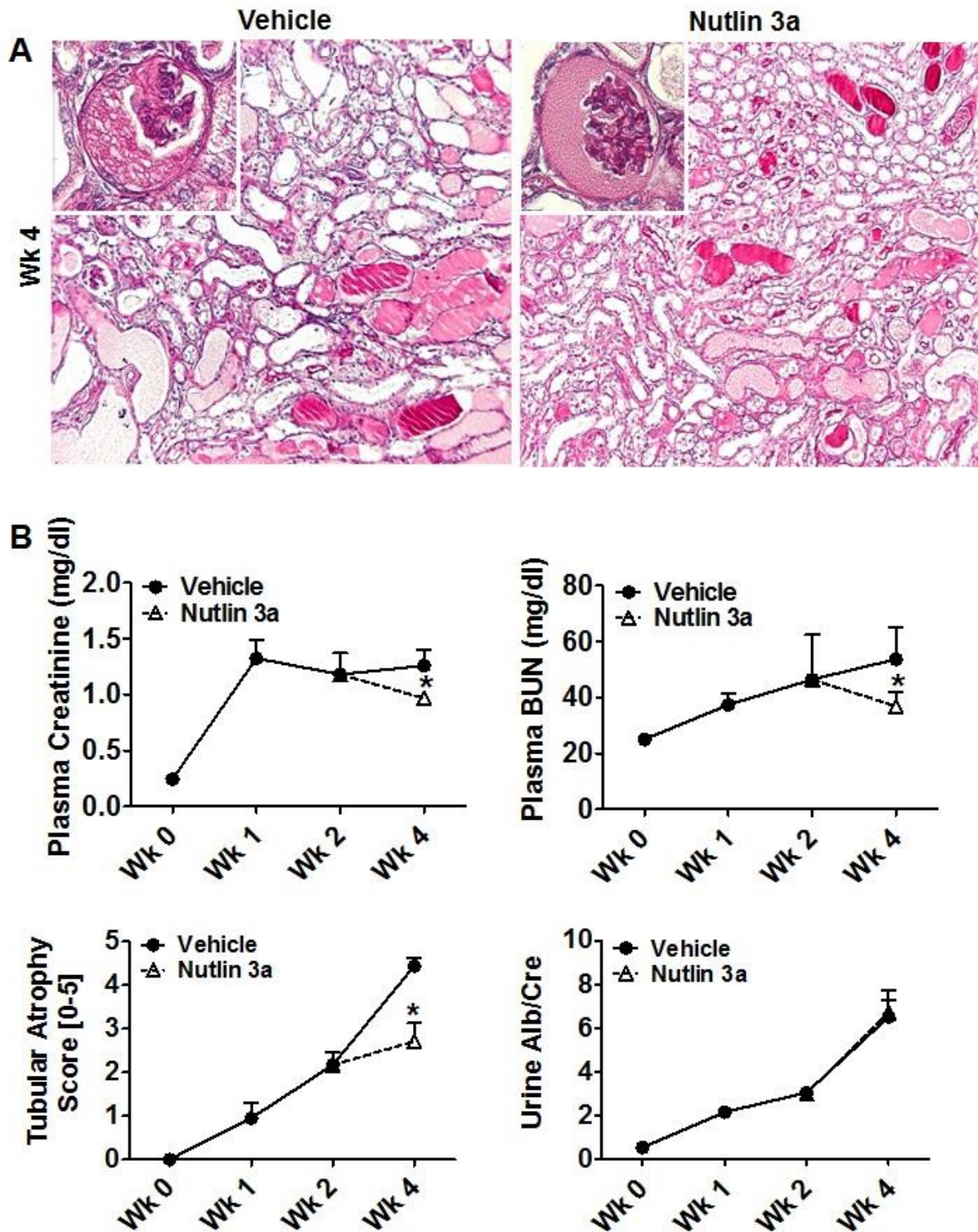


Figure 31 MDM2 blockade and progression of AN A: Representative images of kidneys at week 2 from PAS stains of vehicle- and nutlin-3a- treated groups are shown at a magnification of 100x. Inserts show representative glomeruli from the same kidneys at a magnification of 400x. B: Plasma creatinine, plasma BUN, and proteinuria were determined at several time points as indicated. Semi-quantitative analysis of tubular atrophy was compared between vehicle- and nutlin-3a- treated groups as described in methods. Data are means \pm SEM. * $p < 0.05$ nutlin-3a- versus vehicle-treated mice at week 4.

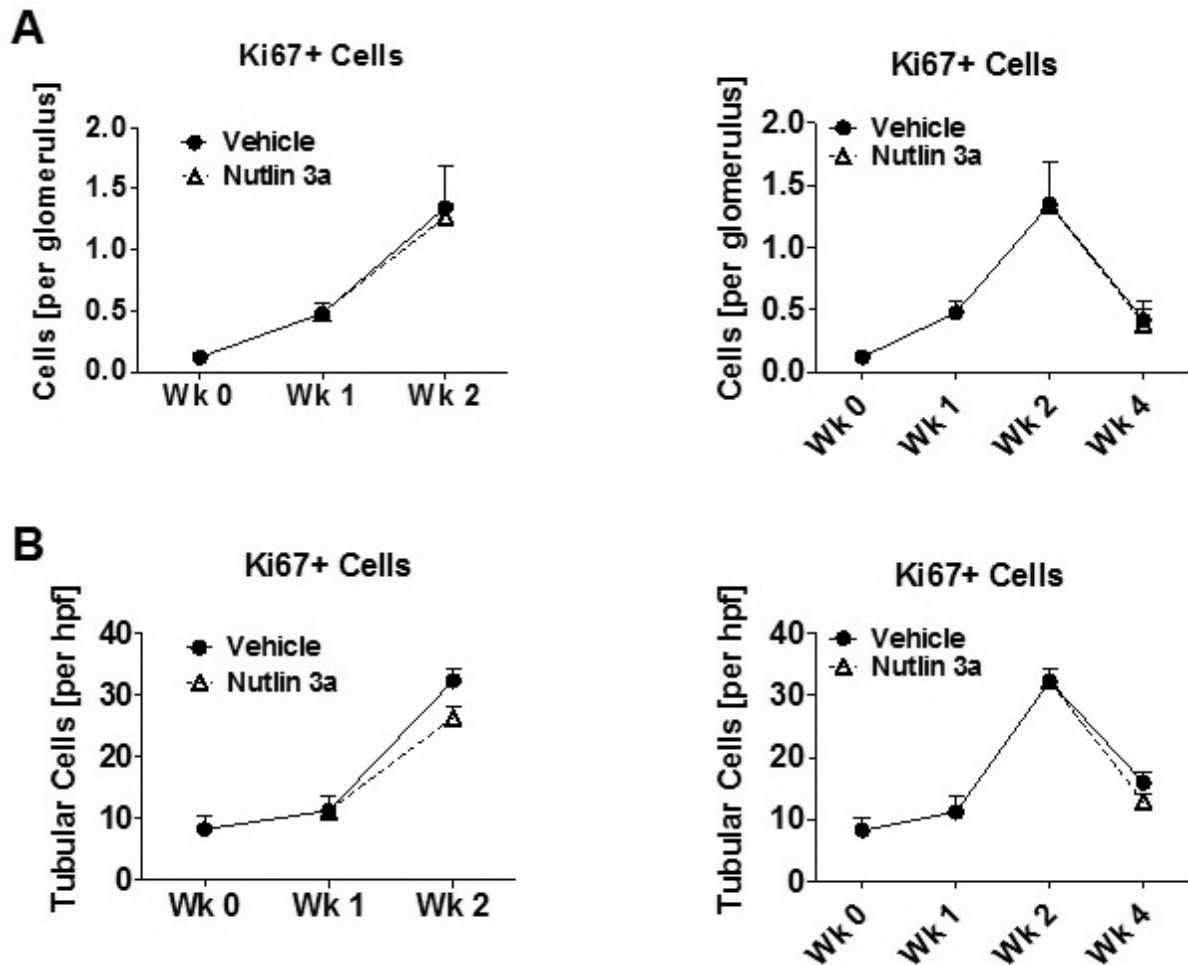


Figure 32 MDM2 blockade and proliferation of kidney cells Renal sections from vehicle- and nutlin-3a-treated kidneys were stained for different Ki-67, a cell proliferation marker as described in methods. A: Quantitative assessment of number of proliferating glomerular cells from vehicle- and nutlin-3a- treated kidneys at respective time points, from week 1-2 (left graph) and from week 2-4 (right graph). B: Quantitative assessment of number of proliferating tubular cells from vehicle- and nutlin-3a- treated kidneys at respective time points, from week 1-2 (left graph) and from week 2-4 (right graph). Data are means \pm SEM.

with a significant reduction of interstitial F4/80+ macrophages and CD3+ T cells (Figure 33B).

Thus, delayed MDM2 blockade prevents CKD progression and prevents tubular atrophy by suppressing intrarenal cytokine and chemokine expression and recruitment of leukocytes.

4.2.8 Delayed MDM2 blockade prevents AN-related interstitial fibrosis

The progression to ESRD involves renal tissue remodeling by replacement of lost renal parenchyma by extracellular matrix¹⁵⁴. As such, renal fibrosis is another histopathological

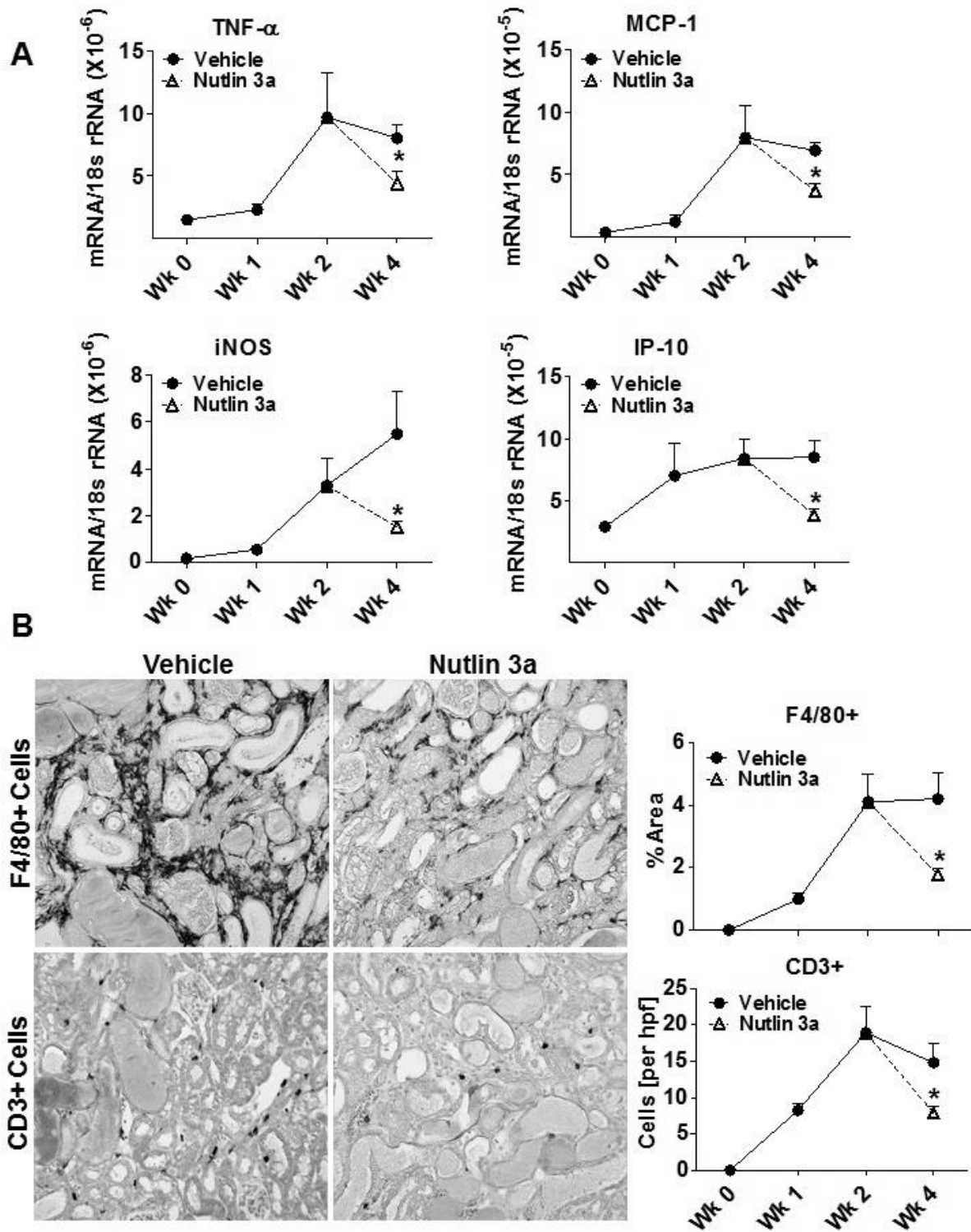


Figure 33 MDM2 blockade and tubulointerstitial inflammation in AN A: Total mRNA was prepared from vehicle- and nutlin-3a- treated kidneys. The mRNA expression levels were determined for the indicated cytokines and chemokines by real-time PCR and expressed as mean of the ratio versus the respective 18s rRNA level \pm SEM. p levels for the comparison of nutlin-3a- versus vehicle treatment are as indicated. B: Renal sections from vehicle- and nutlin-3a- treated kidneys at week 4 were stained for different leukocyte markers as described in methods. F4/80 positive macrophages were quantified by digital morphometry and data are expressed as percentage of hpf. CD3+ T cells were counted per hpf. Data are means \pm SEM of 25 hpf per kidney per group. * $p < 0.05$ nutlin-3a versus vehicle-treated mice at week 4.

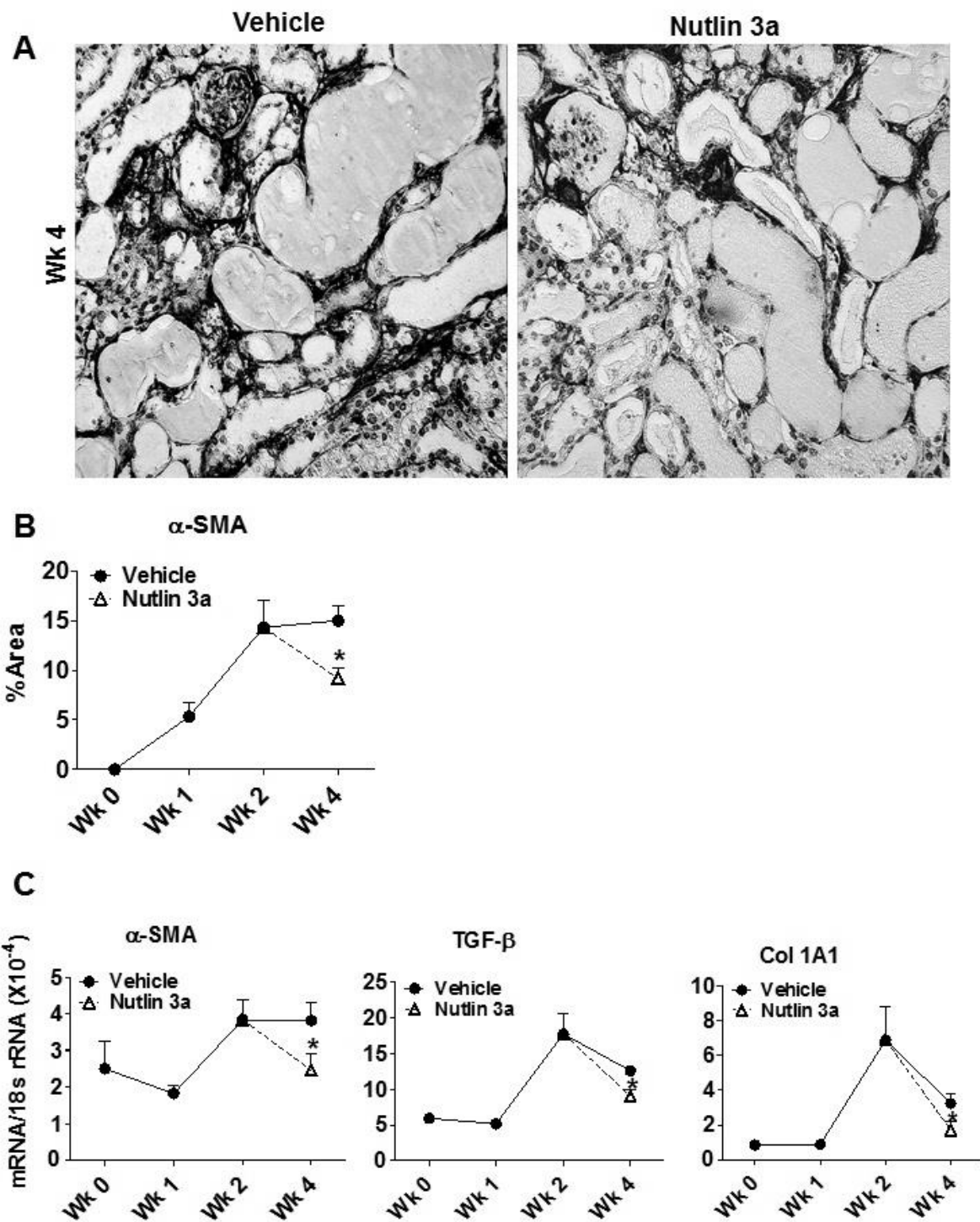


Figure 34 MDM2 blockade and interstitial fibrosis A: Representative images of kidneys at week 4 from α -SMA stains of vehicle- and nutlin-3a- treated groups are shown at a magnification of 200x. B: α -SMA positive area was quantified by digital morphometry and data are expressed as percentage of hpf. C: Total mRNA was prepared from vehicle- and nutlin-3a- treated kidneys. The target mRNA expression levels were determined by real-time PCR and expressed as mean of the ratio versus the respective 18s rRNA level \pm SEM. Data are means \pm SEM. * $p < 0.05$ nutlin-3a- versus vehicle-treated mice at week 4.

marker of CKD and a predictor of ESRD¹⁵³. MDM2 blockade from week 2 to week 4 with nutlin-3a improved intrarenal alpha-smooth muscle actin expression (Figure 34A and 34B) a marker of myofibroblasts that account for most of the extracellular matrix deposited in renal fibrosis¹⁵⁴. This process of transition is triggered by TGF- β , which was also found to be significantly reduced upon nutlin-3a treatment (Figure 34C). Also mRNA expression of alpha-smooth muscle actin and collagen-1alpha1 were significantly reduced (Figure 34C).

These data demonstrate that even delayed MDM2 blockade has the potential to prevent the progression of glomerulosclerosis to CKD due to subsequent tubulointerstitial inflammation and fibrosis.

5. Discussion

MDM2 negatively regulates p53 activity, mainly by inducing the ubiquitin-mediated degradation of p53, thereby suppressing coordinated cell cycle arrest or apoptosis and promoting cell survival and growth¹¹⁹. Therefore, it was hypothesized that the suppressive effect of MDM2 on p53 activity would prevent cell cycle arrest and cell death upon oxidative and/or genotoxic stress and similarly, that MDM2 blockade would aggravate postischemic AKI as well as AN. The finding of the present study that MDM2-mediated suppression of p53 is required for tubular regeneration in the healing phase of AKI is partially consistent with this concept. However, as an unexpected finding, MDM2 also had a p53-independent pro-inflammatory effect in the early injury phase of AKI. This is also true in chronic renal failure, since MDM2 blockade reduced the glomerular as well as tubulointerstitial inflammation in AN. This additional pro-inflammatory function of MDM2 was previously unknown.

The findings of the present study have multiple implications, viz.

1. MDM2 drives and links postischemic inflammation and epithelial healing, two major danger response programs upon acute tissue injuries.
2. MDM2 blockade protected the kidney from AKI despite enhanced p53 activation documenting that intrarenal inflammation, not oxidative stress per se, accounts for most of the tubular damage in postischemic AKI.
3. MDM2 forces the podocytes to undergo NF- κ B-mediated cell death, for example, mitotic catastrophe, a form of cell death resulting from abnormal mitotic spindles and chromosome segregation with multiple nuclei in postmitotic cells^{85,87}.
4. MDM2 blockade rather increased the podocyte number in AN despite p53 activation questioning the well-established concept of p53 dependent apoptosis as a common cause of podocyte loss in AN.
5. Podocyte MDM2 might have a similar role like podocyte mTOR in podocyte injury.
6. Therapeutic MDM2 blockade, e.g., in cancer, may hold the risk of impaired (epithelial) healing during AKI. On the other hand, MDM2 antagonists may delay or halt the progression of glomerular disorders to CKD.

The novel finding coming out of this study is that MDM2 blockade inhibits the induction of pro-inflammatory mediators that mediate leukocyte recruitment and tissue damage in the postischemic kidney. This sterile inflammatory response is triggered by danger-associated molecules that are released from dying cells and that activate TLR2 and TLR4 in renal parenchymal cells and in intrarenal dendritic cells^{5,20,25,26,28,149}. The common signaling adaptor MyD88 links TLR activation to NF- κ B translocation to the nucleus where it binds to the promoter of multiple pro-inflammatory target genes such as ILs, TNF, and chemokines¹⁵⁵. Blocking NF- κ B signaling consistently abrogates postischemic inflammation and AKI¹⁵⁶⁻¹⁵⁸, and lack of NF- κ B signaling inhibitors aggravates renal ischemia–reperfusion injury¹⁵⁹. The data showed here now document that MDM2 is required for TLR-induced NF- κ B signaling.

MDM2 was previously shown to induce the expression of the p65 subunit of NF- κ B by binding to the Sp1 site at the p65 promoter in acute lymphoblastic leukemia cells¹⁶⁰, but in the present study the MDM2-dependent regulation of p65, I κ B, or MAP kinases was not observed. Rather a nonredundant role of MDM2 for NF- κ B interaction with its binding site at a target gene promoter was observed. This observations are also consistent with a previous report showing that MDM2 blockade with nutlin-3a suppresses LPS-induced lung inflammation and that nutlin-3a impairs NF- κ B DNA binding in neutrophils without affecting other components of the TLR signaling pathway¹⁶¹. It is important to note that this pro-inflammatory role of MDM2 is p53 independent as clearly documented by the studies with *p53*- and *p53/Mdm2*-deficient cells and the studies in *wild-type* and *p53*-deficient mice.

In the postischemic kidney, this p53-independent pro-inflammatory effect of MDM2 operates simultaneously to its suppression of p53. This was documented by western blotting of kidney proteins from nutlin-3a-treated mice, which displayed a consistent increase of the protein levels of total p53 and its phosphorylated form. These data document the dual modulatory effect of MDM2 on p53, i.e., its E3 ligase activity that degrades p53 and its direct inhibitory effect on p53 activation¹⁶². Increased p53 activity mediates postischemic tubular cell death and renal dysfunction, and blocking p53 activation attenuates AKI^{9,10}. These data suggest that MDM2 blockade should aggravate postischemic AKI. But the observations in the present study were exactly the opposite, suggesting that in the early phase of AKI the p53-independent pro-inflammatory effect of MDM2 overrides its p53-dependent effects. This finding also clearly documents that postischemic AKI largely results from secondary inflammatory tissue damage as an unnecessary and inappropriate danger response to oxidative stress.

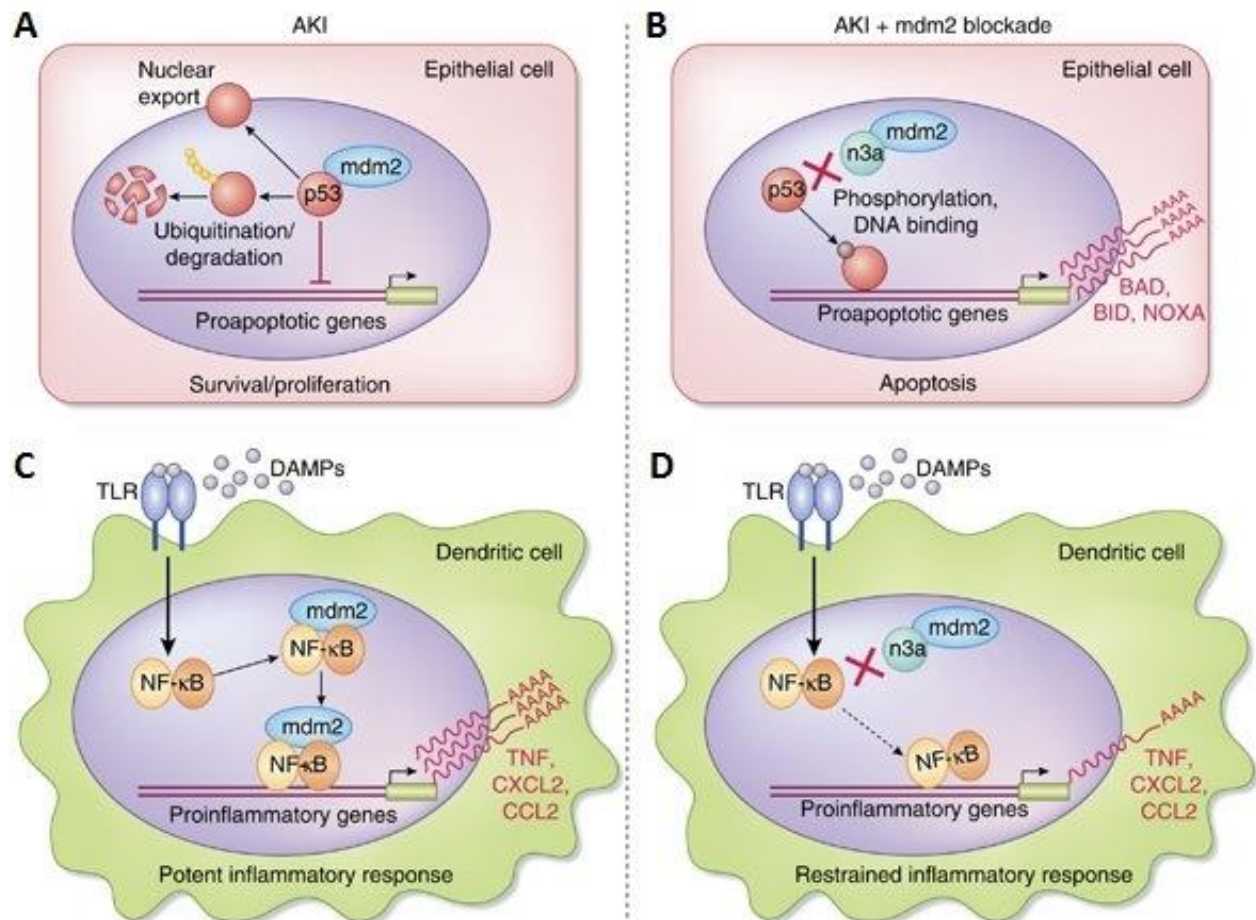


Figure 35 Dual effects of murine double minute-2 blockade during acute kidney injury A. In its best-described role, murine double minute-2 (MDM2) interacts with p53 via an N-terminal domain and targets p53 for nuclear export or, by E3 ubiquitin ligase activity, for proteosomal degradation. During AKI, this function of MDM2 may limit p53-mediated upregulation of proapoptotic genes and, by so doing, promote tubular epithelial cell survival and proliferation during the regenerative phase. B. In the presence of the MDM2 blocker nutlin-3a (n3a), p53-mediated transcription of proapoptotic gene products such as BAD, BID, and NOXA is enhanced, favoring increased epithelial cell apoptosis and inferior recovery of kidney function. C. In cells of the innate immune system such as intrarenal dendritic cells, MDM2 may facilitate binding of the transcription nuclear factor- κ B (NF- κ B) to promoter regions of genes encoding pro-inflammatory mediators such as tumor necrosis factor (TNF), CXCL2, and CCL2 in response to Toll-like receptor (TLR) signaling initiated by release of danger-associated molecular patterns (DAMPs). This property of mdm2 promotes a potent inflammatory response that may exacerbate early tissue damage and cell loss during AKI. D. For this mechanism of action of MDM2, the inhibitor nutlin-3a is associated with attenuated NF- κ B-driven transcription of pro-inflammatory genes, resulting in a restrained inflammatory response and reduced early tissue injury and loss of kidney function. (adapted from McNocholas BA *et. al.* ¹⁶³).

This p53-independent pro-inflammatory effect of MDM2 was also observed in AN. MDM2 blockade with nutlin-3a suppressed the renal cytokines and leukocyte infiltrates in the early (mostly glomerular injury) phase and the later (glomerular and tubulointerstitial injury) phase and therefore protected the mice from AN. This indicates that nutlin-3a as such suppresses

AN like other NF- κ B antagonists¹⁰⁰. From these and other studies it can be assumed that suppressing intraglomerular or tubulointerstitial cytokine and chemokine expression avoids the activation of endothelial cells which is a requirement for the adhesion and transmigration of leukocytes in both of these compartments of the kidney¹⁵¹. Leukocytes arriving into the pro-inflammatory environment of glomerular or tubular injury get activated and amplify the inflammatory milieu they found upon arrival which may indirectly contribute to podocyte loss and subsequent FSGS⁴⁰.

During the later phase of AKI, there is a shift of the balance between inflammation and regeneration (epithelial healing) towards regeneration¹⁶⁴. In accordance with this, in the present study we observed that once the acute inflammatory response had resolved, MDM2-mediated inhibition of p53's effects on the induction of proapoptotic genes and tubular cell death was dominant and was required for tubular regeneration. Epithelial healing is an important element of tissue regeneration after injury of outer or inner surfaces¹⁵⁰. The regeneration of injured tubular cells is conceptually identical to (scratch-induced) injury of cell monolayers in culture and involves the proliferation and migration of surviving epithelial cells⁴⁴. MDM2 blockade impaired this process 5 days after renal ischemia–reperfusion by tilting cell cycle regulation toward p53-dependent tubular cell apoptosis as evidenced by a lack of this phenomenon in p53-deficient mice. The capacity of the MDM2 antagonist nutlin-3a to impair epithelial healing may be clinically important when nutlins will be used to treat cancer^{142,165,166}, and it should be considered that the desired antiproliferative and proapoptotic effects of nutlins in cancer might affect tissue regeneration upon (renal) injuries or wound healing after surgery^{167,168}.

Inside the glomerulus, podocytes are terminally differentiated visceral epithelial cells. MDM2 staining of the kidney sections revealed that, being an epithelial cell lineage MDM2 is strongly expressed by podocytes. Moreover, the finding that MDM2 mediates NF- κ B-dependent death of tubular epithelial cells during postischemic renal inflammation and rather inhibits p53-dependent tubular cell apoptosis raised the question whether MDM2 also modulates podocyte survival upon injury and how. MDM2 inhibition reactivates p53-mediated tumor cell senescence and apoptosis^{28,119,142} making it a rational for use as an anticancer strategy. Therefore, the speculation was that MDM2 blockade would massively enhance podocyte apoptosis during glomerular injury. On the contrary, it has been found that it rather protects podocytes from an inflammatory form of cell death, known as mitotic catastrophe^{86,87,112,169}. These data question podocyte apoptosis as a dominant form of

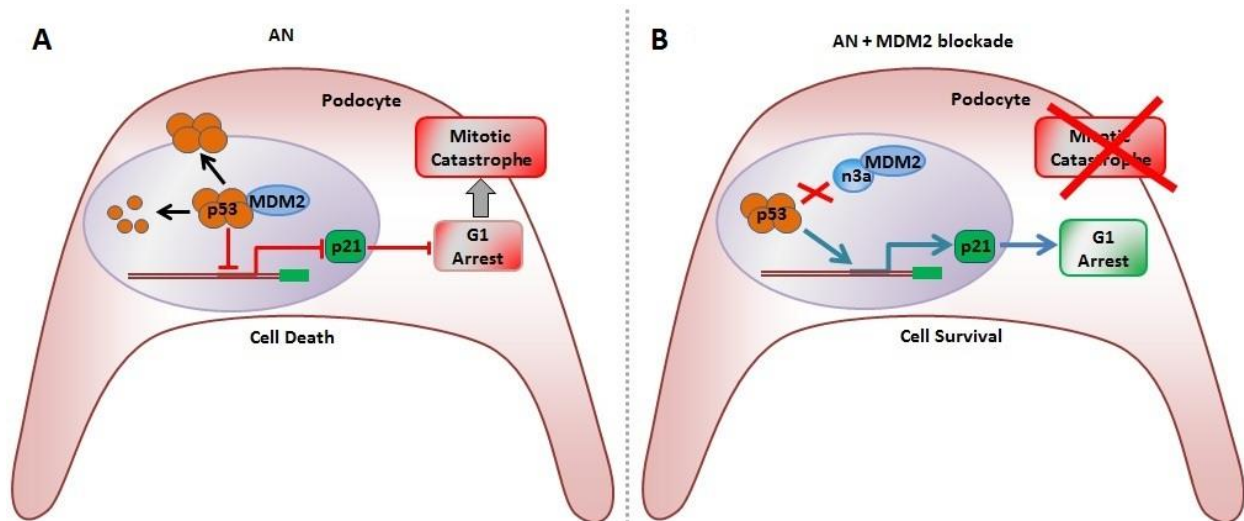


Figure 36 Effect of MDM2 blockade during adriamycin nephropathy A. MDM2 interacts with p53 and facilitates its nuclear export as well as proteosomal degradation by ubiquitylation. During AN, this function of MDM2 lowers the p21 levels, a G1 restriction point, and therefore forces the podocyte to undergo cell division (mitosis). As podocytes are highly differentiated cells, they cannot divide and thus die by a process called mitotic catastrophe. B. In the presence of MDM2 antagonist, nutlin-3a, the p53 dependent expression of p21 is increased. This increase in p21 (G1 restriction point) forbids the podocyte from undergoing cell division (mitosis), resulting in podocyte survival.

cell death during podocyte loss, at least in AN, and document that MDM2 has a non-redundant role in driving renal inflammation, podocyte loss, FSGS, and its progression to CKD. Current concepts of podocyte loss mostly name apoptosis, even though apoptotic podocytes are rarely captured *in-vivo*, e.g. by TUNEL staining⁸². The TUNEL+ podocytes were undetectable in AN in the present study, even upon MDM2 blockade which was expected to increase p53-dependent apoptosis. Thus, the p53-mediated apoptosis as a major element of podocyte loss in AN had been excluded. In contrast, MDM2 blockade rather increased podocyte numbers, which implies that MDM2 is a mediator of podocyte loss. The *in-vitro* studies revealed that MDM2 blockade directly protected podocytes from adriamycin-induced death. A careful analysis identified that MDM2 blockade protected podocytes from mitotic catastrophe. Physiologically, mitotic catastrophe prevents an oncogenic growth of aneuploid cells with significant DNA damage⁸⁵. In the present study adriamycin, an alkylating agent that inhibits topoisomerase II, kills podocytes *in-vitro* and *in-vivo* by inducing oxygen radical formation and DNA damage which then fuel to cause mitotic catastrophe^{86,112,170}. These data are in line with previous studies that had demonstrated that podocytes may enter the S-phase of the cell cycle to increase DNA synthesis and to undergo hypertrophy which they can survive until they get pushed to pass the p21-governed G1 restriction point and

complete the cell cycle^{83,86,88,170-173}. Notch activation, complement activity, and obviously also MDM2 signaling, suppress p21 so that podocyte loss can involve mitotic catastrophe whenever cell cycle arrest genes like p21 are suppressed or absent^{84,86,88,174}.

But why can podocytes not simply complete the cell cycle? Forming the mitotic spindle involves the entire actin cytoskeleton which is hardly compatible with maintaining the secondary foot-processes and, therefore, the slit membranes. Mature podocytes also lack proteins like aurora B which are necessary to complete cytokinesis, i.e. the division of the cytoplasm⁸⁶. Therefore, multinucleated podocytes can be observed in podocytopathies but are most common in collapsing FSGS^{173,175}. These multinucleated podocytes indicate aneuploid, i.e. severely damaged, podocytes which are destined to die, rather than to regenerate the injured podocyte monolayer^{61,173}.

The dual role of MDM2 on inflammation and cell cycle control is conceptually similar to the respective functional roles of the mTOR pathway¹⁷⁶. As such it is noteworthy that MDM2 blockade with nutlin-3a elicits identical effects on AN in Balb/c mice as well as renal IRI in both Balb/c and C57BL/6 mice as mTOR inhibition with rapamycin¹⁷⁷⁻¹⁷⁹. It is likely that podocyte MDM2 has a similar role like podocyte mTOR which was recently shown to be an important element of podocyte injury in diabetic glomerulosclerosis^{180,181}.

In summary, a rapid inflammatory response and subsequent epithelial healing represent effective response programs to minimize the risk of fatal infections after dermal injuries. In the kidney, however, postischemic inflammation is of no benefit in this regard but determines largely postischemic AKI. Also, the inflammatory environment generated after the podocyte injury in the kidney further contributes to the podocyte loss and glomerulosclerosis. The data presented here shows that MDM2 is constitutively and predominantly expressed in all epithelial segments of the nephron from podocytes and PECs to tubular epithelial cells all along the nephron. MDM2 is not regulated during acute and chronic kidney injury but still significantly contributes to renal immunopathology. MDM2 actively contributes to the early inflammatory response after renal IRI, promoting the inflammation in tubular compartment as well as during AN, promoting podocyte loss e.g. via mitotic catastrophe and the subsequent inflammatory response in the glomerular and tubulointerstitial compartment.

The data identifies MDM2 as a factor that drives early postischemic renal inflammation and subsequent epithelial healing via two independent functional properties, i.e., facilitating NF- κ B-target gene expression and suppressing p53-mediated cell cycle arrest and apoptosis respectively. Therefore, the data confirms MDM2 as a link between inflammation and

epithelial healing during acute kidney injury. Moreover, the data presented here indicates that, p53-dependent podocyte apoptosis does not contribute to podocyte loss in AN, which questions p53-dependent apoptosis as a common cause of podocyte loss *in-vivo*.

However, there are some limitations to the conclusions drawn from the present study. Viz. 1. The study lacks supporting evidence from human experiments. But these have to await the results of the ongoing clinical trials with nutlin-3a in cancer. 2. Similar experiments in cell type-specific *Mdm2*-deficient mice will be useful to understand the role of MDM-2 in a particular cell type during kidney injury. These are currently performed in the laboratory by another staff member. 3. Only a single dose of nutlin-3a was used throughout the study based on the previous studies in the laboratory. But it might be possible that higher doses are even more effective. 4. The conclusions were drawn from studying only one animal model of AKI and one of CKD. It might be possible that MDM-2 blockade leads to different results in other disease models.

To summarize, therapeutic MDM2 blockade, e.g., in cancer, may hold the risk of impaired (epithelial) healing during AKI. On the other hand, MDM2 antagonists may delay or halt the progression of glomerular disorders to CKD by reducing renal inflammation and by directly protecting podocytes from mitotic catastrophe.

6. References

1. Lameire, N., Van Biesen, W. & Vanholder, R. The changing epidemiology of acute renal failure. *Nature clinical practice. Nephrology* **2**, 364-377 (2006).
2. Thadhani, R., Pascual, M. & Bonventre, J.V. Acute renal failure. *The New England journal of medicine* **334**, 1448-1460 (1996).
3. Bonventre, J.V. & Yang, L. Cellular pathophysiology of ischemic acute kidney injury. *The Journal of clinical investigation* **121**, 4210-4221 (2011).
4. Eltzschig, H.K. & Eckle, T. Ischemia and reperfusion--from mechanism to translation. *Nature medicine* **17**, 1391-1401 (2011).
5. Basile, D.P. The endothelial cell in ischemic acute kidney injury: implications for acute and chronic function. *Kidney international* **72**, 151-156 (2007).
6. Molitoris, B.A., Dahl, R. & Geerdes, A. Cytoskeleton disruption and apical redistribution of proximal tubule Na(+)-K(+)-ATPase during ischemia. *The American journal of physiology* **263**, F488-495 (1992).
7. Kimura, T., *et al.* Autophagy protects the proximal tubule from degeneration and acute ischemic injury. *Journal of the American Society of Nephrology : JASN* **22**, 902-913 (2011).
8. Kelly, K.J., *et al.* Intercellular adhesion molecule-1-deficient mice are protected against ischemic renal injury. *The Journal of clinical investigation* **97**, 1056-1063 (1996).
9. Molitoris, B.A., *et al.* siRNA targeted to p53 attenuates ischemic and cisplatin-induced acute kidney injury. *Journal of the American Society of Nephrology : JASN* **20**, 1754-1764 (2009).
10. Imamura, R., *et al.* Intravital two-photon microscopy assessment of renal protection efficacy of siRNA for p53 in experimental rat kidney transplantation models. *Cell transplantation* **19**, 1659-1670 (2010).
11. Bonegio, R. & Lieberthal, W. Role of apoptosis in the pathogenesis of acute renal failure. *Current opinion in nephrology and hypertension* **11**, 301-308 (2002).
12. Daemen, M.A., *et al.* Inhibition of apoptosis induced by ischemia-reperfusion prevents inflammation. *The Journal of clinical investigation* **104**, 541-549 (1999).
13. Amaral, J.D., Xavier, J.M., Steer, C.J. & Rodrigues, C.M. The role of p53 in apoptosis. *Discovery medicine* **9**, 145-152 (2010).

14. Dagher, P.C. Apoptosis in ischemic renal injury: roles of GTP depletion and p53. *Kidney international* **66**, 506-509 (2004).
15. Homsy, E., *et al.* p53-Mediated oxidative stress and tubular injury in rats with glycerol-induced acute kidney injury. *American journal of nephrology* **33**, 49-59 (2011).
16. Zhou, L., *et al.* Activation of p53 promotes renal injury in acute aristolochic acid nephropathy. *Journal of the American Society of Nephrology : JASN* **21**, 31-41 (2010).
17. Linkermann, A., *et al.* Rip1 (receptor-interacting protein kinase 1) mediates necroptosis and contributes to renal ischemia/reperfusion injury. *Kidney international* **81**, 751-761 (2012).
18. Price, P.M. & Hodeify, R. A possible mechanism of renal cell death after ischemia/reperfusion. *Kidney international* **81**, 720-721 (2012).
19. White, L.E. & Hassoun, H.T. Inflammatory Mechanisms of Organ Crosstalk during Ischemic Acute Kidney Injury. *International journal of nephrology* **2012**, 505197 (2012).
20. Anders, H.J. Toll-like receptors and danger signaling in kidney injury. *Journal of the American Society of Nephrology : JASN* **21**, 1270-1274 (2010).
21. Nath, K.A. & Norby, S.M. Reactive oxygen species and acute renal failure. *The American journal of medicine* **109**, 665-678 (2000).
22. Akira, S. & Takeda, K. Toll-like receptor signalling. *Nature reviews. Immunology* **4**, 499-511 (2004).
23. Barton, G.M. & Kagan, J.C. A cell biological view of Toll-like receptor function: regulation through compartmentalization. *Nature reviews. Immunology* **9**, 535-542 (2009).
24. Rusai, K., *et al.* Toll-like receptors 2 and 4 in renal ischemia/reperfusion injury. *Pediatr Nephrol* **25**, 853-860 (2010).
25. Leemans, J.C., *et al.* Renal-associated TLR2 mediates ischemia/reperfusion injury in the kidney. *The Journal of clinical investigation* **115**, 2894-2903 (2005).
26. Wu, H., *et al.* TLR4 activation mediates kidney ischemia/reperfusion injury. *The Journal of clinical investigation* **117**, 2847-2859 (2007).
27. Allam, R., *et al.* Histones from Dying Renal Cells Aggravate Kidney Injury via TLR2 and TLR4. *Journal of the American Society of Nephrology : JASN* (2012).
28. Wu, H., *et al.* HMGB1 contributes to kidney ischemia reperfusion injury. *Journal of the American Society of Nephrology : JASN* **21**, 1878-1890 (2010).

29. Schaefer, L., *et al.* The matrix component biglycan is proinflammatory and signals through Toll-like receptors 4 and 2 in macrophages. *The Journal of clinical investigation* **115**, 2223-2233 (2005).
30. Jiang, D., Liang, J. & Noble, P.W. Hyaluronan as an immune regulator in human diseases. *Physiological reviews* **91**, 221-264 (2011).
31. Vabulas, R.M., *et al.* Endocytosed HSP60s use toll-like receptor 2 (TLR2) and TLR4 to activate the toll/interleukin-1 receptor signaling pathway in innate immune cells. *The Journal of biological chemistry* **276**, 31332-31339 (2001).
32. Powers, K.A., *et al.* Oxidative stress generated by hemorrhagic shock recruits Toll-like receptor 4 to the plasma membrane in macrophages. *The Journal of experimental medicine* **203**, 1951-1961 (2006).
33. Palsson-McDermott, E.M. & O'Neill, L.A. Signal transduction by the lipopolysaccharide receptor, Toll-like receptor-4. *Immunology* **113**, 153-162 (2004).
34. Li, Q. & Verma, I.M. NF-kappaB regulation in the immune system. *Nature reviews. Immunology* **2**, 725-734 (2002).
35. Wan, X., *et al.* Small interfering RNA targeting IKKbeta prevents renal ischemia-reperfusion injury in rats. *American journal of physiology. Renal physiology* **300**, F857-863 (2011).
36. Wan, X., *et al.* Inhibition of IkappaB Kinase beta attenuates hypoxia-induced inflammatory mediators in rat renal tubular cells. *Transplantation proceedings* **43**, 1503-1510 (2011).
37. Barnes, T.C., Anderson, M.E., Edwards, S.W. & Moots, R.J. Neutrophil-derived reactive oxygen species in SSc. *Rheumatology (Oxford)* (2012).
38. Friedewald, J.J. & Rabb, H. Inflammatory cells in ischemic acute renal failure. *Kidney international* **66**, 486-491 (2004).
39. Burne-Taney, M.J., *et al.* B cell deficiency confers protection from renal ischemia reperfusion injury. *J Immunol* **171**, 3210-3215 (2003).
40. Anders, H.J. & Ryu, M. Renal microenvironments and macrophage phenotypes determine progression or resolution of renal inflammation and fibrosis. *Kidney international* **80**, 915-925 (2011).
41. Persy, V.P., Verhulst, A., Ysebaert, D.K., De Greef, K.E. & De Broe, M.E. Reduced postischemic macrophage infiltration and interstitial fibrosis in osteopontin knockout mice. *Kidney international* **63**, 543-553 (2003).

42. Nadasdy, T., Laszik, Z., Blick, K.E., Johnson, L.D. & Silva, F.G. Proliferative activity of intrinsic cell populations in the normal human kidney. *Journal of the American Society of Nephrology : JASN* **4**, 2032-2039 (1994).
43. Bonventre, J.V. Dedifferentiation and proliferation of surviving epithelial cells in acute renal failure. *Journal of the American Society of Nephrology : JASN* **14 Suppl 1**, S55-61 (2003).
44. Humphreys, B.D., *et al.* Intrinsic epithelial cells repair the kidney after injury. *Cell stem cell* **2**, 284-291 (2008).
45. Kale, S., *et al.* Bone marrow stem cells contribute to repair of the ischemically injured renal tubule. *The Journal of clinical investigation* **112**, 42-49 (2003).
46. Lin, F., *et al.* Hematopoietic stem cells contribute to the regeneration of renal tubules after renal ischemia-reperfusion injury in mice. *Journal of the American Society of Nephrology : JASN* **14**, 1188-1199 (2003).
47. Duffield, J.S., *et al.* Restoration of tubular epithelial cells during repair of the postischemic kidney occurs independently of bone marrow-derived stem cells. *The Journal of clinical investigation* **115**, 1743-1755 (2005).
48. Humphreys, B.D., *et al.* Repair of injured proximal tubule does not involve specialized progenitors. *Proceedings of the National Academy of Sciences of the United States of America* **108**, 9226-9231 (2011).
49. Angelotti, M.L., *et al.* Characterization of Renal Progenitors Committed Toward Tubular Lineage and Their Regenerative Potential in Renal Tubular Injury. *Stem Cells* (2012).
50. Price, P.M., Safirstein, R.L. & Megyesi, J. Protection of renal cells from cisplatin toxicity by cell cycle inhibitors. *American journal of physiology. Renal physiology* **286**, F378-384 (2004).
51. Miller, R.P., Tadagavadi, R.K., Ramesh, G. & Reeves, W.B. Mechanisms of Cisplatin nephrotoxicity. *Toxins* **2**, 2490-2518 (2010).
52. Price, P.M., *et al.* Dependence of cisplatin-induced cell death in vitro and in vivo on cyclin-dependent kinase 2. *Journal of the American Society of Nephrology : JASN* **17**, 2434-2442 (2006).
53. Johnson, S.M., *et al.* Mitigation of hematologic radiation toxicity in mice through pharmacological quiescence induced by CDK4/6 inhibition. *The Journal of clinical investigation* **120**, 2528-2536 (2010).

54. Yang, L., Besschetnova, T.Y., Brooks, C.R., Shah, J.V. & Bonventre, J.V. Epithelial cell cycle arrest in G2/M mediates kidney fibrosis after injury. *Nature medicine* **16**, 535-543, 531p following 143 (2010).
55. Shapiro, G.I. Cyclin-dependent kinase pathways as targets for cancer treatment. *Journal of clinical oncology : official journal of the American Society of Clinical Oncology* **24**, 1770-1783 (2006).
56. Levey, A.S., *et al.* Definition and classification of chronic kidney disease: a position statement from Kidney Disease: Improving Global Outcomes (KDIGO). *Kidney international* **67**, 2089-2100 (2005).
57. Ju, W., Smith, S. & Kretzler, M. Genomic biomarkers for chronic kidney disease. *Translational research : the journal of laboratory and clinical medicine* **159**, 290-302 (2012).
58. Kitiyakara, C., Kopp, J.B. & Eggers, P. Trends in the epidemiology of focal segmental glomerulosclerosis. *Seminars in nephrology* **23**, 172-182 (2003).
59. Barisoni, L., Schnaper, H.W. & Kopp, J.B. A proposed taxonomy for the podocytopathies: a reassessment of the primary nephrotic diseases. *Clinical journal of the American Society of Nephrology : CJASN* **2**, 529-542 (2007).
60. Wharram, B.L., *et al.* Podocyte depletion causes glomerulosclerosis: diphtheria toxin-induced podocyte depletion in rats expressing human diphtheria toxin receptor transgene. *Journal of the American Society of Nephrology : JASN* **16**, 2941-2952 (2005).
61. D'Agati, V.D., Kaskel, F.J. & Falk, R.J. Focal segmental glomerulosclerosis. *The New England journal of medicine* **365**, 2398-2411 (2011).
62. Gbadegesin, R., Lavin, P., Foreman, J. & Winn, M. Pathogenesis and therapy of focal segmental glomerulosclerosis: an update. *Pediatr Nephrol* **26**, 1001-1015 (2011).
63. Wiggins, R.C. The spectrum of podocytopathies: a unifying view of glomerular diseases. *Kidney international* **71**, 1205-1214 (2007).
64. Matsusaka, T., *et al.* Genetic engineering of glomerular sclerosis in the mouse via control of onset and severity of podocyte-specific injury. *Journal of the American Society of Nephrology : JASN* **16**, 1013-1023 (2005).
65. Matsusaka, T., *et al.* Podocyte injury damages other podocytes. *Journal of the American Society of Nephrology : JASN* **22**, 1275-1285 (2011).

-
66. Leeuwis, J.W., Nguyen, T.Q., Dendooven, A., Kok, R.J. & Goldschmeding, R. Targeting podocyte-associated diseases. *Advanced drug delivery reviews* **62**, 1325-1336 (2010).
 67. Haraldsson, B., Nystrom, J. & Deen, W.M. Properties of the glomerular barrier and mechanisms of proteinuria. *Physiological reviews* **88**, 451-487 (2008).
 68. Chen, Y.M. & Miner, J.H. Glomerular basement membrane and related glomerular disease. *Translational research : the journal of laboratory and clinical medicine* (2012).
 69. Mochizuki, T., *et al.* Identification of mutations in the alpha 3(IV) and alpha 4(IV) collagen genes in autosomal recessive Alport syndrome. *Nature genetics* **8**, 77-81 (1994).
 70. Jarad, G., Cunningham, J., Shaw, A.S. & Miner, J.H. Proteinuria precedes podocyte abnormalities in *Lamb2*^{-/-} mice, implicating the glomerular basement membrane as an albumin barrier. *The Journal of clinical investigation* **116**, 2272-2279 (2006).
 71. Haraldsson, B. & Sorensson, J. Why do we not all have proteinuria? An update of our current understanding of the glomerular barrier. *News in physiological sciences : an international journal of physiology produced jointly by the International Union of Physiological Sciences and the American Physiological Society* **19**, 7-10 (2004).
 72. Smeets, B., Dijkman, H.B., Wetzels, J.F. & Steenbergen, E.J. Lessons from studies on focal segmental glomerulosclerosis: an important role for parietal epithelial cells? *The Journal of pathology* **210**, 263-272 (2006).
 73. Smeets, B., *et al.* The parietal epithelial cell: a key player in the pathogenesis of focal segmental glomerulosclerosis in Thy-1.1 transgenic mice. *Journal of the American Society of Nephrology : JASN* **15**, 928-939 (2004).
 74. Hinkes, B.G., *et al.* Nephrotic syndrome in the first year of life: two thirds of cases are caused by mutations in 4 genes (NPHS1, NPHS2, WT1, and LAMB2). *Pediatrics* **119**, e907-919 (2007).
 75. Ryu, M., *et al.* Plasma leakage through glomerular basement membrane ruptures triggers the proliferation of parietal epithelial cells and crescent formation in non-inflammatory glomerular injury. *The Journal of pathology* (2012).
 76. Kim, Y.H., *et al.* Podocyte depletion and glomerulosclerosis have a direct relationship in the PAN-treated rat. *Kidney international* **60**, 957-968 (2001).
 77. Mundel, P. & Shankland, S.J. Podocyte biology and response to injury. *Journal of the American Society of Nephrology : JASN* **13**, 3005-3015 (2002).

78. Macconi, D., *et al.* Podocyte repopulation contributes to regression of glomerular injury induced by ACE inhibition. *The American journal of pathology* **174**, 797-807 (2009).
79. Remuzzi, G., Benigni, A. & Remuzzi, A. Mechanisms of progression and regression of renal lesions of chronic nephropathies and diabetes. *The Journal of clinical investigation* **116**, 288-296 (2006).
80. He, J.S., *et al.* Identification of cellular origin of type I collagen in glomeruli of rats with crescentic glomerulonephritis induced by anti-glomerular basement membrane antibody. *Nephrology, dialysis, transplantation : official publication of the European Dialysis and Transplant Association - European Renal Association* **16**, 704-711 (2001).
81. Cockwell, P., Howie, A.J., Adu, D. & Savage, C.O. In situ analysis of C-C chemokine mRNA in human glomerulonephritis. *Kidney international* **54**, 827-836 (1998).
82. Shankland, S.J. The podocyte's response to injury: role in proteinuria and glomerulosclerosis. *Kidney international* **69**, 2131-2147 (2006).
83. Petermann, A.T., *et al.* Mitotic cell cycle proteins increase in podocytes despite lack of proliferation. *Kidney international* **63**, 113-122 (2003).
84. Pippin, J.W., *et al.* DNA damage is a novel response to sublytic complement C5b-9-induced injury in podocytes. *The Journal of clinical investigation* **111**, 877-885 (2003).
85. Galluzzi, L., *et al.* Molecular definitions of cell death subroutines: recommendations of the Nomenclature Committee on Cell Death 2012. *Cell death and differentiation* **19**, 107-120 (2012).
86. Lasagni, L., *et al.* Notch activation differentially regulates renal progenitors proliferation and differentiation toward the podocyte lineage in glomerular disorders. *Stem Cells* **28**, 1674-1685 (2010).
87. Castedo, M., *et al.* Cell death by mitotic catastrophe: a molecular definition. *Oncogene* **23**, 2825-2837 (2004).
88. Marshall, C.B., Krofft, R.D., Pippin, J.W. & Shankland, S.J. CDK inhibitor p21 is prosurvival in adriamycin-induced podocyte injury, in vitro and in vivo. *American journal of physiology. Renal physiology* **298**, F1140-1151 (2010).
89. Vakifahmetoglu, H., Olsson, M. & Zhivotovsky, B. Death through a tragedy: mitotic catastrophe. *Cell death and differentiation* **15**, 1153-1162 (2008).

90. Ryu, M., Mulay, S.R., Miosge, N., Gross, O. & Anders, H.J. Tumour necrosis factor-alpha drives Alport glomerulosclerosis in mice by promoting podocyte apoptosis. *The Journal of pathology* **226**, 120-131 (2012).
91. Ryu, M., *et al.* Bacterial CpG-DNA accelerates Alport glomerulosclerosis by inducing an M1 macrophage phenotype and tumor necrosis factor-alpha-mediated podocyte loss. *Kidney international* **79**, 189-198 (2011).
92. Anders, H.J., *et al.* CC chemokine ligand 5/RANTES chemokine antagonists aggravate glomerulonephritis despite reduction of glomerular leukocyte infiltration. *J Immunol* **170**, 5658-5666 (2003).
93. Anders, H.J., *et al.* Bacterial CpG-DNA aggravates immune complex glomerulonephritis: role of TLR9-mediated expression of chemokines and chemokine receptors. *Journal of the American Society of Nephrology : JASN* **14**, 317-326 (2003).
94. Wang, Y., *et al.* Ex vivo programmed macrophages ameliorate experimental chronic inflammatory renal disease. *Kidney international* **72**, 290-299 (2007).
95. Anders, H.J. Four danger response programs determine glomerular and tubulointerstitial kidney pathology: Clotting, inflammation, epithelial and mesenchymal healing. *Organogenesis* **8**(2012).
96. Lee, S.B. & Kalluri, R. Mechanistic connection between inflammation and fibrosis. *Kidney international. Supplement*, S22-26 (2010).
97. Vielhauer, V., *et al.* CCR1 blockade reduces interstitial inflammation and fibrosis in mice with glomerulosclerosis and nephrotic syndrome. *Kidney international* **66**, 2264-2278 (2004).
98. Rangan, G.K., Wang, Y., Tay, Y.C. & Harris, D.C. Cytokine gene expression in Adriamycin nephropathy: effects of antioxidant nuclear factor kappaB inhibitors in established disease. *Nephron* **86**, 482-490 (2000).
99. Tak, P.P. & Firestein, G.S. NF-kappaB: a key role in inflammatory diseases. *The Journal of clinical investigation* **107**, 7-11 (2001).
100. Rangan, G.K., Wang, Y., Tay, Y.C. & Harris, D.C. Inhibition of nuclear factor-kappaB activation reduces cortical tubulointerstitial injury in proteinuric rats. *Kidney international* **56**, 118-134 (1999).
101. Zhang, W., Li, Q., Wang, L. & Yang, X. Simvastatin ameliorates glomerulosclerosis in Adriamycin-induced-nephropathy rats. *Pediatr Nephrol* **23**, 2185-2194 (2008).
102. Zheng, G., *et al.* The role of tubulointerstitial inflammation. *Kidney international. Supplement*, S96-100 (2005).

103. Cao, Q., *et al.* IL-25 induces M2 macrophages and reduces renal injury in proteinuric kidney disease. *Journal of the American Society of Nephrology : JASN* **22**, 1229-1239 (2011).
104. Cao, Q., *et al.* IL-10/TGF-beta-modified macrophages induce regulatory T cells and protect against adriamycin nephrosis. *Journal of the American Society of Nephrology : JASN* **21**, 933-942 (2010).
105. Wang, Y.M., *et al.* Regulatory T cells participate in CD39-mediated protection from renal injury. *European journal of immunology* (2012).
106. Wang, Y. & Harris, D.C. Macrophages in renal disease. *Journal of the American Society of Nephrology : JASN* **22**, 21-27 (2011).
107. Vernon, K.A. & Cook, H.T. Complement in glomerular disease. *Advances in chronic kidney disease* **19**, 84-92 (2012).
108. Lenderink, A.M., *et al.* The alternative pathway of complement is activated in the glomeruli and tubulointerstitium of mice with adriamycin nephropathy. *American journal of physiology. Renal physiology* **293**, F555-564 (2007).
109. Turnberg, D., *et al.* Complement activation contributes to both glomerular and tubulointerstitial damage in adriamycin nephropathy in mice. *J Immunol* **177**, 4094-4102 (2006).
110. Lee, V.W. & Harris, D.C. Adriamycin nephropathy: a model of focal segmental glomerulosclerosis. *Nephrology (Carlton)* **16**, 30-38 (2011).
111. Gewirtz, D.A. A critical evaluation of the mechanisms of action proposed for the antitumor effects of the anthracycline antibiotics adriamycin and daunorubicin. *Biochemical pharmacology* **57**, 727-741 (1999).
112. Eom, Y.W., *et al.* Two distinct modes of cell death induced by doxorubicin: apoptosis and cell death through mitotic catastrophe accompanied by senescence-like phenotype. *Oncogene* **24**, 4765-4777 (2005).
113. De Boer, E., Navis, G., Tiebosch, A.T., De Jong, P.E. & De Zeeuw, D. Systemic factors are involved in the pathogenesis of proteinuria-induced glomerulosclerosis in adriamycin nephrotic rats. *Journal of the American Society of Nephrology : JASN* **10**, 2359-2366 (1999).
114. Jeansson, M., Bjorck, K., Tenstad, O. & Haraldsson, B. Adriamycin alters glomerular endothelium to induce proteinuria. *Journal of the American Society of Nephrology : JASN* **20**, 114-122 (2009).

115. Wang, Y., Wang, Y.P., Tay, Y.C. & Harris, D.C. Progressive adriamycin nephropathy in mice: sequence of histologic and immunohistochemical events. *Kidney international* **58**, 1797-1804 (2000).
116. Bottero, V., *et al.* Activation of nuclear factor kappaB through the IKK complex by the topoisomerase poisons SN38 and doxorubicin: a brake to apoptosis in HeLa human carcinoma cells. *Cancer research* **61**, 7785-7791 (2001).
117. Cahilly-Snyder, L., Yang-Feng, T., Francke, U. & George, D.L. Molecular analysis and chromosomal mapping of amplified genes isolated from a transformed mouse 3T3 cell line. *Somatic cell and molecular genetics* **13**, 235-244 (1987).
118. Momand, J., Zambetti, G.P., Olson, D.C., George, D. & Levine, A.J. The mdm-2 oncogene product forms a complex with the p53 protein and inhibits p53-mediated transactivation. *Cell* **69**, 1237-1245 (1992).
119. Vazquez, A., Bond, E.E., Levine, A.J. & Bond, G.L. The genetics of the p53 pathway, apoptosis and cancer therapy. *Nature reviews. Drug discovery* **7**, 979-987 (2008).
120. Grier, J.D., Xiong, S., Elizondo-Fraire, A.C., Parant, J.M. & Lozano, G. Tissue-specific differences of p53 inhibition by Mdm2 and Mdm4. *Molecular and cellular biology* **26**, 192-198 (2006).
121. Leach, F.S., *et al.* p53 Mutation and MDM2 amplification in human soft tissue sarcomas. *Cancer research* **53**, 2231-2234 (1993).
122. Eischen, C.M. & Lozano, G. p53 and MDM2: antagonists or partners in crime? *Cancer cell* **15**, 161-162 (2009).
123. Shangary, S. & Wang, S. Small-molecule inhibitors of the MDM2-p53 protein-protein interaction to reactivate p53 function: a novel approach for cancer therapy. *Annual review of pharmacology and toxicology* **49**, 223-241 (2009).
124. Bouska, A. & Eischen, C.M. Mdm2 affects genome stability independent of p53. *Cancer research* **69**, 1697-1701 (2009).
125. Chene, P. Inhibiting the p53-MDM2 interaction: an important target for cancer therapy. *Nature reviews. Cancer* **3**, 102-109 (2003).
126. Marine, J.C. & Lozano, G. Mdm2-mediated ubiquitylation: p53 and beyond. *Cell death and differentiation* **17**, 93-102 (2010).
127. Clegg, H.V., Itahana, K. & Zhang, Y. Unlocking the Mdm2-p53 loop: ubiquitin is the key. *Cell Cycle* **7**, 287-292 (2008).

128. Ringshausen, I., O'Shea, C.C., Finch, A.J., Swigart, L.B. & Evan, G.I. Mdm2 is critically and continuously required to suppress lethal p53 activity in vivo. *Cancer cell* **10**, 501-514 (2006).
129. Montes de Oca Luna, R., Wagner, D.S. & Lozano, G. Rescue of early embryonic lethality in mdm2-deficient mice by deletion of p53. *Nature* **378**, 203-206 (1995).
130. Tang, Y., Zhao, W., Chen, Y., Zhao, Y. & Gu, W. Acetylation is indispensable for p53 activation. *Cell* **133**, 612-626 (2008).
131. Sherr, C.J. Divorcing ARF and p53: an unsettled case. *Nature reviews. Cancer* **6**, 663-673 (2006).
132. Deisenroth, C. & Zhang, Y. Ribosome biogenesis surveillance: probing the ribosomal protein-Mdm2-p53 pathway. *Oncogene* **29**, 4253-4260 (2010).
133. Gajjar, M., *et al.* The p53 mRNA-Mdm2 interaction controls Mdm2 nuclear trafficking and is required for p53 activation following DNA damage. *Cancer cell* **21**, 25-35 (2012).
134. Brekman, A., Singh, K.E., Polotskaia, A., Kundu, N. & Bargonetti, J. A p53-independent role of Mdm2 in estrogen-mediated activation of breast cancer cell proliferation. *Breast cancer research : BCR* **13**, R3 (2011).
135. Gu, L., *et al.* Regulation of XIAP translation and induction by MDM2 following irradiation. *Cancer cell* **15**, 363-375 (2009).
136. McDonnell, T.J., *et al.* Loss of one but not two mdm2 null alleles alters the tumour spectrum in p53 null mice. *The Journal of pathology* **188**, 322-328 (1999).
137. Polanski, R., *et al.* MDM2 interacts with NME2 (non-metastatic cells 2, protein) and suppresses the ability of NME2 to negatively regulate cell motility. *Carcinogenesis* **32**, 1133-1142 (2011).
138. Di Conza, G., *et al.* IGF-1R/MDM2 Relationship Confers Enhanced Sensitivity to RITA in Ewing Sarcoma Cells. *Molecular cancer therapeutics* **11**, 1247-1256 (2012).
139. Patel, S. & Player, M.R. Small-molecule inhibitors of the p53-HDM2 interaction for the treatment of cancer. *Expert opinion on investigational drugs* **17**, 1865-1882 (2008).
140. Joseph, T.L., Madhumalar, A., Brown, C.J., Lane, D.P. & Verma, C.S. Differential binding of p53 and nutlin to MDM2 and MDMX: computational studies. *Cell Cycle* **9**, 1167-1181 (2010).

141. Zhang, F., *et al.* Whole-body physiologically based pharmacokinetic model for nutlin-3a in mice after intravenous and oral administration. *Drug metabolism and disposition: the biological fate of chemicals* **39**, 15-21 (2011).
142. Vassilev, L.T., *et al.* In vivo activation of the p53 pathway by small-molecule antagonists of MDM2. *Science* **303**, 844-848 (2004).
143. Lin, F., Moran, A. & Igarashi, P. Intrarenal cells, not bone marrow-derived cells, are the major source for regeneration in postischemic kidney. *The Journal of clinical investigation* **115**, 1756-1764 (2005).
144. Lindoso, R.S., *et al.* Paracrine interaction between bone marrow-derived stem cells and renal epithelial cells. *Cellular physiology and biochemistry : international journal of experimental cellular physiology, biochemistry, and pharmacology* **28**, 267-278 (2011).
145. Maeshima, A., Yamashita, S. & Nojima, Y. Identification of renal progenitor-like tubular cells that participate in the regeneration processes of the kidney. *Journal of the American Society of Nephrology : JASN* **14**, 3138-3146 (2003).
146. Lasagni, L. & Romagnani, P. Glomerular epithelial stem cells: the good, the bad, and the ugly. *Journal of the American Society of Nephrology : JASN* **21**, 1612-1619 (2010).
147. Romagnani, P. Parietal epithelial cells: their role in health and disease. *Contributions to nephrology* **169**, 23-36 (2011).
148. Abuelo, J.G. Normotensive ischemic acute renal failure. *The New England journal of medicine* **357**, 797-805 (2007).
149. Rock, K.L., Latz, E., Ontiveros, F. & Kono, H. The sterile inflammatory response. *Annual review of immunology* **28**, 321-342 (2010).
150. Gurtner, G.C., Werner, S., Barrandon, Y. & Longaker, M.T. Wound repair and regeneration. *Nature* **453**, 314-321 (2008).
151. Vielhauer, V., Anders, H.J. & Schlondorff, D. Chemokines and chemokine receptors as therapeutic targets in lupus nephritis. *Seminars in nephrology* **27**, 81-97 (2007).
152. Kriz, W. & Lemley, K.V. The role of the podocyte in glomerulosclerosis. *Current opinion in nephrology and hypertension* **8**, 489-497 (1999).
153. Bohle, A., *et al.* The pathogenesis of chronic renal failure in diabetic nephropathy. Investigation of 488 cases of diabetic glomerulosclerosis. *Pathology, research and practice* **187**, 251-259 (1991).

154. Zeisberg, M. & Neilson, E.G. Mechanisms of tubulointerstitial fibrosis. *Journal of the American Society of Nephrology : JASN* **21**, 1819-1834 (2010).
155. Takeuchi, O. & Akira, S. Pattern recognition receptors and inflammation. *Cell* **140**, 805-820 (2010).
156. Sanz, A.B., *et al.* NF-kappaB in renal inflammation. *Journal of the American Society of Nephrology : JASN* **21**, 1254-1262 (2010).
157. Thurman, J.M. Triggers of inflammation after renal ischemia/reperfusion. *Clin Immunol* **123**, 7-13 (2007).
158. Cao, C.C., *et al.* In vivo transfection of NF-kappaB decoy oligodeoxynucleotides attenuate renal ischemia/reperfusion injury in rats. *Kidney international* **65**, 834-845 (2004).
159. Lassen, S., *et al.* Ischemia reperfusion induces IFN regulatory factor 4 in renal dendritic cells, which suppresses postischemic inflammation and prevents acute renal failure. *J Immunol* **185**, 1976-1983 (2010).
160. Gu, L., Findley, H.W. & Zhou, M. MDM2 induces NF-kappaB/p65 expression transcriptionally through Sp1-binding sites: a novel, p53-independent role of MDM2 in doxorubicin resistance in acute lymphoblastic leukemia. *Blood* **99**, 3367-3375 (2002).
161. Liu, G., Park, Y.J., Tsuruta, Y., Lorne, E. & Abraham, E. p53 Attenuates lipopolysaccharide-induced NF-kappaB activation and acute lung injury. *J Immunol* **182**, 5063-5071 (2009).
162. Marine, J.C., *et al.* Keeping p53 in check: essential and synergistic functions of Mdm2 and Mdm4. *Cell death and differentiation* **13**, 927-934 (2006).
163. McNicholas, B.A. & Griffin, M.D. Double-edged sword: a p53 regulator mediates both harmful and beneficial effects in experimental acute kidney injury. *Kidney international* **81**, 1161-1164 (2012).
164. Furuichi, K., Kaneko, S. & Wada, T. Chemokine/chemokine receptor-mediated inflammation regulates pathologic changes from acute kidney injury to chronic kidney disease. *Clinical and experimental nephrology* **13**, 9-14 (2009).
165. Vassilev, L.T. MDM2 inhibitors for cancer therapy. *Trends in molecular medicine* **13**, 23-31 (2007).
166. Klein, C. & Vassilev, L.T. Targeting the p53-MDM2 interaction to treat cancer. *British journal of cancer* **91**, 1415-1419 (2004).

167. Saif, M.W. & Mehra, R. Incidence and management of bevacizumab-related toxicities in colorectal cancer. *Expert opinion on drug safety* **5**, 553-566 (2006).
168. Payne, W.G., *et al.* Wound healing in patients with cancer. *Eplasty* **8**, e9 (2008).
169. Curry, C.L., *et al.* Notch inhibition in Kaposi's sarcoma tumor cells leads to mitotic catastrophe through nuclear factor-kappaB signaling. *Molecular cancer therapeutics* **6**, 1983-1992 (2007).
170. Shankland, S.J., Pippin, J.W. & Couser, W.G. Complement (C5b-9) induces glomerular epithelial cell DNA synthesis but not proliferation in vitro. *Kidney international* **56**, 538-548 (1999).
171. Knight, A.W., Keenan, P.O., Goddard, N.J., Fielden, P.R. & Walmsley, R.M. A yeast-based cytotoxicity and genotoxicity assay for environmental monitoring using novel portable instrumentation. *Journal of environmental monitoring : JEM* **6**, 71-79 (2004).
172. Shkreli, M., *et al.* Reversible cell-cycle entry in adult kidney podocytes through regulated control of telomerase and Wnt signaling. *Nature medicine* **18**, 111-119 (2012).
173. Nagata, M., Yamaguchi, Y., Komatsu, Y. & Ito, K. Mitosis and the presence of binucleate cells among glomerular podocytes in diseased human kidneys. *Nephron* **70**, 68-71 (1995).
174. Niranjan, T., *et al.* The Notch pathway in podocytes plays a role in the development of glomerular disease. *Nature medicine* **14**, 290-298 (2008).
175. Barisoni, L., Kriz, W., Mundel, P. & D'Agati, V. The dysregulated podocyte phenotype: a novel concept in the pathogenesis of collapsing idiopathic focal segmental glomerulosclerosis and HIV-associated nephropathy. *Journal of the American Society of Nephrology : JASN* **10**, 51-61 (1999).
176. Thomson, A.W., Turnquist, H.R. & Raimondi, G. Immunoregulatory functions of mTOR inhibition. *Nature reviews. Immunology* **9**, 324-337 (2009).
177. Lui, S.L., *et al.* Rapamycin attenuates the severity of murine adriamycin nephropathy. *American journal of nephrology* **29**, 342-352 (2009).
178. Goncalves, G.M., *et al.* The role of immunosuppressive drugs in aggravating renal ischemia and reperfusion injury. *Transplantation proceedings* **39**, 417-420 (2007).
179. Lui, S.L., *et al.* Effect of rapamycin on renal ischemia-reperfusion injury in mice. *Transplant international : official journal of the European Society for Organ Transplantation* **19**, 834-839 (2006).

-
180. Godel, M., *et al.* Role of mTOR in podocyte function and diabetic nephropathy in humans and mice. *The Journal of clinical investigation* **121**, 2197-2209 (2011).
 181. Inoki, K., *et al.* mTORC1 activation in podocytes is a critical step in the development of diabetic nephropathy in mice. *The Journal of clinical investigation* **121**, 2181-2196 (2011).

7. Abbreviations

A		R	
AKI	Acute Kidney Injury	ROS	Reactive Oxygen Species
AN	Adriamycin Nephropathy	T	
B		THP	Tamm–Horsfall protein
BUN	Blood Urea Nitrogen	TLR	Toll Like Receptor
C		TUNEL	Terminal Deoxytransferase Uridine Triphosphate Nick End Labeling
CDK	Cyclin Dependent Kinase		
CKD	Chronic Kidney Disease		
D			
DAMP	Danger Associated Molecular Pattern		
DCs	Dendritic Cells		
E			
ESRD	End Stage Renal Disease		
F			
FSGS	Focal Segmental Glomerulosclerosis		
G			
GBM	Glomerular Basement Membrane		
GFP	Green Fluorescent Protein		
GFR	Glomerular Filtration Rate		
I			
ICAM-1	Intracellular Adhesion Molecule-1		
IRI	Ischemic Reperfusion Injury		
K			
KIM-1	Kidney Injury Molecule-1		
L			
LPS	Lipopolysaccharide		
LRC	Label Retaining Cells		
M			
MDM2	Murine Double Minute-2		
MEFs	Mouse Embryonic Fibroblasts		
N			
NGAL	Neutrophil gelatinase-associated lipocalin		
NK	Natural Killer		
P			
PAMP	Pattern Associated Molecular Pattern		
PECs	Parietal Epithelial Cells		
PPR	Pattern Recognition Receptors		

8. Appendix

Composition of buffers used

FACS buffer :

Sterile DPBS	500 ml
Na Azide	500 mg (0.1 %)
BSA	1 g (0.2 %)

Paris Buffer:

20 mM Tris-HCL, 125 mM NaCl, 10 mM KCl, 10 mM Sodium acetate,
5 mM Glucose.

For 1000 ml:

Tris-HCL (MW 121.14)	2.4228 g
NaCl (MW 58.44)	7.31 g
KCl (MW 74.56)	0.74556 g
Sod. Acetate (MW 82.03)	0.8203 g
D-Glucose (MW 180.16)	0.9 g

10X HBSS (Hank's Balanced Saline Solution) with Ca, Mg:

For 1000 ml

KCl	4 g
KH_2PO_4	0.6 g
NaCl	80 g
$\text{Na}_2\text{HPO}_4 \cdot 2\text{H}_2\text{O}$	0.621 g
NaHCO_3	3.5 g
CaCl_2	1.4 g (or $\text{CaCl}_2 \cdot 2\text{H}_2\text{O}$ 1.854 g)
$\text{MgCl}_2 \cdot 6\text{H}_2\text{O}$	1 g
$\text{MgSO}_4 \cdot 7\text{H}_2\text{O}$	1 g
D-Glucose	10 g

Dissolve in 900 ml of distilled water and adjust to pH 7.4 with 1N HCl or 1N NaOH.
Make up the volume with distilled water to 1000 ml.

10X HBSS (Hank's Balanced Saline Solution) without Ca, Mg:

For 1000 ml

KCl	4 g
KH ₂ PO ₄	0.6 g
NaCl	80 g
Na ₂ HPO ₄ · 2H ₂ O	0.621 g

Dissolve in 1000 ml and autoclave.

DNase stock solution (1 mg/ml):

DNase (type III) 15000 U/6 mg (Sigma D5025)

To prepared 1 mg/ml solution:

Add 6 ml of 50 % (w/v) Glycerol in 20 mM Tris-HCl (pH 7.5), 1 mM MgCl₂.

Can be kept at -20 °C for several weeks.

Caution: Solution is stable only for 1 week at 4 °C.

50 % Glycerol in 20 mM Tris-HCl (pH 7.5), 1 mM MgCl₂:

- 0.48 g of Tris-HCl in 100 ml of distilled water, adjust pH to 7.4 (= 40 mM)
- 50 ml of Glycerol 100 % + 50 ml of 40 mM Tris-HCl (20 mM)
- Add 100 ul of 1M MgCl₂ solution.

Collagenase / DNase solution:

1 mg/ml Collagenase, 0.1 mg/ml DNase in 1X HBSS (with Ca, Mg)

For 10 ml:

Collagenase (type I) (Sigma C0130)	10 mg
1 mg/ml DNase stock solution	1 ml
HBSS (with Ca, Mg)	9 ml

To be preheated in 37 °C water bath before use.

Caution: Prepare freshly every time (Stable only for few days)

Collagenase solution:

1 mg/ml Collagenase in 1X HBSS (with Ca, Mg)

For 10 ml:

Collagenase (type I)	10 mg
HBSS (with Ca, Mg)	10 ml

To be preheated in 37 °C water bath before use.

Caution: Prepare freshly every time (Stable only for few days)

EDTA 2 mM:

EDTA 7.44 mg in 10 ml HBSS (without Ca, Mg)

To be preheated in 37 °C water bath before use.

MACS Buffer:

PBS pH 7.2

0.5% bovine serum albumin

2 mM EDTA

Citrate buffer 10X:

110 mM Sodiumcitrate in ddH₂O

with 2N NaOH to pH 6

PBS:

2.74 M NaCl

54 mM KCl

30 mM KH₂PO₄

130 mM Na₂HPO₄

in ddH₂O

Adjust pH to 7.5 with HCl

Gel Running Buffer (10x):

Tris 30g

Glycine 144g

SDS 5g

Make up volume to 1000ml (pH 8.3)

Transfer Buffer (1x):

Tris 1.5g

Glycine 7.2g

Make up volume to 500ml

TBS (10x):

Tris	24.23g
NaCl	80.06g
Conc. HCL	around 17.5ml

Make up volume to 1000ml (pH 7.6)

TBS-T (1x):

TBS (1x)	1000ml
Tween 20	1ml

Sample buffer:

Milipore water	3,8 ml
0,5 M Tris HCl, pH 6,8	1 ml
Glycerol	0,8 ml
10% SDS	1,6 ml
2- mercaptoethanol	0,4 ml
1% (w/v) bromophenol blue	0,4 ml
Total	8 ml

Separating Buffer (1x):

Tris (1.5mM)	18,2g
SDS	400mg

Make up volume to 100ml (pH 8.8)

Stacking Buffer (1x):

Tris (0.5mM)	6,05g
SDS	400mg

Make up volume to 100ml (pH 6.8)

Staining solution:

Methanol	500ml
Acetic acid	100ml
Water	400ml

Coomasie Brilliant blue R : 2.5 g (0.25%)

Destaining solution:

Methanol	150ml
Acetic acid	100ml
Water	750ml

9. Acknowledgement

There are many who have helped and inspired me during my doctoral study, I would like to convey my gratitude to all those people.

Firstly, I would like to thank **God Almighty** for inspiring, guiding and accompanying me through thick and thin. Without his blessing I could not have reached this far in my career.

I take this opportunity to thank my mentor & guide; **Prof. Hans-Joachim Anders**. He patiently provided the vision, encouragement and advice necessary for me to proceed through the doctoral program. Thanks a lot for giving me this opportunity to work here at Klinische Biochemie, LMU; instilling the confidence in me and your help with the transition to a new professional perspective. I would also like to thank **Dr. Volker Vielhauer, Dr. Bruno Luckow** and **Dr. Peter Nelson** for their constant encouragement of my research work and constructive suggestions throughout my stay at Klinische Biochemie, LMU and **Prof. Paola Romagnani**, University of Florence, Italy for sharing her knowledge and cooperation to complete this thesis.

I thank all my **lab buddies**, Adriana, Anji, Dana, Khader, Kirstin, Maciej, Mi, Murthy, Onkar, Santhosh, Simone, Sufyan and all medical students for the wonderful time we had together. Especially to **Dana**, for sharing your skills and knowledge and **Onkar**, for everything; be it lab or personal life... your constant support and guidance helped me a lot and will always be remembered. Chain of gratitude would be incomplete if I forget to thank Henny, Dan, Jana, Nuru and Ewa for providing skillful technical assistance to carry out the research work successfully. I am also indebted to my **other friends** Supriya, Jyaysi, Dilip, Pankaj, Hari, Jaydeep & others; thanks for your love & support. One of the most important reasons why I love Munich is having all you guys being around. Thank you all for giving me the life long memories, engraved in my heart. I would also like to thank Pravin, Sachin, Tushar, Ujwal, Vijay, Vishal and Yogesh for always being there with me.

There are no words to express my feeling, love and affectionate gratitude to **my family**, my mother, my brother, my sister, my sister-in-law and my uncle for their faith, love, inspiration, selfless sacrifices and constant encouragement throughout my life.

I am grateful to everybody who has been part of my life and helped in some way or other, but if I failed to mention their names, **thank you all**.

It is my duty to express my tearful acknowledgement to the animals, which have been sacrificed for the betterment of human being.

Date:

Shrikant Ramesh Mulay

Curriculum Vitae



Shrikant Ramesh Mulay, M.S. Pharm.

Post doctoral Research Fellow (since Feb. 2013),

AG. Prof. Dr. Anders, Klinische Biochemie, Schillerstr-42, 80336, Munich, Germany.

Email: Shrikant_Ramesh.Mulay@med.uni-muenchen.de

Phone : 0049- 17670539503, 0049-89218075856

Fax : 0049-89218075860

Post-doctoral Fellow

Department of Clinical Biochemistry, Faculty of Medicine, Ludwig Maximilians University of Munich (LMU)

** Pharmacologist * Immunology * Kidney Diseases / Nephrology * Molecular Biology techniques * Immunohistology * Flow Cytometry * Cell culture techniques**

PROFILE

A young professional with combination of scientific research experience and technical skills

- PhD in human biology (thesis submitted Sep 12) with 3 first author and 8 co-author publications in peer reviewed journals.
- Experience of working with several animal models, *in-vivo* techniques.
- Experience of working in cell culture, *in-vitro* techniques.
- Excellent academic profile.

PROFESSIONAL EXPERIENCE

Feb 2013 – till date Department of Clinical Biochemistry, Faculty of Medicine, LMU, Germany

Post-doctoral fellow

I am involved in the projects aimed to investigate the role of the innate immune system and inflammation in the pathogenesis of different renal diseases and their putative role in renal repair after acute as well as chronic kidney injury.

Simultaneously my other responsibilities are writing grants to raise money for research as well as teaching and mentoring the students in the laboratory.

Jan 2010 – Feb 2013 Department of Clinical Biochemistry, Faculty of Medicine, LMU, Germany

PhD fellow (Thesis submitted 09/12)

During my PhD I have worked on the thesis entitled "Role of murine double minute (MDM)-2 in kidney injury and repair". Major findings of the project are (a) MDM2 is a link between inflammation and tubular regeneration, two danger response programs operating during acute renal injury, in p53-independent and p53-dependent manner

respectively (b) MDM2 promotes the podocytes to undergo mitotic catastrophe during chronic kidney failure, suggesting that MDM2 antagonists, e.g. nutlin-3a, have therapeutic potential to treat chronic renal failure. However, their use in acute kidney injury may hold the risk of impaired epithelial healing.

Key Achievements:

- **Three first author** publications in peer reviewed journals (**highest Impact factor 13.06**), **Eight co-author** publications in peer reviewed journals (**Cumulative Impact factor 79.54**)

Jun 2007 – Jun 2009 National Institute of Pharmaceutical Education and Research, Mohali, India

Research Scholar

During these two years I have established the role of TGF- β /smad signaling pathway in the development of diabetic nephropathy (STZ model). Major finding of the study was this pathway is activated leading to renal inflammation and fibrosis during the progression of diabetic nephropathy. Blockade of this pathway with the combination of aspirin and telmisartan reduced the renal inflammation and fibrosis during diabetic nephropathy.

Key Achievements:

- **One first author** publication in peer reviewed journal.
- **Research Fellowship** for two years.

TECHNICAL EXPERTISE

- **In-vivo techniques:** Experienced in Animal handling, Retro-orbital bleeding, organ collection, ways of drug dosing, surgical techniques likes renal ischemia reperfusion, unilateral nephrectomy, unilateral ureteral obstruction etc.
- **In-vitro techniques:** Experienced in Cell culture techniques including isolation of primary cell lines, maintenance of primary, immortalized as well as hybridoma cell lines in cell culture, Cell proliferation and cell death assays, Cell stimulation assays, isolation and purification of monoclonal antibodies from cell supernatants etc.
- **Molecular biology/Immunology techniques:** Experienced in isolation of cytosolic and nuclear proteins from cell culture as whole tissue samples, SDS-PAGE, Western Blot, EMSA, RNA isolation, cDNA synthesis, RT-PCR, ELISA, Co-immunoprecipitation and other biochemical assays etc.
- **Other techniques:** Experienced in Flow cytometry (four color flow cytometer, BD biosciences), Microscopy (Light and Florescence) and Immunohistochemistry techniques etc.

EDUCATION: PhD in Human Biology (Pharmacologist)

PhD in human biology (Jan 2010 – Feb 2013)

Department of Clinical Biochemistry, Faculty of Medicine, LMU, Germany

Masters in Pharmacy (Pharmacology and Toxicology) (Jun 2007 – Jun 2009)

National institute of Pharmaceutical Education and Research (NIPER), Mohali, India

Bachelors in Pharmacy (Jun 2003 - Jun 2007)

Pune University, Nashik, India

Publications:

**Impact
Factor**

First-Author

- **Mulay SR**, Thomasova D, Ryu M, Kulkarni OP, Migliorini A, Bruns H, Gröbmayer R, Lazzeri E, Lasagni L, Liapis H, Romagnani P, Anders HJ. Podocyte loss 6.31

involves MDM2-driven mitotic catastrophe of podocytes. *J Pathol*. *Accepted*.

- **Mulay SR**, Kulkarni OP, Rupanagudi KV, Migliorini A, Darisipudi MN, Vilaysane A, Muruve D, Shi Y, Munro F, Liapis H, Anders HJ. Calcium oxalate crystals induce renal inflammation by NLRP3-mediated IL-1 β secretion. *J Clin Invest*. 2013 Jan 2; 123(1):236-46. 13.06
- **Mulay SR***, Thomasova D*, Ryu M, Anders HJ. Murine double minute-2 links inflammation and tubular healing in acute kidney injury of mice. *Kidney Int*. 2012 Jun; 81(12):1199-21. *Equal Contribution 6.60
- **Mulay SR**, Gaikwad AB, Tikoo K. Combination of aspirin with telmisartan suppresses the augmented TGF β /smad signaling during the development of streptozotocin-induced type I diabetic nephropathy. *Chem Biol Interact*. 2010 Apr 29; 185(2):137-42. 3.06

Co-Author

- Migliorini A, Angelotti ML, **Mulay SR**, Kulkarni OP, Demleitner J, Dietrich A, Sagrinati C, Ballerini L, Peired A, Shankland SJ, Liapis H, Romagnani P, Anders HJ. The antiviral cytokines IFN- α and IFN- β modulate parietal epithelial cells and podocyte loss. Implications for IFN toxicity, viral glomerulonephritis, and glomerular regeneration. *Am J Pathol*. *Accepted*. 5.71
- Schwarz M, Taubitz A, Eltrich N, **Mulay SR**, Allam R, Vielhauer V. TNF-mediated recruitment and activation of glomerular dendritic cells in mouse kidneys: analyzed by compartment-specific flow cytometry. *Kidney Int*. 2013 Mar 6. doi: 10.1038. 6.60
- Hagemann JH*, Thomasova D*, **Mulay SR**, Anders HJ. NRF2 signaling promotes tubular epithelial cell survival and regeneration via murine double minute (MDM)-2. *Nephrol Dial Transplant*. 2013 Mar 8. *Equal Contribution 3.40
- Thomasova D, **Mulay SR**, Bruns H, Anders HJ. The p53-independent role of MDM2 in NF- κ B signaling. Implications for cancer therapy, wound healing, and autoimmune diseases. *Neoplasia*. 2012 Dec; 14(12):1097-1101. 5.95
- Darisipudi MN*, Thomasova D*, **Mulay SR**, Brech D, Noessner E, Liapis H, Anders HJ. Uromodulin Triggers IL-1 β -Dependent Innate Immunity via the NLRP3 Inflammasome. *J Am Soc Nephrol*. 012 Nov; 23(11):1783-9. *Equal Contribution 9.07
- Allam R*, Scherbaum CR*, Darisipudi MN*, **Mulay SR**, Hägele H, Lichtnekert J, Hagemann JH, Rupanagudi KV, Ryu M, Schwarzenberger C, Hohenstein B, Hugo C, Uhl B, Reichel CA, Krombach F, Monestier M, Moreth K, Schaefer L, Anders HJ. Histones from dying renal cells aggravate acute kidney injury via TLR2 and TLR4. *J Am Soc Nephrol*. 2012 Aug; 23(8):1375-88. *Equal Contribution 9.07
- Ryu M, **Mulay SR**, Miosge N, Gross O, Anders HJ. Tumour necrosis factor- α drives Alport glomerulosclerosis in mice by promoting podocyte apoptosis. *J Pathol*. 2012 Jan; 226(1):120-31. 6.31
- Lichtnekert J*, Kulkarni OP*, **Mulay SR**, Rupanagudi KV, Ryu M, Allam R, Vielhauer V, Muruve D, Lindenmeyer MT, Cohen CD, Anders HJ. Anti-GBM Glomerulonephritis Involves IL-1 but Is Independent of NLRP3/ASC Inflammasome-Mediated Activation of Caspase-1. *PLoS One*. 2011; 6(10):e26778. *Equal Contribution 4.4

Total Impact Factor 79.54

Book Chapters:

- Darisipudi MN, **Mulay SR**, Anders HJ. L'inflammasome NLRP3: un nouvel element de signalisation du danger qui favorise l'inflammation renale. In Actualites Nephrologiques Jean Hamburger. Medicine Sciences Publications. Paris 2013

Oral Presentations:

- "Role of murine double minute-2 in inflammation and tubular repair during acute kidney injury" at 23rd meeting of *The European Renal Cell Study Group* at Desenzano del Garda, *Italy* (March 2011).
- "Effect of aspirin in combination with telmisartan on STZ induced type 1 diabetic nephropathy" at IGSDHD selection workshop at *University of Cologne, Germany* (June 2009).

Poster Presentations:

- **American society of nephrology** (ASN) at San Diego, CA, USA (Nov 2012).
- **European Renal Association - European Dialysis and Transplant Association** (ERA-EDTA) at Paris, France (May 2012).
- **American society of nephrology** (ASN) at Philadelphia, PA, USA (Nov 2011).
- **European Renal Association - European Dialysis and Transplant Association** (ERA-EDTA) at Prague, Czech Republic (Jun 2011).
- **International symposium on Nuclear Architecture & Chromatin Dynamics'08** at Centre for Cellular & Molecular Biology (CCMB) Hyderabad, India (November 2008).

Honors and Awards:

- "**Hugo Wilhelm von Ziemssen-Preis 2013**" Medical Clinic and Policlinic IV, LMU Munich, Germany (Jan 2013).
- **The publication**, 'Murine double minute-2 links inflammation and tubular healing in acute kidney injury of mice. *Kidney Int.* 2012 Jun; 81(12):1199-21' is selected for "**Faculty of 1000: post publication peer review**" (July 2012).
- "**Travel Grant Award**" for ERA-EDTA (European Renal Association - European Dialysis and Transplant Association) at Paris, France (May 2012).
- "**Research Fellowship**" at National Institute of Pharmaceutical Education and Research (NIPER) SAS Nagar, Punjab, India (July 2007- June 2009).

CERTIFICATES:

- **Federation of European Laboratory Animal Science Associations (FELASA), Category B:** Appropriate education and training of laboratory animal handling and care for persons carrying out animal experiments for scientific purposes (April 2012).
- **Pharmacist:** Registered Pharmacist in Maharashtra State Pharmacy Council, India (Aug 2012 – Dec 2040).

KEY BEHAVIORAL SKILLS:

Team building, multi-tasking, confident, strong grasping skills, change management & leading

PERSONAL INFORMATION:

- **Nationality** : Indian
- **Date of Birth** : 19th May 1986
- **Languages known:** English, Hindi, Marathi, German (Beginner)

I hereby solemnly declare that all the information provided here is as per the best of my knowledge.

Date: - May 30, 2013

Signature: *SR Mulay*